UNIVERSITY OF VAASA

FACULTY OF TECHNOLOGY

AUTOMATION TECHNOLOGY

Thomas Höglund

ENERGY HARVESTING SOLUTION FOR THE UWASA NODE

Applications for Wind Turbine Monitoring

Master's thesis for the degree of Master of Science in Technology submitted for inspection, Vaasa, 6 October, 2014

Supervisor	Professor Timo Mantere
Instructor	Reino Virrankoski

PREFACE

In the recent years the internet of things has become an extremely popular topic. The concept is very broadly defined and there are huge expectations on the connected devices of the near future. Wireless sensor nodes are central in the internet of things, but their lifetime is limited by the capacity of their batteries. Energy harvesting promises to make ubiquitous sensing possible by charging batteries or supplying wireless sensor nodes directly with power, so that the nodes become maintenance free and their lifetime grows to possibly tens of years. For this master's thesis I developed a small, but powerful energy harvester and management circuit for the UWASA Node.

This thesis builds on research I did as a research assistant in the Communications and Systems Engineering Group (ComSys) at the University of Vaasa from November 2012 until August 2014. I find there is a large number of energy harvesting circuits available on the market, with new, more optimized solutions emerging every year. These can easily be used in almost any project that can run on a small amount of power and I expect I will have good use of my acquired knowledge of energy harvesting.

I would like to thank my instructor Reino Virrankoski and supervisor Timo Mantere for giving me the opportunity to work with such an interesting topic. I would like to thank my colleagues Markus Madetoja, Mike Mekkanen, Tomi Voltti, Caner Çuhac, Linh Le Manh and Maiwulan Wulayinjiang for their kindness and tireless support. I thank my wife Anna for all the support and encouragement. I thank Rayko Toshev for involving me in 3D printing and quadcopter awesomeness as a balance to my demanding studies. A special thank you goes to Mr. Ali Yusein for his active support and positive attitude.

Last, but most of all, I would like to thank all my fellow board members of Wasa Teknologförening rf for believing in our cause and giving me a fantastic time as an engineering student, a time that sadly now is over, but I pledge to continue my support for the Swedish speaking engineering students in Vaasa.

TABLE OF CONTENTS **page**

SYMBOLS AND ABBREVIATIONS

Roman letters

A	Area
P	Power
V	Volts
V	Volume
W	Watts
Z	Impedance

Greek letters

Ω	Resistance, ohms

Subscripts

ESR	Equivalent series resistance
L	Load
MPPC	Maximum power point control
MPPT	Maximum power point tracking
S	Source

Abbreviations

ADC	Analog-to-digital converter/conversion
DSP	Digital signal processor
EDA	Electronic design automation
EH	Energy harvesting/energy harvester
ESR	Equivalent series resistance
FPGA	Field-programmable gate array
IC	Integrated circuit
kbps	Kilobits per second
LDO	Low dropout voltage regulator
LDR	Light dependent resistor
Li-Ion	Lithium-ion
lx	Lux

MOSFET	Metal-oxide-semiconductor field-effect transistor
MPP	Maximum power point
MPPC	Maximum power point control
MPPT	Maximum power point tracking
NiCd	Nickel-cadmium
NiMH	Nickel-metal hydride
PCB	Printed circuit board
PV	Photovoltaics
PWM	Pulse width modulation
RF	Radio frequency
RISC	Reduced instruction set computer
RTC	Real-time clock
SPICE	Simulation program with integrated circuit emphasis
UVLO	Undervoltage lock-out
UWASA	University of Vaasa, Finland
WSN	Wireless sensor network/node

VASA UNIVERSITET
Tekniska fakulteten
Författare: John Thomas Höglund
Diplomarbetets titel: Energy Harvesting Solution for the UWASA Node: Applications for Wind Turbine Monitoring
Övervakare: Professor Timo Mantere
Handledare: Reino Virrankoski
Examen: Diplomingenjör
Utbildningsprogram: Utbildningsprogrammet för elektro- och energiteknik
Inriktning: Automationsteknik
Studierna inleddes: 2008
Diplomarbetet färdigställdes: 2014 **Sidantal:** 86

ABSTRACT

Syftet med detta diplomarbete var att utveckla en lösning för energiskörd för den trådlösa sensornoden UWASA Node för användning i vindkraftverk. Med energiskörd menas utvinnande av energi från omgivningen i små mängder för förbrukning i elektronik såsom trådlösa sensornoder. Den utvecklade lösningen för energiskörd klarar av att försörja UWASA Node med tillräckligt med energi för att utföra många olika uppgifter på obegränsad tid, utan att dess batteri behöver bytas. Den trådlösa sensornoden kan t.ex. avläsa givare med hög samplingsfrekvens och lagra mätdata eller sända det trådlöst. Den kan även utföra invecklade beräkningar och reagera på förändringar i dess omgivning. Ett planerat användningsändamål var övervakning av vibrationer i rotorblad på vindkraftverk, men fälttest har inte ännu utförts.

Detta diplomarbete bygger vidare på forskningsresultaten från mitt kandidatarbete, Höglund (2014) i källförteckningen. I kandidatarbetet undersöktes olika metoder för energiskörd för att finna de lämpligaste metoderna för detta projekt. I detta diplomarbete utvecklades och testades en prototyp för energiskörd och energiförvaltning. Prototypen kan utvinna tiotals milliwatt ur en liten solcell. Den kan också modifieras för att utvinna energi ur en annan energikälla i omgivningen, eller från flera källor samtidigt.

Varje del av energiskördaren och energiförvaltningskretsen diskuteras i detalj och laboratorietest presenteras. Olika metoder för maximum power point tracking (en typ av effektanpassning) provades och utvärderades. Energiskördarprototypen byggdes modulärt så att energiskörd från flera energikällor enkelt kan möjliggöras genom att lägga till några få komponenter för varje energikälla till kretsen.

Sensornodens programmering måste också anpassas så att den fungerar optimalt på den skördade energin genom att schemalägga mätning och trådlös kommunikation. En energisnål realtidsklocka och en vippande brytare lades till på prototypens kretskort för att slå på och av strömtillförseln till sensornoden, så att en minimal mängd energi förbrukas när sensornoden är inaktiv.

NYCKELORD: Energiskörd, autonom sensor, energihantering

VAASAN YLIOPISTO
Teknillinen tiedekunta
Tekijä: John Thomas Höglund
Diplomityön nimi: Energy Harvesting Solution for the UWASA Node: Applications for Wind Turbine Monitoring
Valvojan nimi: Professori Timo Mantere
Ohjaajan nimi: Reino Virrankoski
Tutkinto: Diplomi-insinööri
Koulutusohjelma: Sähkö- ja energiatekniikan koulutusohjelma
Suunta: Automaatiotekniikka
Opintojen aloitusvuosi: 2008
Diplomityön valmistumisvuosi: 2014 **Sivumäärä:** 86

TIIVISTELMÄ

Tämän diplomityön tavoitteena oli kehittää ratkaisu energian harvestointiin UWASA Node:lle tuulivoimalatarkoituksiin. Energian harvestointi tarkoittaa energian keräämistä ympäristöstä pienissä määrissä elektroniikkaa varten, esim. langatonta anturinodia varten. Kehitetty energian harvestointiratkaisu pystyy syöttämään riittävää määrää energiaa UWASA Node:lle, niin että se voi suorittaa monta erilaista toimintoa pidemmän ajan ilman että sen paristoa tarvitse vaihtaa. Langaton anturinodi voi esimerkiksi lukea antureita korkealla näytteenottotaajuudella ja tallentaa tai lähettää nämä lukemat langattomasti. Se voi myös suorittaa monimutkaisia laskuja ja reagoida ympäristön muutoksiin. Yksi suunniteltu käyttötarkoitus oli värinän tarkkailu tuulivoimalan lavassa, mutta kenttäkokeita ei ole vielä tehty.

Tämä diplomityö rakentuu kandidaattityöni tuloksilla, Höglund (2014) lähteissä. Kandidaattityössä eri energian harvestointitapoja tutkittiin ja tähän projektiin sopivin tapa valittiin. Tässä diplomityössä energian harvestointi ja -hallintapiiriä kehitettiin ja testattiin. Prototyyppi pystyy harvestoimaan kymmeniä milliwatteja pienestä aurinkokennosta. Sitä voi myös muokata niin, että se harvestoi toista ympäristön energianlähdettä tai useita lähteitä yhtäaikaisesti.

Jokaista energian harvestointi ja -hallintapiirin osaa pohditaan yksityiskohtaisesti ja laboratoriokokeiden tuloksia esitetään. Eri maximum power point tracking-menetelmiä (eräänlainen impedanssisovitus) testattiin ja arvioitiin. Energian harvestointiprototyypiä rakennettiin modulaarisesti, niin että useiden energialähteiden yhtäaikainen harvestointi onnistuu helposti lisäämällä piiriin vain muutaman komponentin jokaista lähdettä kohtaan.

Anturinodin ohjelmointia pitää myös soveltaa niin, että se käyttää kerätyn energiamäärän optimaalisesti aikatauluttamalla anturilukemia ja langatonta kommunikaatiota. Anturinodin virrankulutusta minimoitiin kytkemällä sen virransyötön pois anturinodin ollessa toimettomassa tilassa. Tätä varten lisättiin pienitehoinen reaaliaikakello ja kiikkukytkin prototyyppipiirilevylle.

AVAINSANAT: Energian harvestointi, itsenäinen sensori, energian hallinta

UNIVERSITY OF VAASA
Faculty of Technology
Author: John Thomas Höglund
Topic of the Thesis: Energy Harvesting Solution for the UWASA Node: Applications for Wind Turbine Monitoring
Supervisor: Professor Timo Mantere
Instructor: Reino Virrankoski
Degree: Master of Science in Technology
Degree Programme: Degree Programme in Electrical and Energy Engineering
Major of Subject: Automation Technology
Year of Entering the University: 2008
Year of Completing the Thesis: 2014 **Pages:** 86

ABSTRACT

The aim of this thesis was to develop an energy harvesting solution for the UWASA Node for wind power station applications. Energy harvesting is the process by which small amounts of ambient energy is collected for use by electronics such as wireless sensor nodes. The developed energy harvesting solution is capable of supplying enough energy for the UWASA Node to perform a wide variety of tasks indefinitely, without the need for changing its battery. The wireless sensor node can for example read sensors at high sampling rates and store or wirelessly transmit these readings. It can also perform complex computations and react to changes in its environment. One intended use was monitoring vibrations of wind turbines blades, but field tests have yet to be done.

This master's thesis builds on the findings of my bachelor's thesis, Höglund (2014) in the references. In the bachelor's thesis different methods of energy harvesting were investigated to find the most suitable methods for this project. In this master's thesis a prototype energy harvester and energy management circuit was developed and tested. The prototype is capable of harvesting tens of milliwatts from a small solar cell. It could also be modified to harvest another ambient energy source or several sources at once.

Every part of the energy harvester and energy management circuit is discussed in detail and laboratory tests are presented. Different means of maximum power point tracking were tested and evaluated. The prototype energy harvester was built using a modular approach so that energy harvesting from multiple sources of energy easily can be accomplished by adding a few components for each source to the harvesting circuit.

The programming of the sensor node also needs to be adapted so that it runs optimally from the harvested energy by scheduling measurements and wireless communication. A low-power real-time clock and a latching switch were included on the prototype PCB for switching on and off the power to the sensor node completely in order to consume as little energy as possible when the sensor node is inactive.

KEYWORDS: Energy harvesting, wireless sensor node, energy management

1. INTRODUCTION

This master's thesis was written as part of the RIWA project, in which University of Vaasa, Aalto University and VTT cooperated. The acronym RIWA is derived from Reliable and Real-Time Wireless Automation. The primary goal of the project was to develop robust hardware and software components and design tools for industrial applications.

The purpose of this thesis was to research energy harvesting methods suitable for the UWASA Node and to implement an energy harvesting solution for supplying the UWASA Node with power in wind turbine monitoring applications. The UWASA Node is a wireless sensor node developed by University of Vaasa and Aalto University as part of the RIWA project. In my bachelor's thesis several different methods of energy harvesting were researched and analyzed to find the most suitable way of powering the UWASA Node (Höglund 2014). Different ways of implementing the energy management and storage circuit were also examined. In this thesis the results of my bachelor's thesis are further studied and an energy harvesting system is implemented.

This thesis focuses especially on developing an energy harvester capable of powering the UWASA Node in wind turbine monitoring applications. The UWASA Node could for example be installed on a wind turbine blade to monitor the vibrations and performance of the blade to find if it is degraded over time. The UWASA Node should be powered by an energy harvester so that changing batteries would not be necessary.

Energy harvesting, also known as energy scavenging, is the process of gathering and storing ambient energy for powering small electronic devices, making them self-sufficient for a long time. Potentially any energy form could be used as a source, but only a few methods have reached widespread commercial use. The total market for what can be regarded as energy harvesting amounts to a few hundred million dollars yearly with photovoltaics (PV) in the lead. (Harrop 2009.)

According to Harrop (2009), 90 % of envisaged Wireless Sensor Networks (WSN) would be impractical without energy harvesting because in networks with a large num-

ber of nodes batteries would be inaccessible or prohibitively expensive to access and change. A few examples of where energy harvesting WSNs could be especially useful are: In buildings where a large number of sensor nodes are embedded, in engines, in monitoring a large number of trees and in weather sensors and other environmental sensors located in inaccessible places.

It is thought that the proliferation of wireless sensor networks will have a vast impact on many aspects of our human existence. WSN make it possible to monitor things such as utilization of resources, behaviour of people and animals, environmental changes, production systems and security. Not only can WSN monitor things but they can also be used to control complex systems. When used in large numbers, wireless sensor nodes need to be low cost and low maintenance. The performance of batteries is improving and the power consumption of electronics for WSNs is decreasing, but they are still not good enough for demanding, long lifetime WSN applications. Therefore, there is considerable interest in developing energy harvesting WSNs. (Gilbert & Balouchi 2008.)

Wireless sensor nodes (WSN) consume different amounts of energy depending on what components are used and depending on the schedule of the program. If actuators are used, those usually consume the most energy. Often there is no need for actuators, and in that case the wireless communication typically consumes the most energy. Some other components that may consume much energy are sensors, processors and voltage regulators. The choice of a low-power microcontroller and clock speed are critical when designing a WSN to be powered by energy harvesting. The power consumption of a WSN can be greatly reduced by shutting off peripherals when they are not needed and setting the microcontroller and sensors into sleep mode. WSNs are often very different and used in different ways that affect how much energy they consume and when they consume it. Therefore an energy harvesting solution for a WSN needs to be optimized for the specific application. (Gilbert & Balouchi 2008.)

This thesis is organized as follows: Chapter 2 summarizes the methods of energy harvesting that were deemed suitable for this project in Höglund (2014). Chapter 3 describes what the UWASA Node is and what it is intended for. Its power requirements and compatibility with energy harvesting hardware are investigated. Chapter 4 explains

how to maximize the amount of energy harvested and how to minimize losses. Chapter 5 presents the measurement devices and techniques used in the tests. In chapter 6 all the parts of the developed energy harvesting solution are covered, with those related to energy management and storage in chapter 6.6. Chapter 7 looks at the performance of the developed prototype and in chapter 8 possible applications related to wind power stations are discussed.

2. METHODS OF ENERGY HARVESTING

For wind turbine monitoring applications solar energy harvesting is the most suitable method of energy harvesting because of the good availability of sunlight in such locations and the good availability and proven technology of solar cells. Energy harvesters using sunlight as their energy source can provide power on the order of 10 mW/cm^2 under ideal circumstances. (Höglund 2014.)

When implementing an energy harvester there are several factors that need to be optimized in order to extract maximum power. Especially voltage conversion can waste much energy, but is necessary because the energy harvester outputs a varying voltage and the energy needs to be stored in order to minimize the size of the energy harvesting system. The optimal method of energy harvesting is always case specific because of the very different availability of energy over time from different sources and locations and the very much varying power consumption of wireless sensor nodes. (Höglund 2014.)

Based on the findings of my bachelor's thesis (Höglund 2014), there are three methods of energy harvesting that are feasible for supplying the UWASA Node with power in wind turbine monitoring applications: solar energy harvesting using photovoltaic (PV) cells, vibration energy harvesting using a piezoelectric cantilever and wind energy harvesting using a microscale wind turbine with an electromagnetic generator. These three methods could also be used in parallel in a hybrid energy harvester.

2.1. PV-Cell Energy Harvesting

Using a PV cell as the energy source would be a safe choice, because it is a well-established technology. Solar cells are readily available in all sizes and in many different configurations with conversion efficiencies around 15 % (Gilbert & Balouchi 2008). A suitable number of photovoltaic fingers should be connected in series in the cell to give an optimum nominal output voltage and more fingers can be connected in parallel to cover the rest of the available area. The generic 92x61 mm, 0.45 W solar cell sold by SparkFun Electronics would be a suitable one, because its open circuit voltage is ap-

prox. 5 V and its size is approximately that of the UWASA Node. Why 5 V is suitable is explained in chapter 6.4. If more energy is needed it is possible to connect more than one such cell in parallel to the energy harvester, while still keeping the maximum power point (MPP) voltage and energy harvesting circuit the same.

PV cells are made for outdoor use and are not damaged by rain or large temperature changes. Energy can reliably be harvested from them whenever the ambient illuminance is high enough. A suitable harvesting schedule can be estimated by analyzing weather data to find out how much energy can be generated on average at a given time of day and time of year. A large fraction of the available energy is lost when the PV-cell is not directed straight against the sun, but this is typically unavoidable. If possible, the PV-cell should be directed in the direction of average maximum sunlight. The reflectiveness of the surroundings highly influences the received energy and a heavy cloud cover reduces the available energy by approximately an order of magnitude (Gilbert & Balouchi 2008). In the worst case the PV-cell will get bright enough conditions for so short a time that not enough energy can be harvested for the load to operate. Seasonal and weather conditions may make it impossible to harvest a sufficient amount of energy for a long time and therefore it is important to store enough energy for the WSN to operate during such times.

2.2. Piezoelectric Energy Harvesting

Of the different vibration energy harvesters, the piezoelectric cantilever is probably the best choice for small applications. Its efficiency is relatively high and it is readily available from several companies. As most vibration energy harvesters, it needs to be tuned to resonate at one of the fundamental frequencies of the source. If the frequency of the source varies much the harvester needs to be tuned or else not much energy can be harvested.

In case a piezoelectric vibration energy harvester would be installed on a blade or stay of a wind turbine, the typical vibrations of that structure would need to be known so that the harvester can be tuned before installation. Those vibrations could be measured by a

first test of the UWASA Node (possibly powered by another type of energy harvester) and then a vibration harvester could be included in the second installation, optimized based on the results from the first installation.

2.3. Microscale Wind Energy Harvesting

A small wind turbine could be used to drive a miniature electromagnetic generator. A benefit of this method would be that it generates energy when it is windy and measurements need to be taken on the wind power station. The small turbine would, however, be unreliable due to the moving parts that can fail. Such a system would probably not work well in freezing conditions, as the turbine would jam when subjected to snow and icing.

Mounting a miniature wind turbine on a full scale turbine blade is probably not a good idea. Mounting one on a large, fixed object such as a stay would work better. A microscale wind turbine can generate quite much energy when it is windy. Azevedo & Santos (2012) were able to harvest between 41–1256 mW at wind speeds of 3–9 m/s using a three-blade horizontal axis wind turbine with 7 cm long blades. This is more than enough for basic intermittent sensing and transmission. Microscale wind turbines would be especially useful for powering sensor nodes that require a large amount of energy in locations where the energy harvester can be large and mounted in a fixed place. A large energy harvester could for example be installed on a base station that communicates with other WSNs.

2.4. A Hybrid Energy Harvester

Several different energy harvesting sources can be harvested simultaneously using a modular energy harvester. Harvesting both solar and wind or vibrational energy would reduce the down time of the harvester and produce power more evenly. The largest drawback of using several sources is the increased requirement for space. Park & Chou (2006) developed a modular energy harvesting system called AmbiMax. They propose

to use a reservoir capacitor array, i.e. a separate supercapacitor for each energy harvester. These supercapacitors need to be able to reach the same voltage in order to power the common voltage rail. If the voltage over one of the capacitors is higher than that of the others, only that one will supply the voltage rail. If more than one capacitor is used like this, diodes may be necessary to prevent backflow from the voltage rail to the capacitors. Diodes should be avoided when possible, as they cause a small voltage drop and power loss. An energy harvester that outputs less power than the other harvesters needs to have a smaller supercapacitor so that it can reach the target voltage fast enough to be efficient (reaching its maximum power point). The voltage rail can be used to power the WSN and/or a battery charger. (Park & Chou 2006.)

3. THE UWASA NODE

The UWASA Node is a wireless sensor node developed by Aalto university and University of Vaasa. It is a modular and stackable platform that can be adapted for diverse applications by stacking different slave boards onto the main board. This allows the engineer to create custom solutions for any application. In its simplest form, called the basic stack, only the main module and the power module are used. These are enough to provide processors, a wireless communication interface, peripheral interfaces and power management and distribution. (Çuhac 2012.)

3.1. The Main Module

The main module of the UWASA Node contains two processors: one main controller and one radio frequency controller. The radio frequency controller can handle all computation and communication in simple applications and then the main controller need not be used. For more demanding applications the main controller is preferable. The main controller is an LPC2378 ARM7TDMI-S based high-performance 32-bit RISC microcontroller by NXP Semiconductors.

3.2. Operating System and Software

The modularity of the UWASA Node is realized by both the hardware and the software architectures. The FreeRTOS (Free Real Time Operating System) was chosen for the UWASA Node in order to enable real time operation and preemptive multitasking. The UWASA Node can thus handle many communication, measurement and control tasks simultaneously. (Çuhac 2012.)

Middleware has been written for the UWASA Node to provide device drivers and hardware abstractions that are used to provide a uniform programming interface for both the main controller and the radio frequency controller. The same API functions can thus be used for programming both controllers. (Çuhac 2012.)

Automated daemons run in the background, taking care of tasks related to power management, time synchronization and system diagnostics. (Çuhac 2012.)

3.3. Auxiliary Hardware

The UWASA Node can be connected to a number of slave modules by using the hardware stack connectors with a total of 160 pins per module. These connectors provide all necessary inter-modular connections for signals and power supplies. The slave modules can be any peripherals such as sensors, actuators and drivers.

3.4. Power Source and Energy Management

The energy management of the UWASA Node is handled by the power module which is a separate module that can be stacked onto the main module. The power module has four different power inputs: a battery input, a charger (external energy source) input, a USB input and an input for the real-time clock, which is integrated in the main controller. The battery can be connected directly to the power module, but a battery can also be connected to the optional generic slave module. If two batteries are connected in this way, the battery connected to the power module will supply the system. (Çuhac 2012.)

The power module features dynamic power path management and is capable of choosing the most suitable power source and charging a battery if one is connected and enough power is supplied. There is a battery monitoring chip that accurately measures current, voltage and temperature. This can be used for calculating the energy state of the battery and for measuring the power consumption of different applications.

The charger input accepts an input voltage in the range 4.35–6.4 V. This is normally supplied by an external battery eliminator, but could for example be supplied directly by a solar cell or an energy harvesting circuit. The charger input is connected to a linear voltage regulator which consumes some energy and therefore it would be better to connect an energy harvester with an external, optimized battery charger to the battery input.

The battery input is designed for one cell lithium ion batteries with a nominal voltage of 3.7 V. It accepts voltages between 1.8–4.2 V. The charger features an undervoltage lock-out (UVLO) that cuts the power when the charger voltage is below 3.3 V. During undervoltage lock-out a very small, but nontrivial current (tens of milliamperes were measured) is drawn from the charger input. Similarly, a very small but nontrivial current flows into the battery input when the battery voltage is below 1.8 V and the charger is in short circuit mode. To eliminate this loss, an external, very low-power UVLO circuit is proposed for energy harvesting applications.

The power module has 10 independent voltage regulator outputs, two of which are fixed voltages for the main module and the remaining outputs provide adjustable voltages for different slave modules and can be independently enabled or disabled. Voltage regulators are necessary for many peripherals, but can in energy harvesting applications waste nontrivial amounts of energy due to quiescent current if unused but connected. In that respect the UWASA Node is not very suitable for energy harvesting because it uses so many regulators and peripherals.

3.5. Power Consumption

Figure 1, reproduced from Çuhac (2012), shows how the hardware components of the power module are interconnected. The input current always passes through the charger and into the VIN_REG voltage rail that supplies the voltage regulators. If power is input into the charger input, power is lost in the protection circuitry and Texas Instruments BQ24075 charger and power management IC. If the power is input into the battery input, less power is lost, because of how the charger and voltage regulators operate.

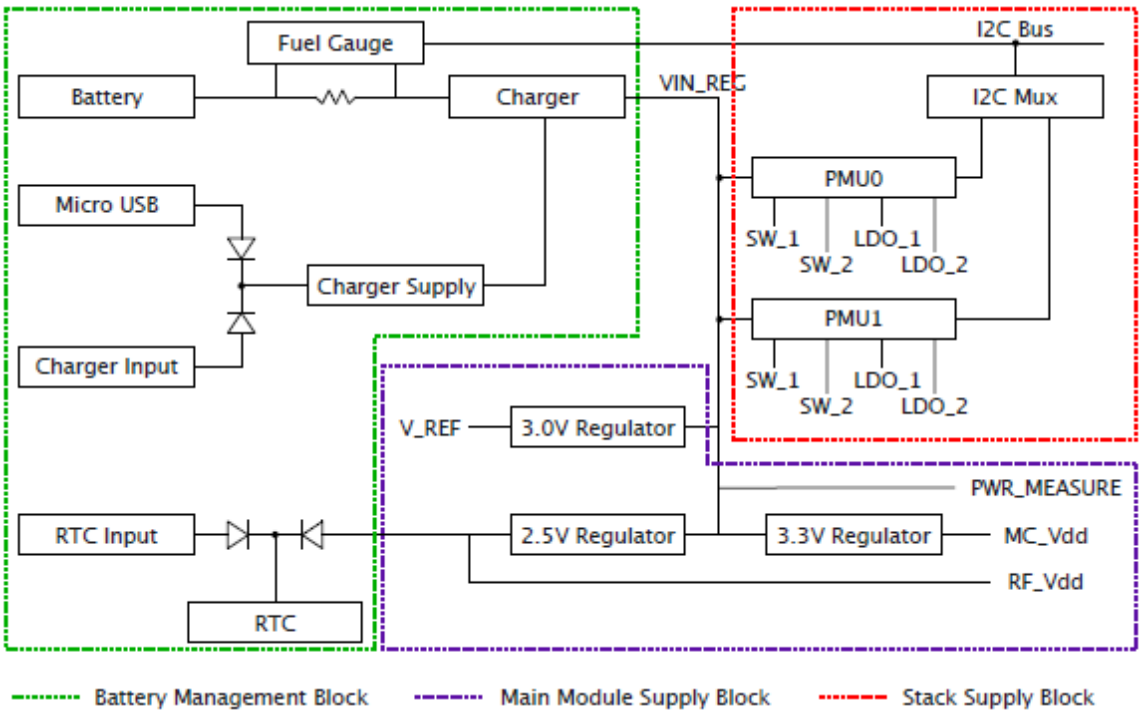

Figure 1. The logical structure of the power module hardware blocks

To investigate the power consumption of the UWASA Node, a number of measurements were conducted under different circumstances. Figure 2 shows how much power the power module draws without the main module, with the supply connected to the charger input and with no battery connected. The graph shows that the power drops when the UVLO is activated below 3.3 V. In UVLO about 10–100 µW of power is still lost depending on the voltage and this loss may be significant, depending on the size of the harvester and the application. Below five volts the power drops rapidly, probably indicating that the charger and other circuitry stop functioning at that low a voltage. The charger input is specified to accept voltages down to 4.35 V. How low the voltage can drop before a UWASA node stops working depends on the running application. The measurements were taken using two basic digital multimeters measuring voltage and current. The measurements are not very reliable because of the few data points, but give a good indication of how the device works. The current sensing multimeter causes a voltage drop on the order of 100 mV, but the voltage measurement was taken on the load side of that multimeter to avoid this error.

A battery at 3.5 V was connected to the battery input and the charger input voltage was reduced until the charger stopped charging the battery. This occurred at a voltage slightly below 5 V. If an energy harvester is ever to be connected to the charger input and a battery to the battery input, it would be important to investigate what voltage the energy harvester should optimally output. This voltage would probably depend on the battery voltage and the power consumption of the UWASA Node, and if so, the energy harvester should take these into account and change its output voltage if possible and efficient.

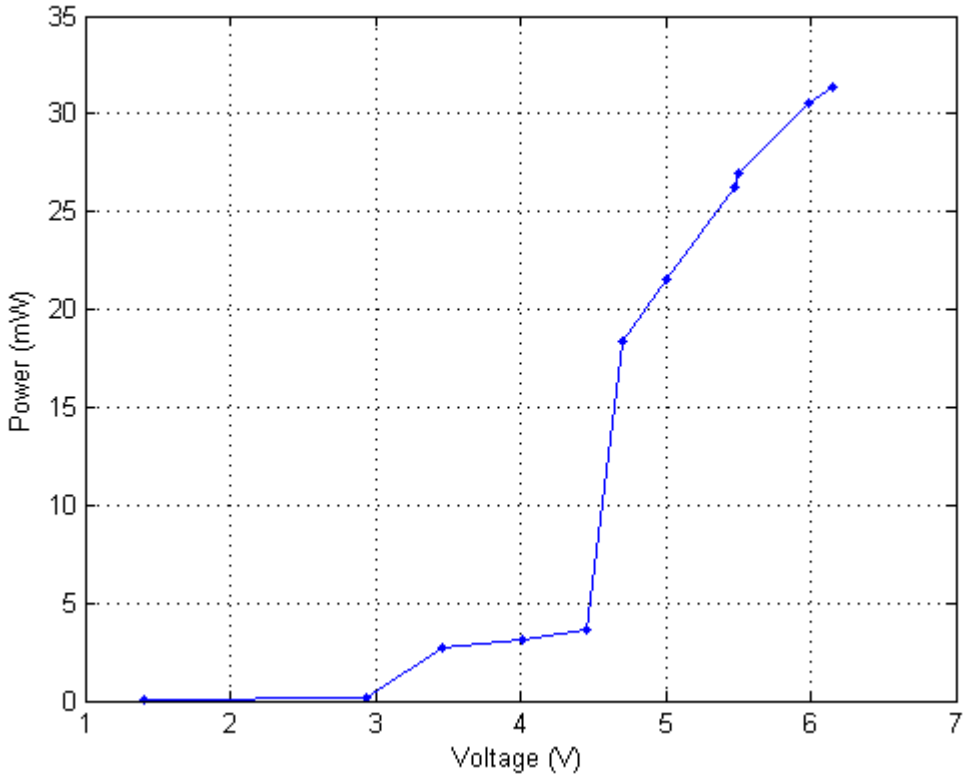

Figure 2. Voltage over and power consumed by charger input with power module only and no battery

In Figure 3 the upper graph shows how much power is consumed when different voltages are applied to the battery input of the power module, with no main module connected. The lower graph shows the same, but with also the main module connected, running a program that continuously transmits data wirelessly. Comparing Figure 2 and Figure 3, it is evident that less power is lost in the power module when the supply is

connected to the battery input than when it is connected to the charger input. When the voltage drops in Figure 3, there are power peaks in both graphs, but at slightly different voltages. This voltage shift might be due to the voltage regulator requiring a higher input voltage when the load is larger. The measurements are not intended to be exact, but give a crude indication of the order of magnitude of the power consumed. Ideally the power consumed by the UWASA Node should be measured while running the actual program that will be running when the node is deployed.

The lowest battery input voltage at which the UWASA Node can operate also depends on the program and how it uses peripherals. Therefore, if an energy harvester is to power the battery input, it is important for the program running on the main module to check that the battery input voltage is high enough for the tasks that need to be executed, before executing them. If not enough power is available, the program will fail, waste power and possibly prevent the energy harvester from ever charging its energy storage. The program should first power up in an energy conserving state before doing heavy duty processing or wireless communication.

To roughly test how much power the UWASA Node will draw in a worst case scenario, a program sending data wirelessly at 32 kbps was uploaded to the node and a 3.8 V battery was connected to the power module. This resulted in a power consumption of 456 mW, which would be a lot for an energy harvesting application of a small size. The power consumption would have been even greater if more peripherals would have been connected. This shows how important it is to write code specifically intended to run on harvested energy.

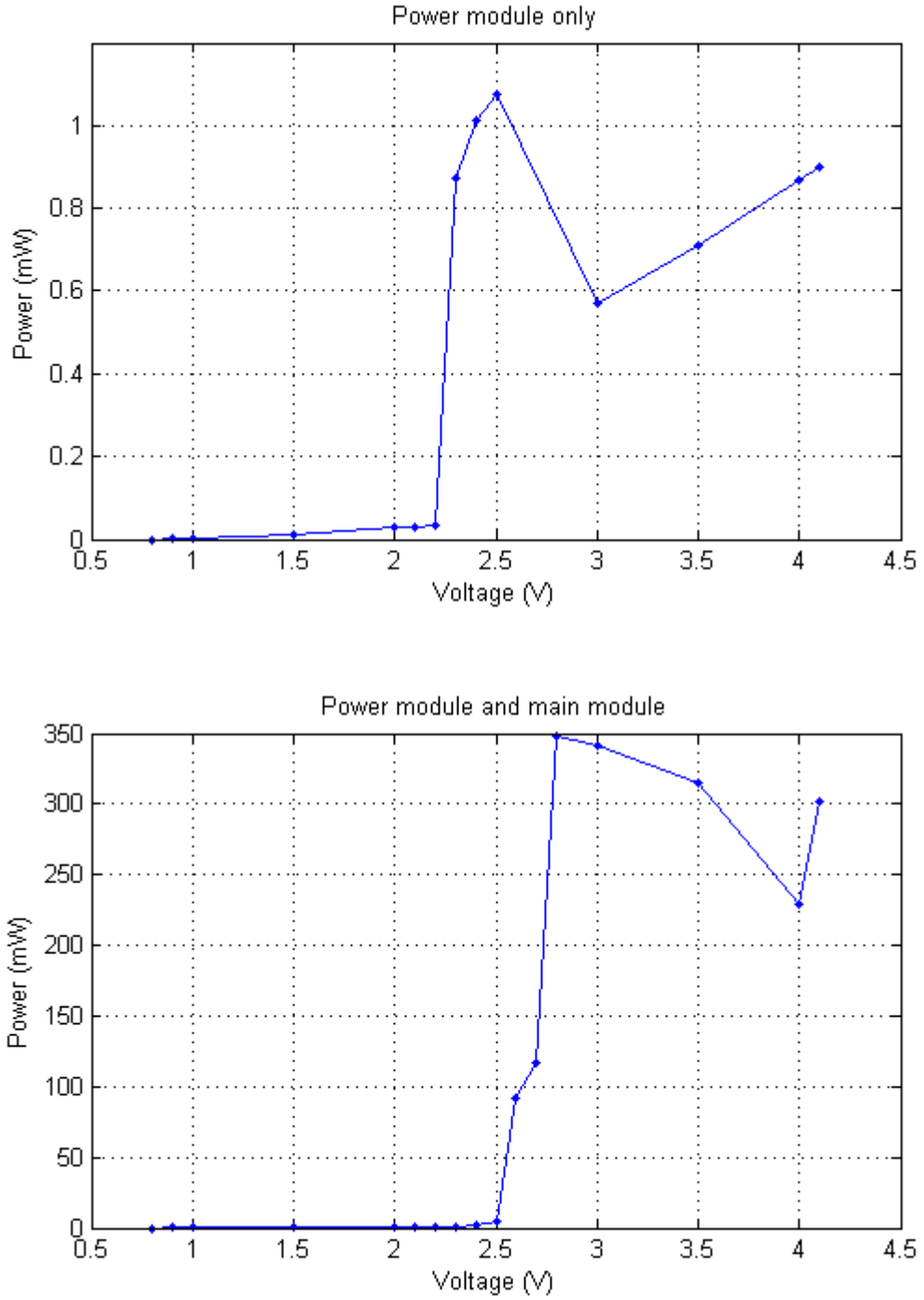

Figure 3. Power consumed when powering the battery input vs. input voltage without and with the main module

To investigate how much energy the UWASA Node consumes when performing different tasks three different test programs were written. The UWASA Node power, main and auxiliary modules were connected and a battery at 3.98 V was connected to the power module. For the first test a 9 degrees of freedom board by SparkFun Electronics was connected to the UWASA Node using the auxiliary board and the I2C2 port. Acceleration was read over I2C with 10-bit precision at a sampling rate of 500 Hz for two seconds (1000 samples), consuming 912 mW. Multiplying the power by the time gives a total energy consumption of 1.824 J, or 1.824 mJ per acceleration measurement. The voltage, current and time were measured using an oscilloscope and a µCurrent active current sensor as described in chapter 5. These power and energy calculations were later used for choosing a solar panel of suitable power.

The second program performed 10 000 loops of analog-to-digital conversion on three pins using the internal ADC of the main controller. The ADC pins were left floating. The initialization part of the code consumed 1.489 J over 1868 ms. An average of 850 mW was consumed during 469 ms, which amounts to approx. 400 mJ, or 40.0 µJ per round of three-pin measurements. Here the results were discarded and it should be noted that storing them or performing calculations on them would consume significantly more energy.

The third program tested how much energy was consumed by wireless transmission of 10 bytes 10 000 times. 678 mW were consumed during 516 ms amounting to 350 mJ, or 35.0 µJ per transmission on average. In practice there seems to need to be a short delay (100 ms) between each transmission in order for the receiver to properly receive the data because of how the transmission is coded. This test result is inconclusive, because another test showed that the sensor node seemed to consume as much power when waiting in between transmission as during transmission. The power consumption apparently needs to be measured in a different way to get more conclusive results, or else there were something wrong with the code. The energy might be buffered somewhere in the UWASA Node, causing power consumption measurements on the battery input to represent an average rather than the instantaneous consumption.

Figure 4 summarizes the power consumptions in the above tests. Contrary to what was expected, the wireless transmission test consumed the least power. This was only a simple test, but it shows that the UWASA Node consumes very much power compared to low power WSNs designed to be powered by energy harvesting. The power consumption can be drastically reduced by properly utilizing sleep modes of the main and RF controllers and some peripherals and by removing unnecessary components such as LEDs, but there was not enough time to test this.

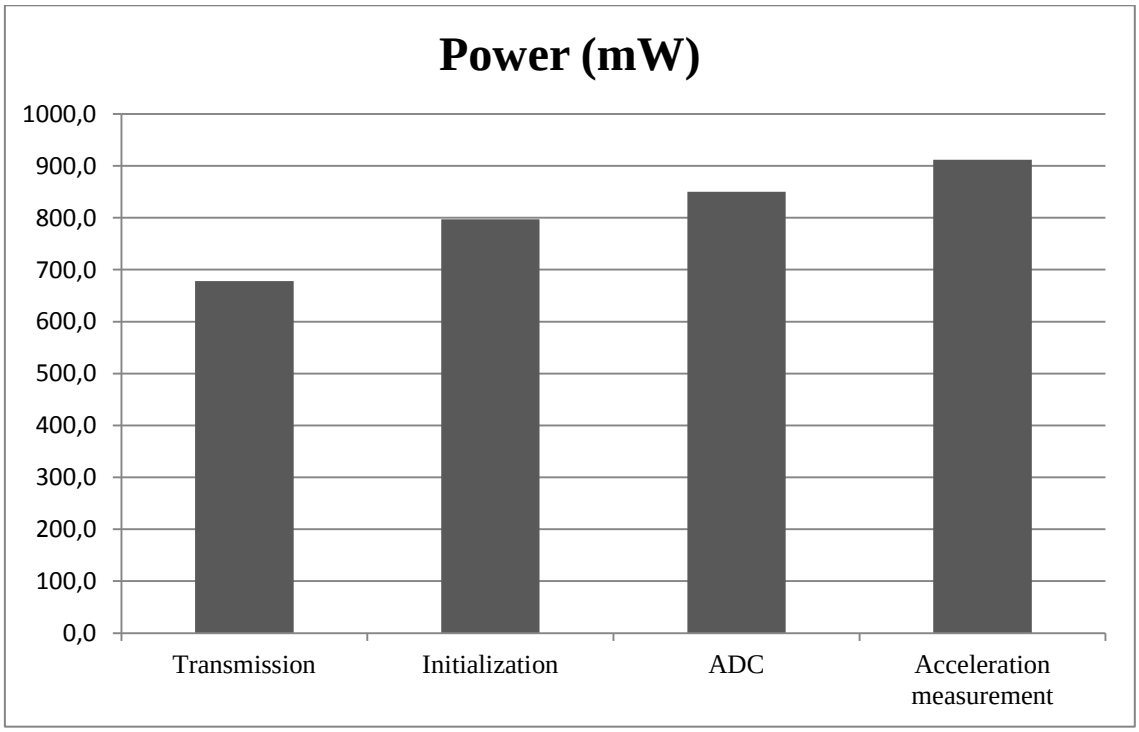

Figure 4. Indicative UWASA Node power consumption for different tasks

4. OPTIMIZING ENERGY HARVESTING

When using an energy harvester to power a wireless sensor node there are many things that require optimization in order to harvest as much energy as possible and to store and use the harvested energy as efficiently as possible. If one part of the system is wasteful, it does not help much to get another part of the system very optimized. Some of the parts of the system that need to be optimized are: harvesting location and schedule, size of the electronics, energy conversion, voltage conversion for storage, electrical switching, energy storage, voltage conversion for consumption, energy consumption of the load circuit, sensor node program execution, wireless communication scheme and transmission power.

As discussed in chapter 3.4 and 3.5, the UWASA Node requires a certain input voltage and is in some ways wasteful compared to a sensor node that is developed specifically to be powered by a certain energy harvester and to perform a narrow range of tasks. The UWASA Node is a modular and multi-purpose sensor node and as such it is not optimized to be powered by energy harvesting. There is, however a new version being developed that consumes less power and would be more suitable for energy harvesting. Even though the UWASA Node is not optimized for energy harvesting, it can still easily be powered by a relatively high power energy harvester.

4.1. Power Density Comparison

The energy harvester and WSN usually need to be as small as possible in order to fit them into tight spaces and make them lightweight. Therefore the power density of the energy harvester, i.e. the power produced per cubic unit of length of the energy harvester, should be as high as possible. Figure 5 is adapted from Gilbert & Balouchi (2008) and compares a number of energy harvesting solutions. It is a plot of power versus volume and power density increases upwards and to the left in the plot. Some of the data was estimated and a few assumptions were made, but the plot gives a good estimate of the power density of different methods. The lines in Figure 5 are based on the assump-

tion that photovoltaic harvesters can be scaled to any size and that the thickness of the solar cell is equal to 5 % of the linear dimensions as in the following equation:

$$V = 0.05A^{3/2}, \tag{4.1}$$

where V is the volume and A is the area of the harvester. Lines of equal power density are parallel to the lines shown for solar energy harvesting.

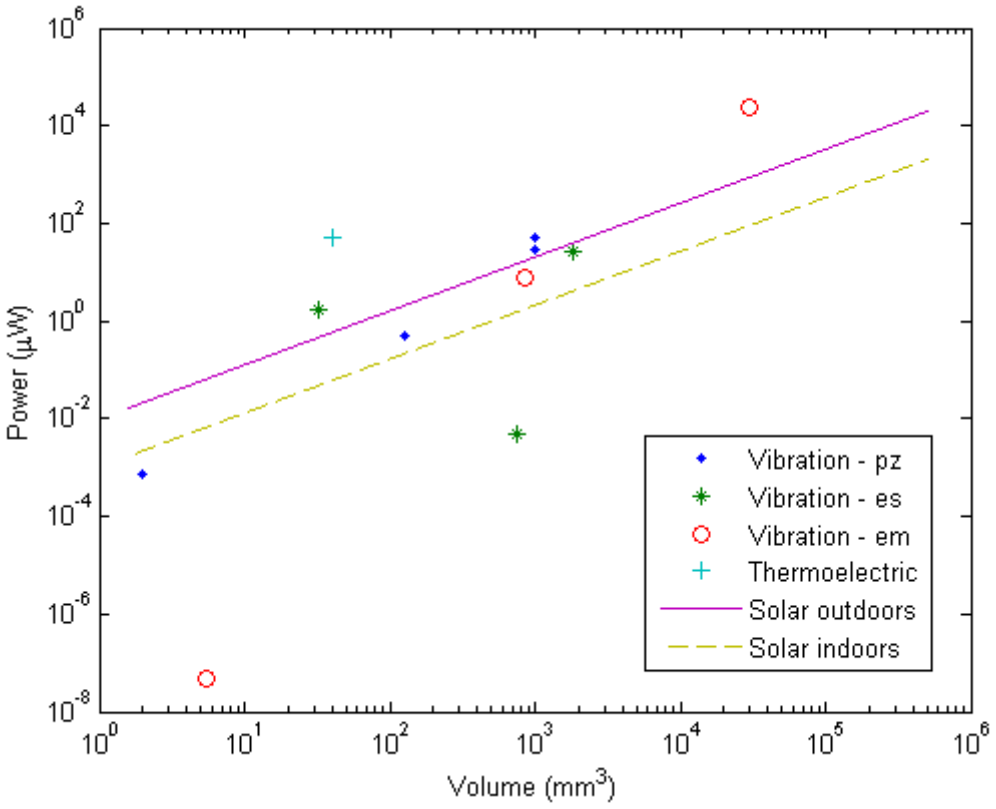

Figure 5. Power vs. volume for different energy harvesters, pz = piezoelectric, es = electrostatic, em = electromagnetic.

In Figure 5 it can be seen that similar types of energy harvesting devices have broadly similar power densities. The smallest harvesters relying on vibration seem to be less efficient than larger ones, but this cannot be interpreted reliably from Figure 5 because of the low number of example sources. Figure 5 does not indicate that any specific vibration harvesting method is much better than the others and therefore it makes sense to make use of the method that is the easiest to implement for the purposes of the target

application of this thesis. It can also be noted that solar energy harvesters are approximately as power dense as vibration harvesters, but they occupy a much larger area.

4.2. Maximum Power Point Tracking

Maximum power point tracking (MPPT) is a method of impedance matching. At the maximum power point (MPP), the energy harvester can harvest the most energy. The MPPT circuit optimizes the load impedance of the energy management circuit. If the output of the energy harvester is DC, the MPPT circuit should set the load resistance to be as close to the source resistance as possible. If it is AC, the MPPT circuit has to be more advanced because it has to set the load impedance (Z_L) to be the complex conjugate of the source impedance (Z_S), as in equation (4.2). This is true for all types of generators. In some cases there may be constraints that make it impractical or impossible to match the impedance exactly. (Toh 2011; Tan & Panda 2011.)

$$Z_S = Z_L^* \tag{4.2}$$

Figure 6, reproduced from Park & Chou (2006), illustrates what a typical solar cell power curve looks like and how MPPT can be performed by keeping the source voltage close to the MPP. Changing the illuminance causes the MPP to shift slightly along the voltage axis. Park & Chou (2006) propose to use a comparator as a hysteresis controller described in chapter 6.5 that rapidly increases and decreases the load to stay close to the MPP.

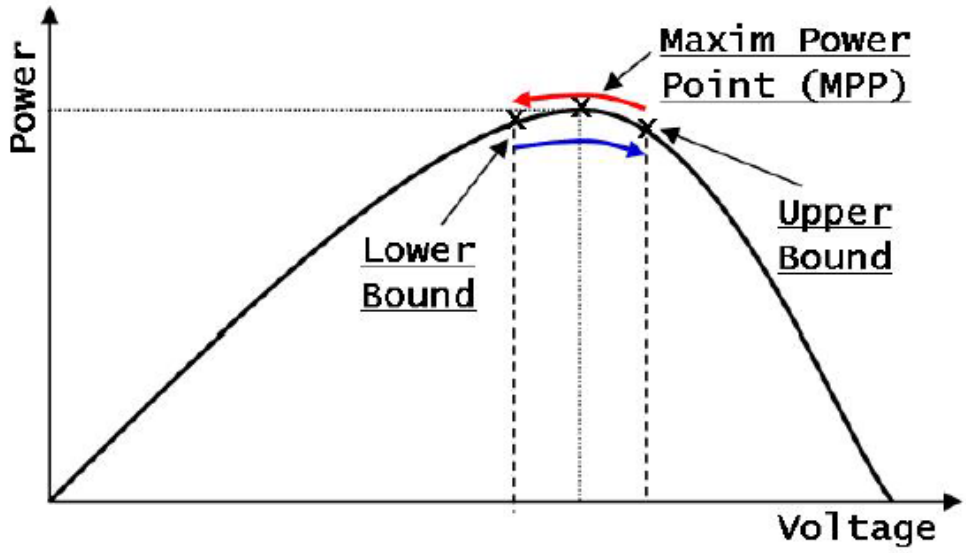

Figure 6. MPPT with an optimum voltage range for bang-bang control

In the simplest case the source impedance is almost constant and the MPPT circuit can just adjust the load impedance to match one single value. In many cases, however, the load impedance varies over varying operating conditions and the MPPT circuit has to actively compensate for this in order to keep the efficiency high. The MPPT circuit often features a low-power microprocessor, operating at low duty cycles, for implementing a control algorithm capable of adapting to varying operating conditions. (Toh 2011.)

Many different types of MPPT circuits have been conceived for use with different types of energy harvesters. Toh (2011) lists a few different MPPT circuits for electromagnetic, piezoelectric and electrostatic energy harvesters. One promising MPPT circuit for electromagnetic sources that Toh describes is a dual-polarity boost converter with rectification, impedance matching, voltage step-up and regulation, all in one circuit. Another is a switched capacitor array. One MPPT circuit for piezoelectric harvesters uses switched inductors. Switched MPPT circuits are common and can be found in many different configurations. (Toh 2011.)

During my visit to the Energy Harvesting & Storage 2014 trade show and conference in Berlin April 1st, 2014, I interviewed a representative from Anagear BV, a company that manufactures integrated circuit solutions for energy harvesting applications. I was told

that the ANG1010 PV power management IC performs MPPT by briefly disconnecting the solar cell once every minute to measure its open-circuit voltage and then it harvests energy from it, keeping it at a percentage of that voltage. A fixed percentage of the open-circuit voltage yields a good enough value for the MPP over the whole range of typical illuminance. In the case of solar energy harvesting a fixed percentage works well, but other DC sources might require a lookup table of voltages and corresponding MPP percentages, or a sensor for finding the MPP.

4.3. Energy Management and Storage

There are complex tradeoffs to be considered when choosing components for the energy management and storage connected to an energy harvester. A source provides the most power in a certain condition at a certain voltage known as its maximum power point as discussed earlier. This voltage may not be optimal for the energy harvesting circuit and voltage regulator that drain the source and supply the voltage rail or storage device with a suitable voltage. Thus a lot of power may be lost if the source and the harvesting circuit are not well matched.

The energy harvesting circuit is also optimally efficient at a certain output voltage. For example, step-up DC/DC converters are the most efficient when their output voltage is only slightly below the input voltage, see Figure 7. When such a converter is charging a battery or a supercapacitor, its output voltage will gradually increase as the load is charged, and the conversion may be efficient only for a short time. For this reason, supercapacitors are commonly used as buffers to let the output voltage rapidly climb to a suitable voltage when harvesting, and then battery charging begins when the optimum voltage is exceeded, thus keeping the output at this voltage until the battery is charged to a higher voltage, after which the efficiency again decreases as the voltage closes in on the setpoint.

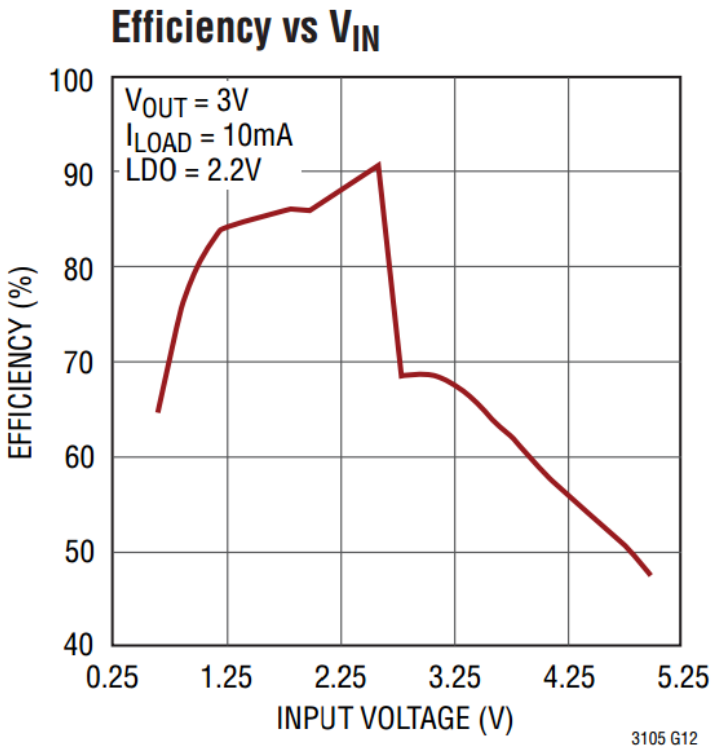

Figure 7. The efficiency of the LTC3105 step-up DC/DC converter, reproduced from its datasheet

Furthermore, the voltage that the sensor node itself is supplied with needs to be constant and therefore voltage regulators are used, causing additional power loss that depends on the regulator type and its input and output voltages. It can be very difficult to optimize the system with so many components in mind. As a rule of thumb the optimum voltages of all components should be as close to equal as possible.

It is unlikely that large WSNs like the UWASA Node could run measurement and transmission programs continuously on harvested energy for an extended period of time because of the high power consumption. A truly optimized energy harvesting system should take into account the limitations of the energy storage circuit and the draining schedule of the storage over time. The wireless sensor node needs to work intermittently and go into sleep mode at certain times in order to conserve energy for coming measurements, data logging and transmissions. The schedule could also be changed by the sensor node based on measurements of the environment. For example the system has to

take into account that no power is harvested from a photovoltaic harvester at night. Schedules of harvesting and consumption can be simulated using computer models before they are tested in hardware in order to make the most of the harvested energy.

5. MEASUREMENT DEVICES AND TECHNIQUES

In order to get precise current measurements without affecting the operation of the load (energy harvester or UWASA Node), the µCurrent active current measurement device was used. Figure 8, which shows the µCurrent version 2, is reproduced from Jones (2010). The µCurrent can be connected to a basic voltage meter or an oscilloscope. It outputs millivolts that correspond to measured milliamperes, microamperes or nanoamperes, depending on the chosen setting. Measuring current using ordinary multimeters causes a voltage drop due to the shunt resistor. This voltage drop is called burden voltage and is approx. 1mV/mA for high-end multimeters (and similar for microamperes), which is inacceptable for many measurements. For truly low power energy harvesters it can even be necessary to measure nanoamperes, which an ordinary multimeter is not capable of. An additional benefit of the µCurrent is that it can be connected to an oscilloscope and then power can be plotted directly if both voltage and current are being measured. This makes it easy to for example tune a maximum power point tracker. Care needs to be taken when using the µCurrent to protect it from overcurrent and to connect the correct reference voltages. During tests some precision resistors were destroyed due to overcurrent, but replacing them was not difficult or expensive. A new version of the µCurrent called the µCurrent Gold has recently been developed and it features larger measurement ranges, increased precision, lower burden voltages and a higher bandwidth of more than 300 kHz (-3 dB). (Jones 2010.)

Figure 8. The µCurrent active current sensor for multimeters and oscilloscopes

A Yokogawa DLM2024 4-channel, 200 MHz, 2.5 GS/s oscilloscope was used for most measurements. Its large screen and four channels were useful when plotting three voltages and a calculated power simultaneously. Its large memory was also useful when logging voltages and currents of the developed energy harvester prototypes over several hours. Measurements and screen captures were saved on a USB memory stick for analysis on a computer and plotting with MATLAB.

For longer tests of energy harvesting prototypes and battery draining a custom voltage logger was built. An Arduino Nano microcontroller platform was used to read voltages every ten seconds and log these to a micro SD card on a separate PCB. These were powered by a separate battery or an AC adapter. A linear 5 V voltage regulator was used to make the voltage reference precise enough. A light dependent resistor (LDR) connected in series with a fixed resistor was used as a voltage divider for measuring the ambient illuminance. The measured voltage was converted to resistance and then to lux using MATLAB. The MATLAB conversion function was created by measuring the resistance of the LDR at 32 different levels of illuminance measured with a lux meter and then making a power regression of that data using the MATLAB Curve Fitting Toolbox. The measurements were conducted indoors using a 20 W adjustable halogen light bulb.

The resulting regression with an R-square goodness value of 0.999 can be seen as a semi-log plot in Figure 9. The LDR used was an A906032 by Excelitas Technologies. The Arduino code for the logger can be found in appendix 8 and the MATLAB script for the resistance vs. illuminance regression plot, containing the regression function, in appendix 9.

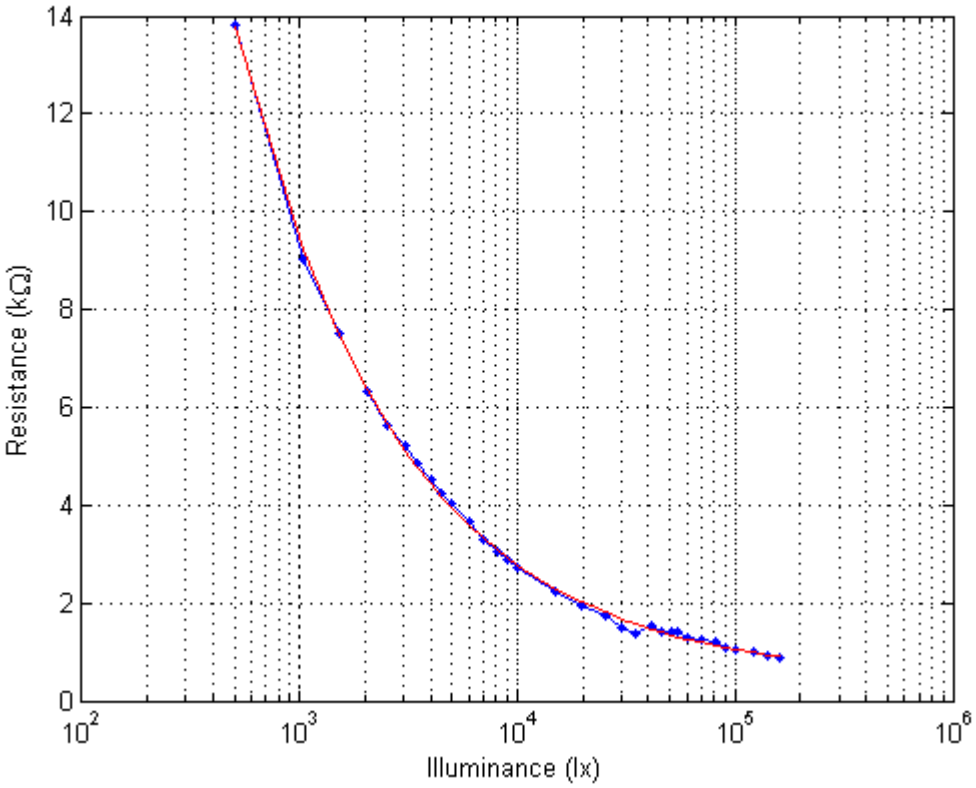

Figure 9. Measured resistance as a function of illuminance (blue) and a power regression (red)

6. ENERGY HARVESTING HARDWARE

After measuring the typical power consumption of the UWASA Node and investigating what forms of energy harvesting would be suitable, an energy harvester prototype was designed and built. The design was made with modularity and expandability in mind. The harvester was designed to work with a small solar cell, but other sources can be added in parallel if some modifications are made. Each separate function of the energy harvester and its power management circuitry were tested as separate PCBs and then combined into a single PCB. These prototype PCBs were designed using CadSoft EAGLE 6.5.0 PCB design software and manufactured by milling using a LPKF ProtoMat S63 circuit board plotter and then soldered by hand under a microscope. After the independent functions were tested on separate PCBs they were merged to a single two sided PCB using the KiCad EDA software suite and sent for production at ITEAD Intelligent Systems Co. Ltd in China. PCB versions 9.0 and newer were produced in China and manually populated in Vaasa.

6.1. The Architecture of the Energy Harvester Prototype

The chosen implementation is based on the AmbiMax system described by Park & Chou (2006). It is an entirely analog energy harvesting system, which was relatively efficient when it was made in 2006, but the power consumption of common, low-power digital controllers has since dropped significantly, making them a viable alternative. The MPPT was not implemented in exactly the same way in this project as in the AmbiMax because newer more efficient analog components were found. Especially the LTC3105 energy harvesting IC described in chapter 6.4 was very useful. The energy management was designed with components similar to those of the AmbiMax. The comparators used in this prototype have smaller quiescent currents and the current limiters have lower resistance than those of the AmbiMax according to their datasheets.

The architecture of the AmbiMax platform can be seen in Figure 10. It consists of a comparator with hysteresis that performs MPPT with the aid of a sensor and controls a

boost regulator. The regulator charges a supercapacitor which is connected to the voltage rail. All these components can be grouped as a subsystem and used in parallel if more than one energy source is used. For the prototype in this work only one such subsystem was implemented. The supercapacitors are connected to the voltage rail via possible protection circuitry and the voltage rail powers the WSN. If the voltage of the voltage rail increases above a certain threshold, the battery is charged from the voltage rail via a current limiter. Conversely, if the voltage of the voltage rail drops to below a certain threshold, the battery feeds the voltage rail as long as its voltage is above a certain threshold. The thresholds are explained in appendix 7. This, in short, is how the AmbiMax and the prototype of this project work. Additionally a low-power undervoltage lock-out (UVLO) circuit and a RTC-controlled latch switch were designed to cut off the voltage rail from the WSN when it drops below a threshold or when the WSN signals it to shut down for a length of time. These were not part of the AmbiMax.

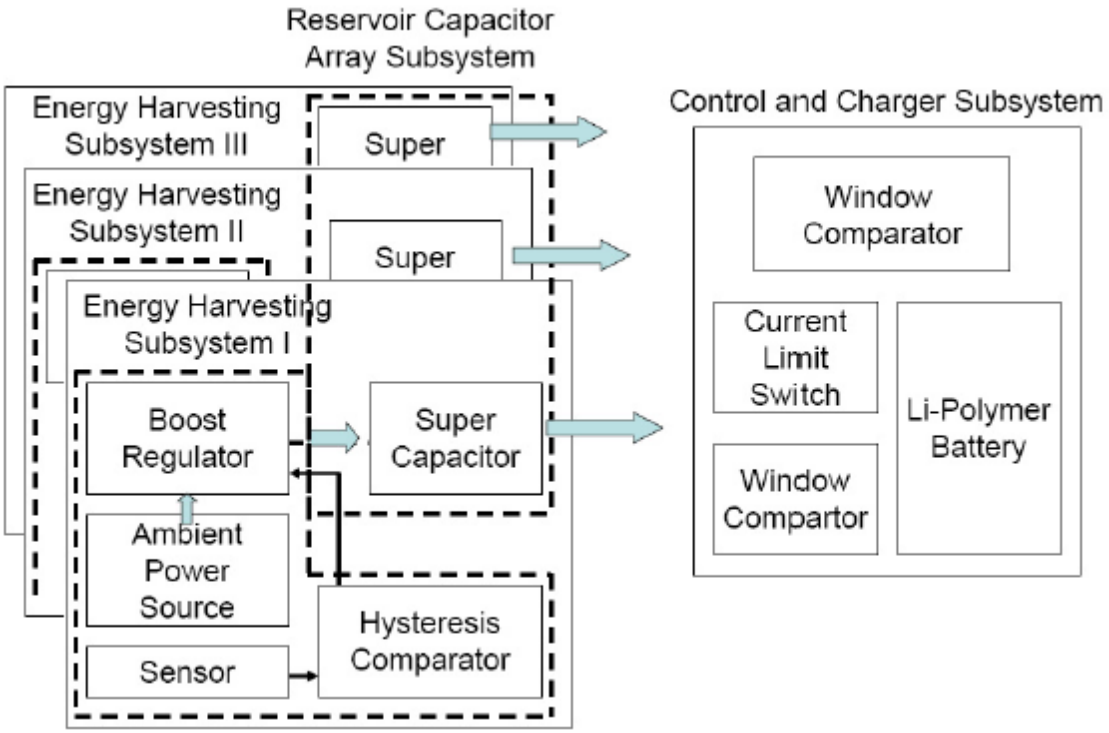

Figure 10. The architecture of the AmbiMax Platform by Park & Chou (2006)

6.2. Developed Prototypes

Versions 4 to 8 of the complete prototype PCB were made as single-sided 51x70 mm boards with mostly surface mount components and some jumpers instead of routing on the bottom side. Pictures of the manufactured prototype version 8 can be found in appendices 3.1 and 3.2. Unfortunately the PCB routing machine did not do a clean job when this circuit was made. Not all versions of the prototype PCB were populated before errors were discovered. A benefit of having all components on one side is that all components and their connections can be seen at once in order to better understand how the circuit works and make it easier to debug.

The 9th version of the PCB was laid out in KiCad so that the separate functions of the board were initially separated as in Figure 11. These blocks of components can be moved and flipped to the other side of the PCB in order to minimize (or customize) its size before final routing and more blocks can easily be added at this stage if more functionality or another harvester needs to be added. All chosen components except the supercapacitors and screw terminals are surface mount devices. Having components related to a specific function close together makes it easier to debug the PCB and easier for people other than the designer to understand it. These functions were also drawn in separate sheets in the KiCad schematic editor. The schematic of the latest prototype, version 9.1, can be found in appendix 1.1 through 1.8 and the layout in appendix 2 and photographs in appendix 3. The 8 schematic sheets are: The parent sheet with terminals, supercapacitors, I^2C pull-up resistors and all other sheets, the UVLO sheet with comparator and MOSFETs, the DoubleComparator sheet with comparator pair, AND gate and current limiter for supplying the voltage rail from the battery, the SolarHarvester sheet with the LTC3105, the ChargerCAP_BAT sheet with comparator and current limiter for charging the battery from the voltage rail, the SHT11 sheet with the temperature and humidity sensor and zero-ohm links for disconnecting the sensor to save power, the V_SENS sheet with voltage dividers for measuring the battery and capacitor voltages with a reference voltage of 3.3 V and finally the RTC_Switch sheet with RTC, latch and MOSFETs for cutting off the load for a given time.

If more energy harvesting sources are to be used, the overall size of the PCB would not grow much, because the energy harvesting circuit itself takes up only a small part of the PCB, see the lower right corner of Figure 11.

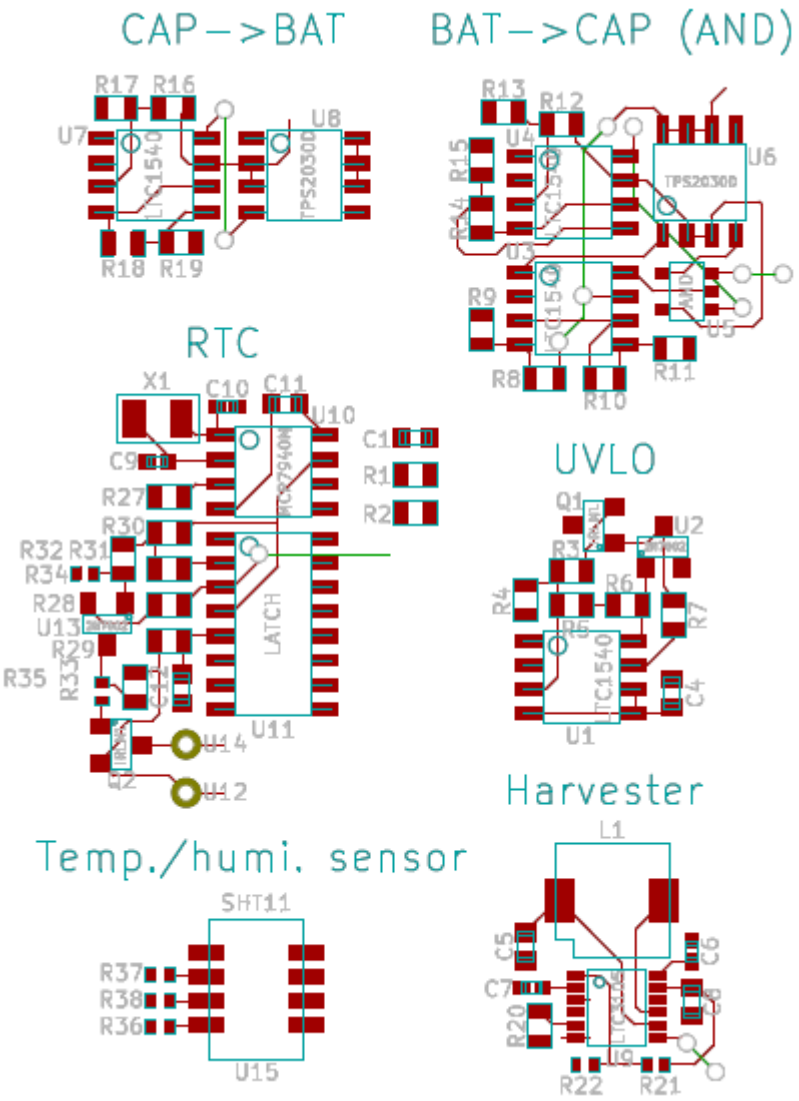

Figure 11. Modular layout of prototype PCB before final routing

In version 8 of the energy harvesting prototype the MPPC pin was connected to three different loads with jumpers as seen in the schematic in appendix 4 and photographs in appendices 6.1 and 6.2. Using the jumpers the MPPC pin can be connected to ground to set the LTC3105 to harvest without MPPT, or to a fixed 360 kA resistor for a fixed MPP of 3.6 V, or to a voltage divider consisting of a LDR and two potentiometers con-

nected between the LDO and ground. After measuring and concluding that the voltage divider was not performing MPPT accurately enough, this option was omitted in later versions of the prototype where only the fixed resistor was implemented.

In version 9.0 an SHT11 temperature and humidity sensor and the RTC-controlled latch switch described in chapter 6.6.5 were added. Version 9.0 featured 9 F supercapacitors, but their physical dimensions were slightly too large to fit them on the same side of the PCB as the screw terminals. Therefore they were replaced by 10 F supercapacitors of smaller physical dimensions in version 9.1. In version 9.1 a pull-up resistor was added to the alarm pin of the RTC and some other minor changes were made.

The total cost of all components for the prototype version 9.1 was approx. 80 €. This cost per unit could be lowered slightly by ordering larger amounts of components at once, but then it would not be feasible to solder the board by hand. A large portion of the cost, 23.65 €, was due to the expensive SHT11 temperature and humidity sensor.

6.3. Solar Cells

Two solar cells (nominally 0.45 W and 2.5 W) were acquired from SparkFun Electronics and a third one (nominally 0.5 W) from Radio Shack for testing. In the module column of Table 1 the nominal values of the solar cells are displayed. The sizes of the cells, in order of increasing power rating, are 92x61x8 mm, 96x54x3 mm and 180x113x8.4 mm. Figure 12 is a photograph of the 92x61x8 mm solar cell. This particular cell seems to have a lot of area that is not covered with photovoltaics. The area of the photovoltaics on the cells (omitting the empty space on the cells) is in the order of increasing power rating: 27 cm^2, 33 cm^2 and 144 cm^2 respectively. Table 1 shows the measured open circuit voltages and short circuit currents and the powers obtained by multiplying these. The listed powers are not attainable because the voltage and current drop when a load is connected, but they are good for comparing the potential power output of the modules. The solar cells were first tested under three different conditions: outdoors under a clear sky and a lightly cloudy sky in the Finnish summer and indoors under fluorescent tube lighting. Fluorescent tubes flicker with the mains frequency and do not emit light of the same spectrum as the sun, but this measurement did not need to be exact since the solar cells were going to be used outdoors and measurements indoors were done only for future reference. The illuminance was measured using a hand-held lux meter.

Figure 12. The 92x61x8 mm, 0.45 W solar cell

Table 1. The tested photovoltaic modules

Module	**Illuminance**	**Open circuit voltage**	**Short circuit current**	**Power**
2.5 W, 8 V	Outdoor, sunny, 147 klx	9.4 V	234 mA	2.2 W
0.45 W, 4.5 V	Outdoor, sunny, 147 klx	5.2 V	104 mA	541 mW
0.5 W, 6 V	Outdoor, sunny, 147 klx	6.9 V	91 mA	628 mW
2.5 W, 8 V	Outdoor, cloudy, 17 klx	8.9 V	31 mA	276 mW
0.45 W, 4.5 V	Outdoor, cloudy, 17 klx	5.0 V	9.0 mA	45 mW
0.5 W, 6 V	Outdoor, cloudy, 17 klx	6.5 V	13 mA	85 mW
2.5 W, 8 V	Indoor, 490 lx	5.3 V	740 µA	3.9 mW
0.45 W, 4.5 V	Indoor, 490 lx	2.5 V	220 µA	550 µW
0.5 W, 6 V	Indoor, 490 lx	3.3 V	200 µA	660 µW

Table 1 shows that the illuminance varies greatly with sun and atmospheric conditions and it will later (in Figure 22) be shown that the output power of a solar cell is directly proportional to the illuminance. The nominal values were quite accurate for comparing the cells. The sunny condition of 147 klx was uncommonly bright because the solar cells were directed straight at the sun. The illuminance rapidly decreases with the angle to the sun when a cell is turned away from the sun and the reflectance of the surroundings also has a large effect on the illuminance. It is therefore important to take the orientation of the solar cell into account when installing it.

In order to measure the MPPs of each solar cell, they were connected to potentiometers used as variable loads. They were then placed under a constant illuminance and their currents and voltages were measured when the load was varied.

The 0.45W solar cell was tested at an illuminance of approximately 2.8 klx. The result is plotted in Figure 12. The MPP occurs at approx. 3.6 V and 6.3 mW. The shape of the curve is very similar to that of Figure 6 in chapter 4.2.

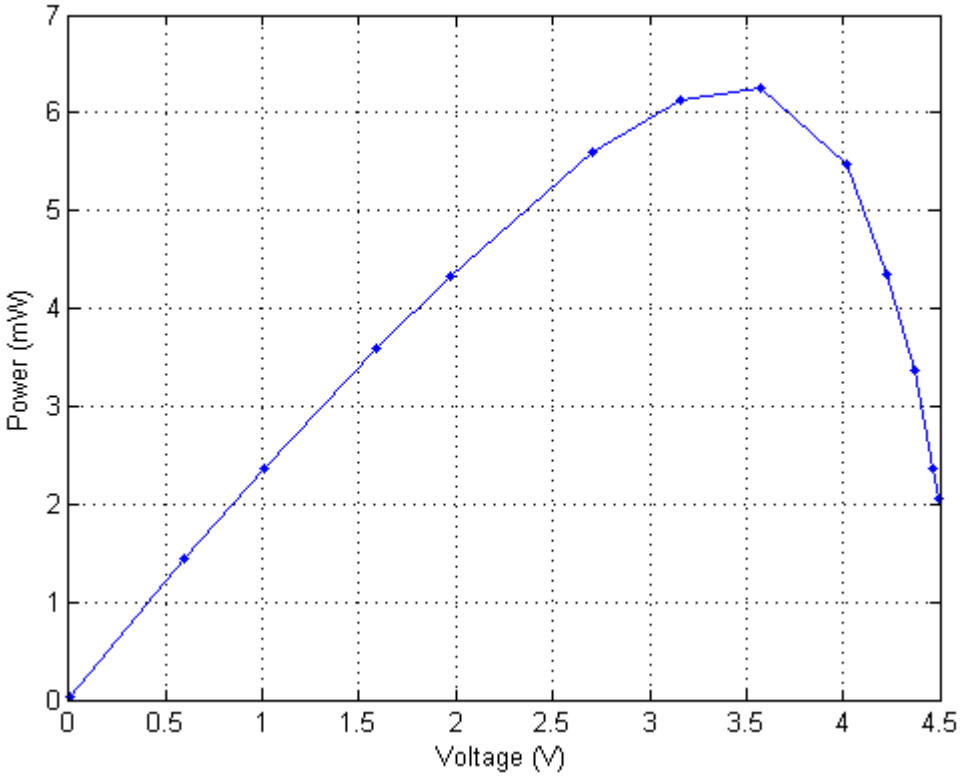

Figure 13. Power vs. voltage for the 0.45 W solar cell at 2.8 klx

The 0.5 W solar cell was only tested indoors at an illuminance of approximately 300 lx. The result is plotted in Figure 14. The MPP occurs at approx. 2.1 V and 290 µW.

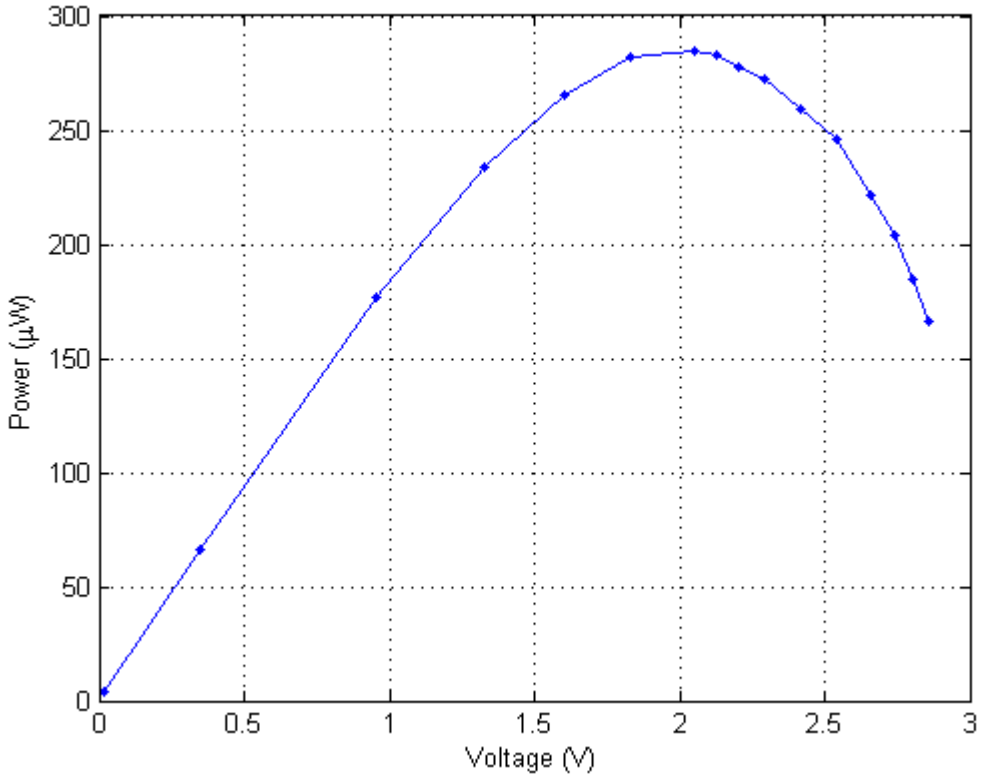

Figure 14. Power vs. voltage for the 0.5 W solar cell at 300 lx

The 2.5W solar cell was first tested indoors at an illuminance of approximately 300 lx. The result is plotted in Figure 15. The MPP occurs at approx. 3.28 V and 1.6 mW. Then it was tested outdoors under three different lighting conditions. The results of the outdoor tests are plotted in Figure 16. Unfortunately a few important data points close to the maximum of each curve were not measured, but the graph gives a good indication of the response to a change of illuminance. It seems that the MPP is almost constantly 7 V in this range of illuminance and this indicates that a fixed MPP could be set for a harvester instead of a moving MPP that is tracked by a MPPT as the illuminance varies. However, the MPP is likely to shift more if the operational range of illuminance is increased.

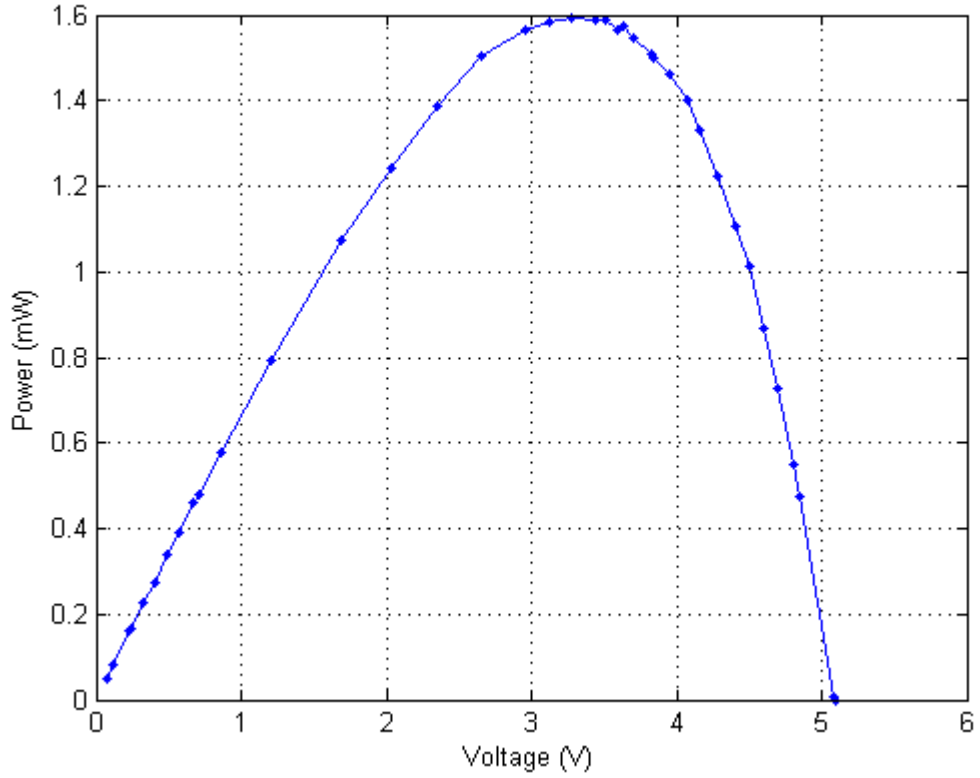

Figure 15. Power vs. voltage for the 2.5 W solar cell at 300 lx

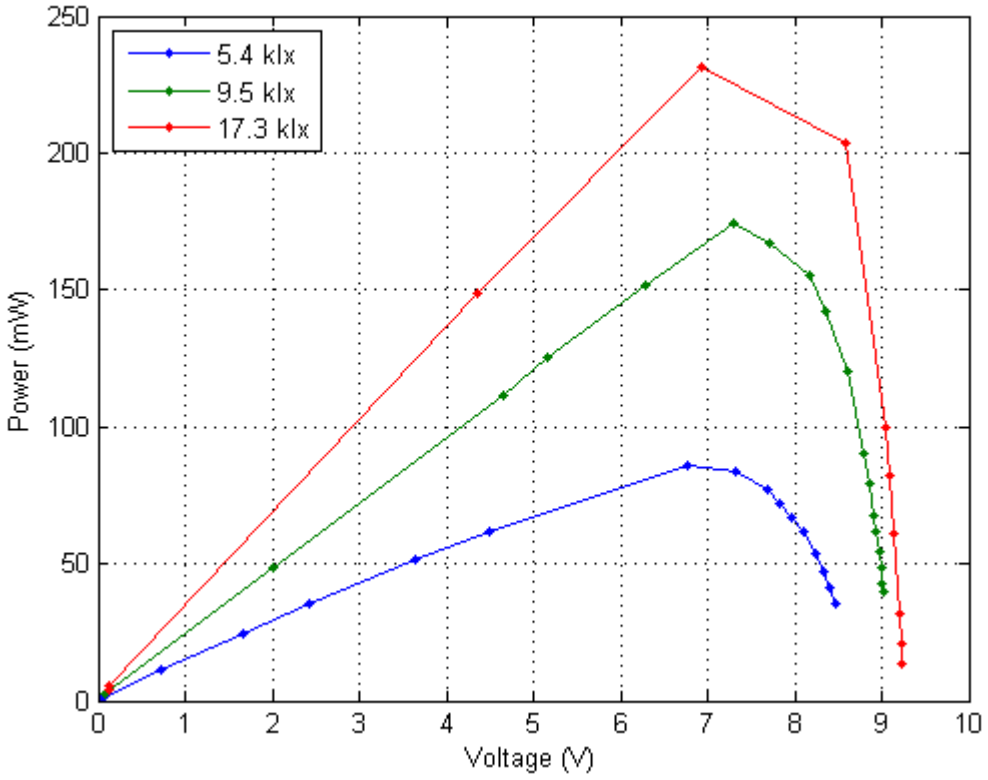

Figure 16. Power vs. voltage for the 2.5 W solar cell at 5.4, 9.5 and 17.3 klx

6.4. The Energy Harvesting Circuit

The LTC3105 energy harvesting IC by Linear Technology was chosen out of many alternatives to be the energy harvester used in the prototype of this project. It is listed as a 400 mA step-up DC/DC converter with maximum power point control and 250 mV start-up voltage. It was chosen based on several factors. The LTC3105 is capable of sourcing up to 5.25 V, which is enough for both the charger input and the battery input of the power module. The prototype is designed to source the battery input and therefore outputs a voltage of 4.2 V, which is the maximum voltage of a one cell Lithium-ion battery. The LTC3105 has a very low start-up voltage of approximately 250 mV in the best case. This allows it to harvest from a photovoltaic that outputs a low voltage due to low ambient illuminance. The low input voltage can also be useful for other types of energy harvesting sources such as thermoelectric, electromagnetic or magnetostrictive sources which output a low voltage and are relatively common.

Figure 17, reproduced from the LTC3105 datasheet, is a schematic of the LTC3105 used as a single PV cell Li-ion trickle charger. The output voltage V_{OUT} and LDO voltage are set using resistors as voltage dividers. The LTC3105 can directly trickle charge a battery, or it can be connected to supercapacitors acting as a buffer, see chapter 6.6.3. The operation of the LTC3105 was simulated using an LTspice IV model provided by the manufacturer to confirm the resistor sizing calculations and the capacitor and inductor recommendations.

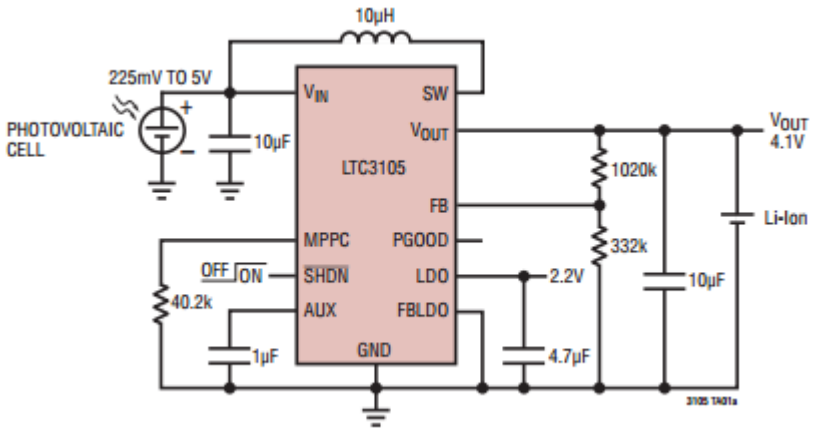

Figure 17. Schematic of LTC3105 used as a single PV cell Li-ion trickle charger

The smaller solar cell from SparkFun Electronics, i.e. the one rated at 0.45 W and 4.5 V, was selected for supplying the prototype of the energy harvester being designed, because the LTC3105 has a maximum operating input voltage of 5 V and the other cells could potentially apply too high a voltage to its input. The 0.45 W solar cell can reach slightly over 5 V if unloaded, but the LTC3105 is rated at a maximum voltage of 6 V on all pins when not in operation. Protection diodes could be used, but the LTC3105 operates most efficiently at input voltages slightly lower than the output voltage as shown previously in chapter 4.3, Figure 7 and therefore the MPP voltage of the solar cell should be lower than the desired output voltage. This small solar cell is a suitable size for many applications, since it is about the size of the UWASA Node.

The small PCB in Figure 18 was manufactured for testing the LTC3105 and its MPPT feature. The 10 µH inductor on this PCB was unnecessarily large in physical dimensions, but had a very low equivalent series resistance (ESR) and suitable inductance. The PCB has connections for power input and output and external variable resistors for the LDO, FBLDO (feedback for LDO) and MPPC pins. The LTC3105 was tested by connecting its input to the 0.45 W solar cell and its output to a pair of uncharged supercapacitors. The resulting output power and efficiency vs. output voltage is plotted in Figure 19. The input voltage was kept at approx. 3.8 V using the MPPC pin. The illuminance was kept constant. The conversion efficiency was precisely proportional to the output power. The power and efficiency increased more rapidly when the output voltage exceeded the input voltage, as expected for a step-up converter. This shows how important the output voltage is for the efficiency. It should also be noted that the LDO can only reach as high a voltage as the output has at a given time. In this case the LDO was set to output 4.15 V, but it reached regulation only when the supercapacitor was fully charged to 4.15 V or when it was disconnected.

In late 2013 Texas Instruments launched the award-winning BQ25505 and BQ25570 ultra low power harvester power management ICs with boost chargers. These feature better specifications than the LTC3105 in many ways and they have integrated MPPT that is done by disconnecting the energy source to measure its open-circuit voltage and then harvest at a configurable percentage of that voltage. If a new low power energy

harvester is to be designed after the prototype described in this thesis, one of these new ICs should be used instead of the LTC3105. One drawback of these ICs is that their maximum input voltage is only 4 V and therefore the solar cell used in this project would need overvoltage protection or some other lower voltage solar cell could be used.

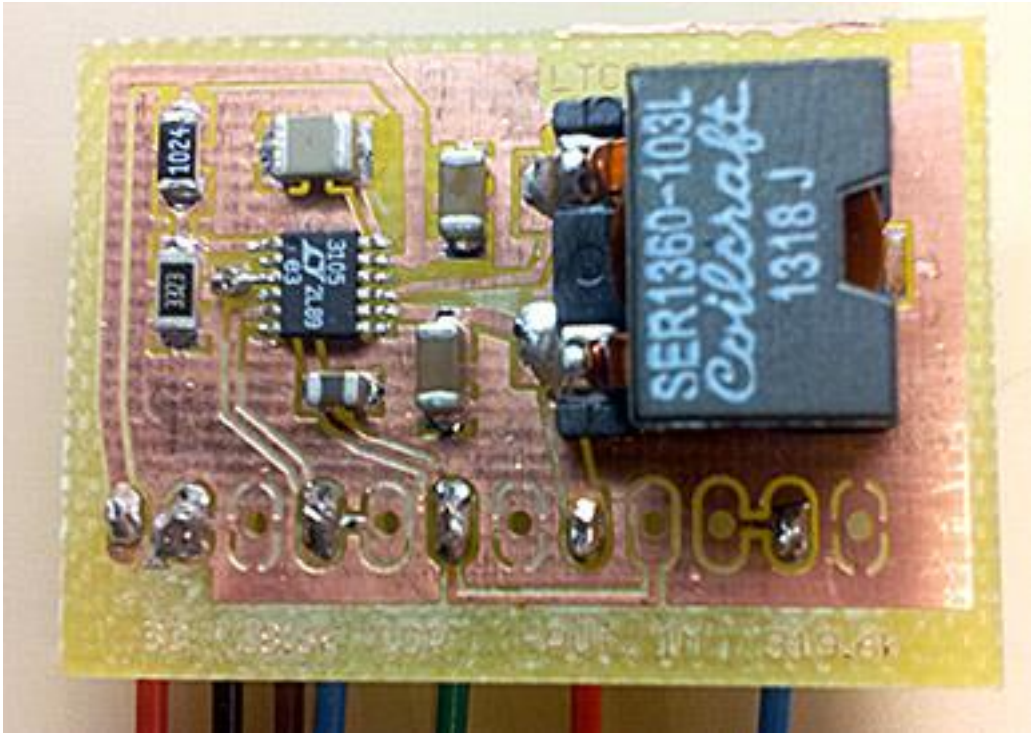

Figure 18. The LTC3105 test PCB

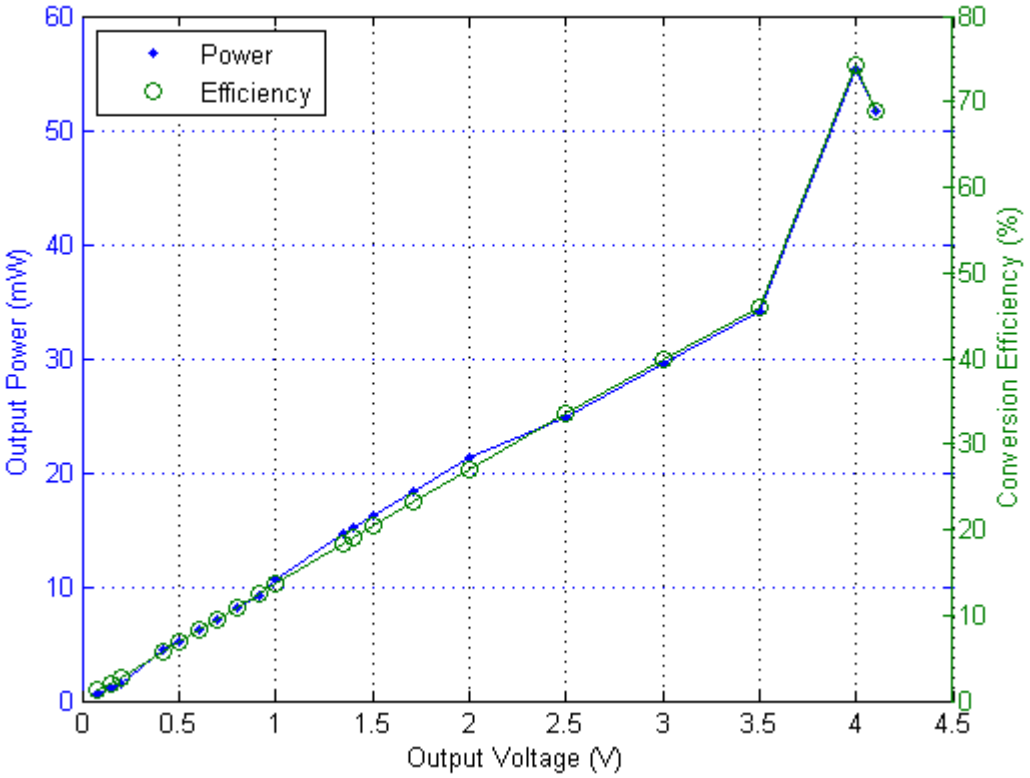

Figure 19. Output power and conversion efficiency vs. output voltage of LTC3105

The voltage rating of a solar cell depends on how many photovoltaic cells are connected in series. The LTC3105 could be used with more than one solar cell rated at 5 V or less in parallel to increase the power output. Having several small cells can be less convenient and when there is little light the voltage drops below a useful level earlier than when a solar cell with a higher voltage rating is used. A solar cell with a higher output voltage could be used with a step-down converter, but then a step-up converter would have to be used at times when it is so dark that the voltage of the solar cell drops below the target output voltage. Another method would be to store enough energy for driving the UWASA Node during the darker hours by choosing a larger cell, but there are usually size constraints. There are voltage regulators such as the Pololu S7V8A that combine a step-up and a step-down converter and such a combination could probably also easily be made using separate step-up and step-down converters, MOSFETS and a comparator to choose which one is active. In future applications, if a large amount of energy is desired at the expense of the size, a larger solar cell could be useful. Therefore the Pololu

S7V8A was tested with the larger cell from SparkFun Electronics, rated at 2.5 W and 8 V.

The Pololu S7V8A is in general the most efficient when it is stepping down and its input voltage is a little higher than its output voltage, as seen in Figure 20 and 21 which are reproduced from the manufacturers' product description Pololu Robotics & Electronics (2014). Figure 20 promises a high efficiency of around 90 % in many cases. A big drawback of the S7V8A is that its minimum input voltage is as high as 2.7 V.

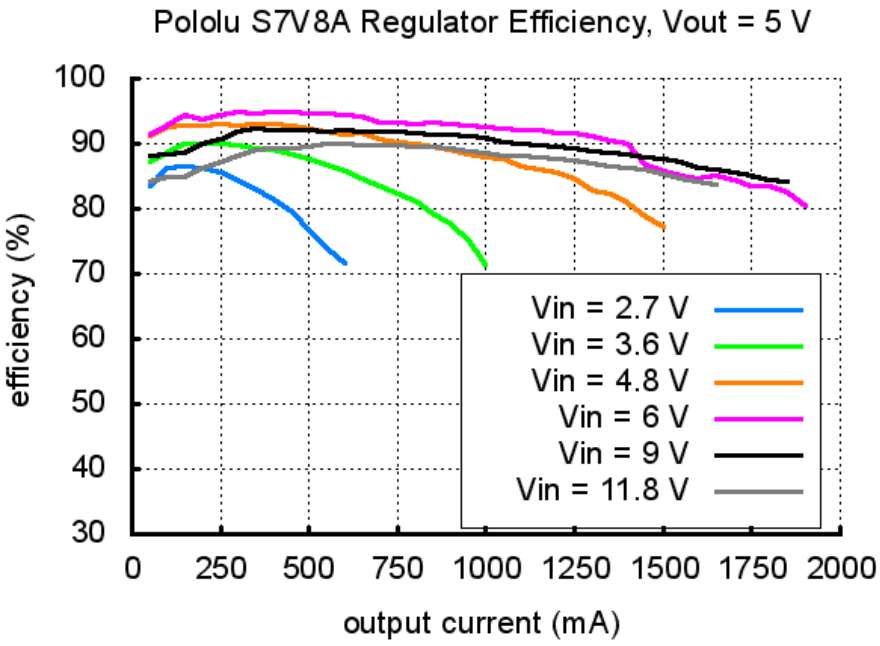

Figure 20. Efficiency of Pololu S7V8A vs. output current at 5 V output and different input voltages

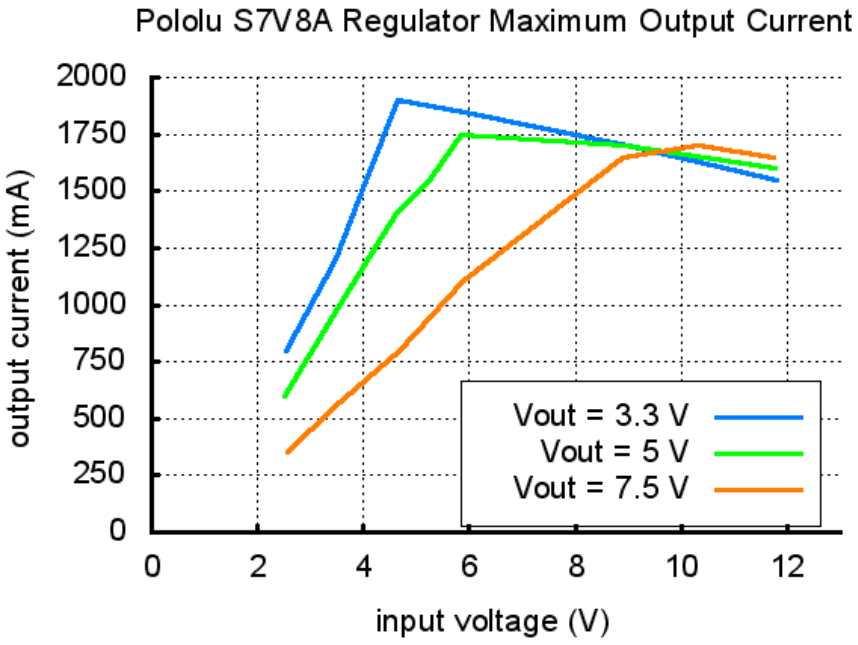

Figure 21. S7V8A maximum output current vs. input voltage for different output voltages

The S7V8A regulator was connected to the 2.5 W solar cell and tested in sunlight in different places with varying illuminance. The regulator was set to output 4.5 V and a 4 kΩ potentiometer was used as a variable load. Impedance matching was performed in each case by tuning the potentiometer to give maximum power output. The output power was maximized when the measured output current was maximized since the output voltage was constant. The plotted result of the measurements is shown in Figure 22. The relationship between the power generated by the solar cell and the illuminance was almost linear. The lower efficiency at lower levels of illuminance was probably due to the lower efficiency of the voltage regulator at lower output currents as seen in Figure 20.

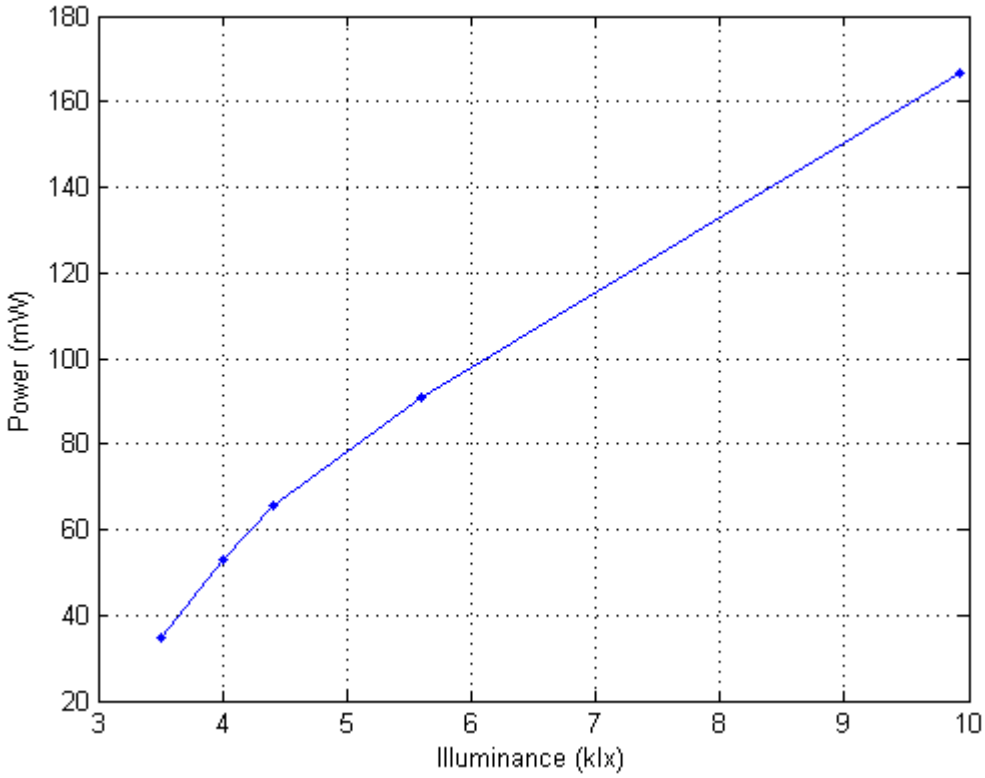

Figure 22. Output power of S7V8A vs. illuminance

The combination of the S7V8A and the 2.5 W solar cell was then tested at a constant illuminance of approximately 10 klx with a potentiometer as a varying load to find the maximum power point as in the previous experiment. Both input and output currents and voltages were measured. The measurement result can be seen in Figure 23. The plotted power is the power consumed by the load. The efficiency η was calculated using equation 6.2.

$$\eta = \frac{P_{out}}{P_{in}} = \frac{U_{in}I_{in}}{U_{out}I_{out}} \tag{6.2}$$

The efficiency did not vary much, but was slightly higher for higher output power. As the load resistance was decreased linearly the power grew exponentially. After reaching 300 mW of output power, the regulator dropped out of regulation when the resistance was further decreased. When in regulation the output voltage was 4.56 V but when the load resistance was too small it dropped to between 0.2–2 V. Once the regulator

dropped out of regulation there was a large hysteresis, meaning that the load resistance needed to increase to much more than it had been just before the dropout for the regulator to reach regulation again. At low illuminance the regulator was unable to get back into regulation even after the load resistance was increased very much or even disconnected. Only after increasing the illuminance in this case, was the regulator able to reach regulation again. This is a big disadvantage if used in energy harvesting where the illuminance may vary greatly. MPPT would be difficult to perform because the output

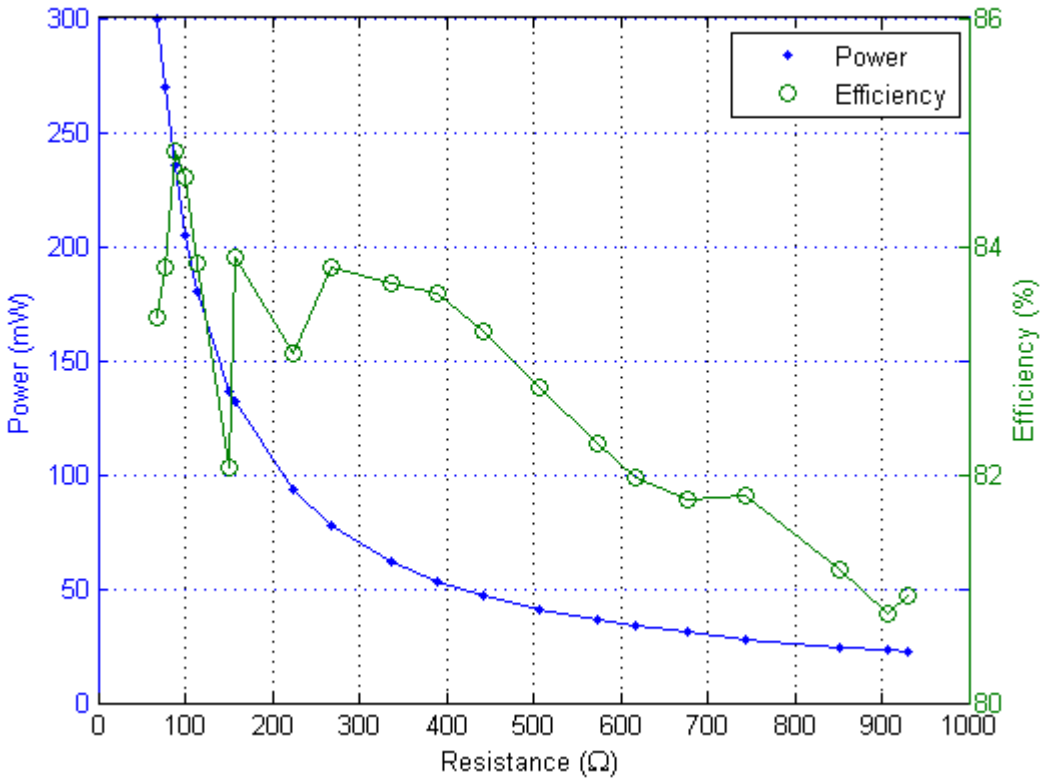

power is the highest close to where the regulator drops out.

Figure 23. Power and efficiency of S7V8A powered by 2.5 W solar cell at an illuminance of 10 klx with a varying load

6.5. Maximum Power Point Tracking

When a step-up or step-down voltage regulator is used for energy harvesting, it can be turned on and off and at a high rate in order to perform MPPT, provided that the regulator has an enable pin and that it responds fast enough. Park & Chou (2006) performed MPPT in this manner by having a comparator with a small hysteresis turn on and off a voltage regulator to keep the source voltage close to the MPP. In effect it produces a pulse width modulated (PWM) output. Since the MPP voltage varies with varying conditions such as illuminance for solar harvesters, a sensor needs to influence the threshold voltage of the comparator to maximize the power output. Figure 24, which is reproduced from Park & Chou (2006), shows how resistive or voltage output sensors can be used for this purpose. Most voltage output sensor implementations consume non-trivial amounts of energy. A small, separate solar cell could be used as a voltage output sensor, but it would have to be rather big to output enough voltage. A small photodiode was tested, but it did not output enough voltage to be useful without amplification. Amplification would be difficult to implement and require a fixed voltage source and was therefore not implemented.

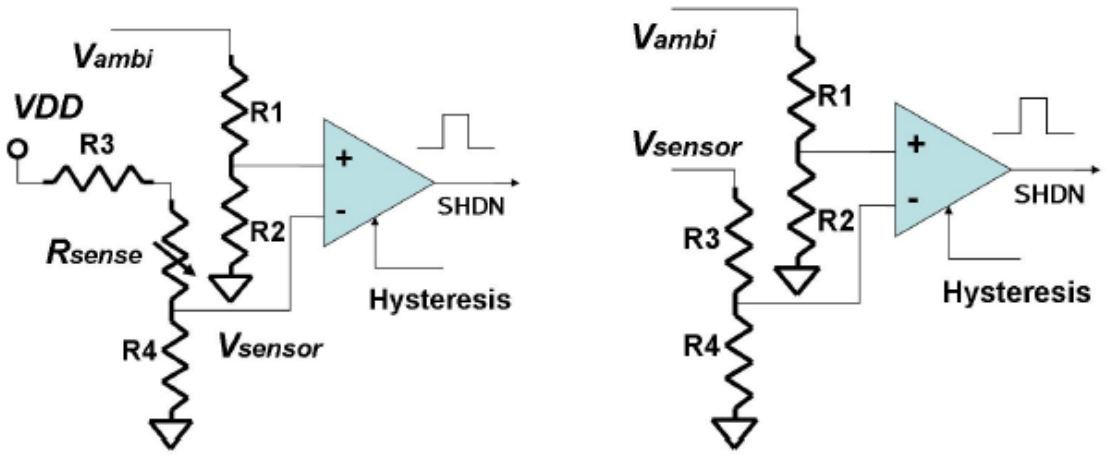

Figure 24. Left: comparator with resistive sensor. Right: comparator with voltage output sensor

Using a step-up voltage converter has the benefit that it can harvest from very low voltages and it protects from reverse current flow like a diode would in a more simple har-

vester that harvests only when the source voltage is higher than the desired voltage, but without the power loss caused by the voltage drop in the diode.

In the case of the LTC3105, the MPPT is integrated on the chip and there is a pin named MPPC. The LTC3105 keeps the source voltage the same as the voltage on the MPPC pin which constantly outputs 10 µA. This pin can thus be connected via a fixed resistor (R_{MPPC}) to ground in order to set the MPP to a fixed voltage (U_{MPPT}) according to equation 6.1.

$$U_{MPPT} = 10\ \mu A * R_{MPPC} \tag{6.1}$$

MPPT will not be performed if the MPPC pin is connected to ground. The datasheet of LTC3105 proposes to use a diode thermally coupled to the solar cell for MPPT, but this is unlikely to work well over the large temperature range of this application. It would also be difficult to make the thermal coupling. Instead, the small MPPT circuit in Figure 25 was designed for connecting to the MPPC pin to change the MPP voltage according to the illuminance at the solar cell. Figure 25 was drawn and simulated in the LTspice IV SPICE simulator. It represents a resistive sensor comparable Figure 24. The ideal current source I1 represents the MPPC pin and the ideal voltage source V1 represents the LDO pin on the LTC3105. The LDO (low dropout linear voltage regulator) is set to output 4.15 V. Unfortunately this is too high a voltage, since it can only reach that voltage when the supercapacitor is charged to at least that voltage and therefore this MPPT should be redesigned. The LDO can output a maximum of 6 mA. R1 is a light dependent resistor (LDR) and R2 is a variable resistor that can be used to tune the MPP. The LDR should be placed so that it receives the same illuminance as the solar cell.

The energy harvesting prototype to be designed does not have any voltage regulator that is constantly outputting a fixed voltage that could be used as V1 in Figure 25. A separate such regulator should not be added because it would consume too much energy compared to what could be won by the resulting increase in accuracy of the MPPT. The resistors in the voltage divider also waste a small amount of power. The values of the components in LTspice IV can quickly be changed to simulate different operating con-

ditions. Other circuits were also simulated for the same purpose, but it proved difficult to design a simple, low-power circuit for performing this MPPT.

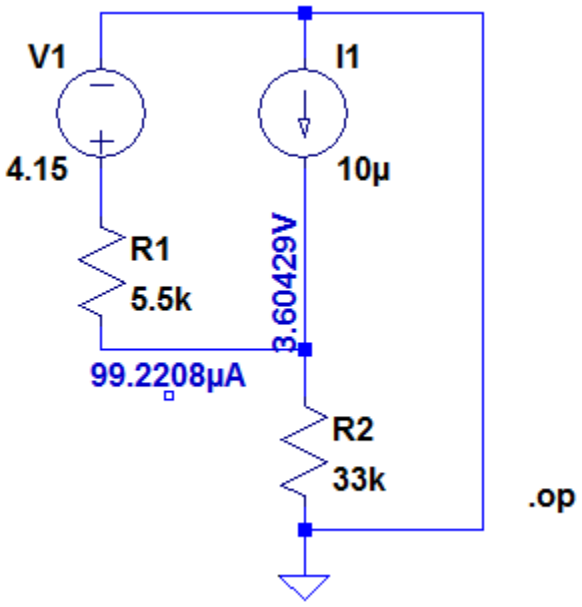

Figure 25. LTspice simulation of MPPT circuit for LTC3105

The maximum power point of the 0.45 W solar cell was measured by hand over a range of illuminance as shown in Figure 26. The illuminance was adjusted by placing the solar cell under an adjustable halogen lamp with a paper in between to disperse the light more evenly. The solar cell was connected to the LTC3105 energy harvester and the voltage on its MPPC pin was tuned by a voltage divider made of potentiometers until the MPP was found at each point. The voltage over the solar cell and its current output were measured using an oscilloscope as described in chapter 5. These were then multiplied by the oscilloscope so that the power could be directly viewed while tuning the load of the circuit manually. Figure 27 is an example of what could be seen in the oscilloscope. Blue is voltage, magenta is current and cyan is the product of the two, i.e. the power. The lower part is a zoom of the power in the upper right part.

The MPP voltage in Figure 26 is not very regular, possibly due to inexact illuminance, but also due to difficulty of tuning at low levels of illuminance where the measured cur-

rent was small and noisy. Filtering the measured millivolts using a capacitor at the output of the µCurrent helped only a little. It would be difficult to choose one fixed MPP only based on this plot. The average MPP voltage over the whole range is 3.58 V, but it would be better to use a higher voltage of approx. 3.9 V for an illuminance of more than 10 klx and a lower voltage of approx. 3.3 V for less illuminance. Using a LDR for MPPT could, based on this result, work in a small region, but not very well over the whole operating range of illuminance because the variation of the MPP voltage is so irregular. The irregularities can in part be explained by measurement error and bad set-up, but that notwithstanding it would still be very difficult to get a good response from a voltage divider with a LDR. The response for higher illuminance should also be tested. Unfortunately the illuminance meter jumped from 40 klx to 60 klx when it reached 40 klx. Further tests should be done with a more reliable illuminance meter. The power output at the MPP of the 0.45 W solar cell is quite linear over the whole measured range of illuminance. As a rule of thumb the power increases with 5 mW for every kilolux.

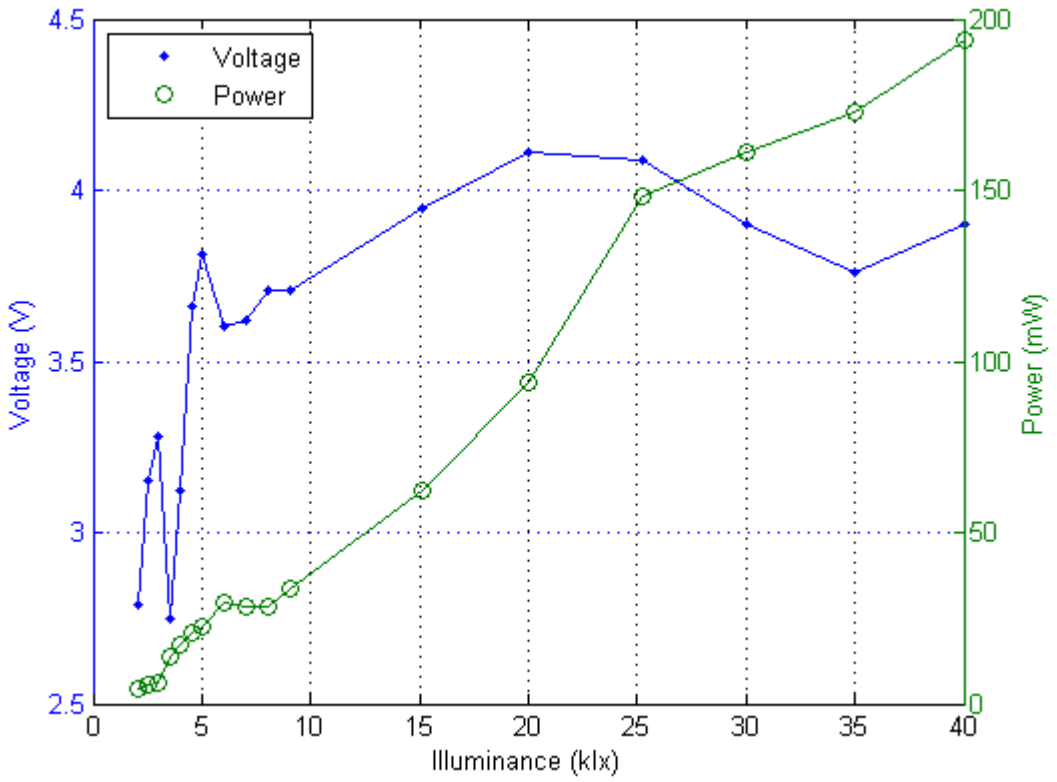

Figure 26. MPP voltage and power vs. illuminance of the 0.45 W solar cell

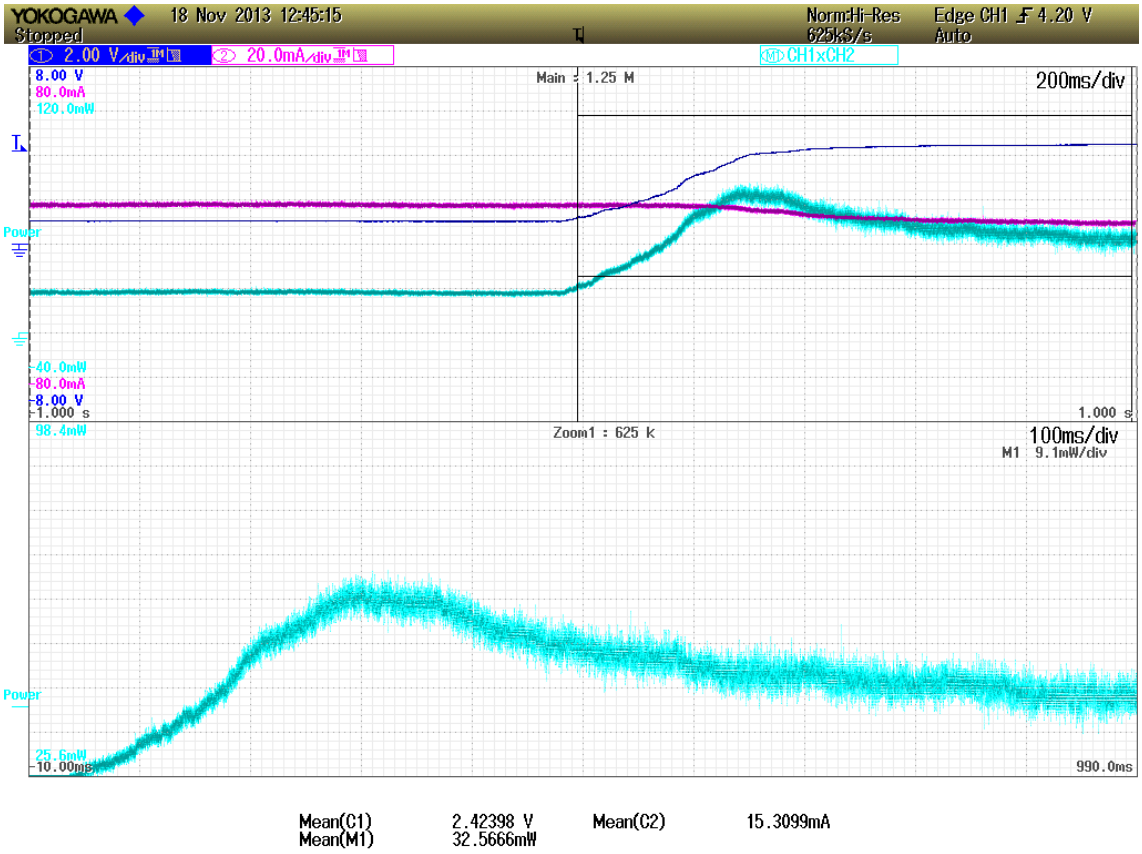

Figure 27. An example of the voltage (blue), current (magenta) and power (cyan) displayed by the oscilloscope while finding the MPPT

Maximum power point tracking could also be performed digitally by a low-power microcontroller, DSP or FPGA. It is easier to calculate the MPP digitally and take several factors into account, such as illuminance and temperature, but unless carefully designed not much power can be saved. A digital MPPT could be a good improvement to the design presented in this report. A microcontroller could calculate the desired MPP voltage, or use a lookup table to find it. MPPT could even be performed by the microcontroller on the WSN itself, but that would require the WSN to be very low-power and it would work only if the MPP needed to be changed at a low rate, allowing the WSN to sleep in between measurements and control. The UWASA Node is not suitable for this purpose due to its high quiescent currents and other power consumption.

The efficiency of the LTC3105 step-up converter depends on its input and output voltages and so MPPT should optimally not only be performed for the solar cell, but for the solar cell and step-up converter combined.

6.6. Energy Management and Storage

The energy management part of the circuit takes care of routing the power in an optimal way between components for maximum performance and lifetime and optimal schedule of operation. The energy management of the energy harvester prototype consists of supercapacitors, a Li-ion polymer battery, nanopower voltage comparators, a logical AND gate, two MOSFETSs and a few current limiters. These are described in detail in the next few chapters.

6.6.1. Batteries

A lithium-ion (Li-ion) 1-cell battery was chosen to power the UWASA Node. More specifically, a cobalt lithium-ion polymer battery was chosen because of the light weight and thin form factor. Lithium-ion batteries are common in portable consumer products because of their high energy density. Lithium-ion polymer batteries have a different structure for holding the electrolyte compared to normal lithium-ion batteries. This allows them to be packaged in laminated sheets instead of a rigid case and this reduces the weight by several percent. Compared to lead acid, NiCd and NiMH battery chemistries Li-ion batteries have longer cycle life, lower fast-charge time and higher peak load current. Li-ion also has a relatively small self-discharge rate of less than 10 %. The initial voltage drop if a Li-ion battery during self-discharge is high, but then the voltage drops very slowly over several months, see Figure 28, reproduced from Sony Corporation (2013). Figure 28 plots the potential discharge energy in percent of its initial value over time. Because of the power consumption of a possible protection circuitry, the battery may need charging once a year or so if stored. (Buchmann 2014a.)

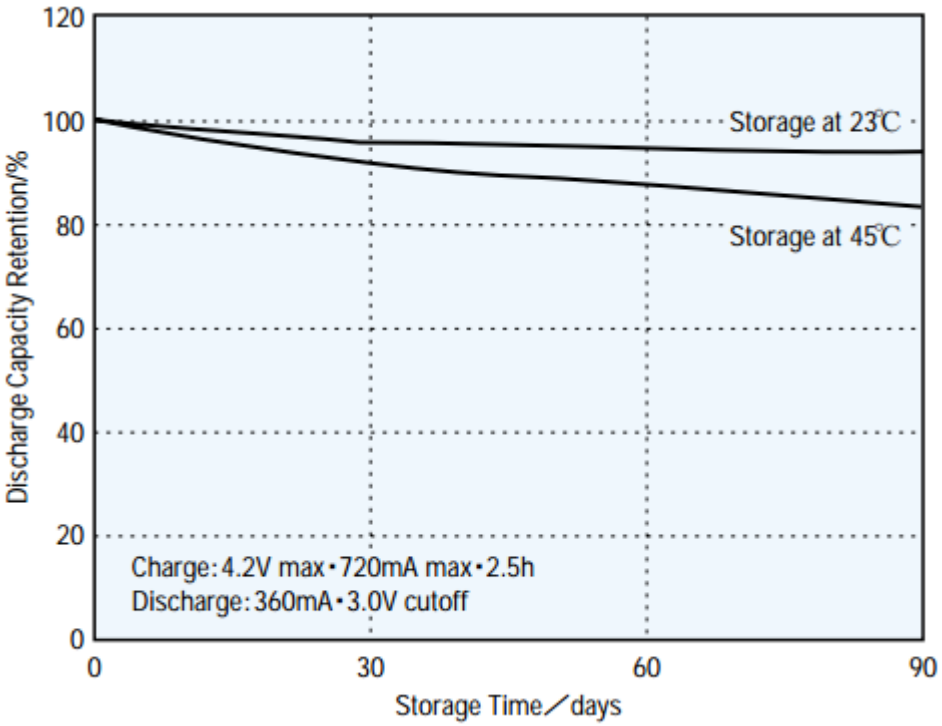

Figure 28. Discharge capacity retention of Li-ion batteries stored at different temperatures

All previously discussed battery chemistries can be used in temperatures down to -20º C, but NiCd, NiMH and Li-ion batteries can only be charged at temperatures above freezing. Unfortunately plating of metallic lithium can occur on the anode of a Li-ion battery when charging in temperatures below 0º C and this reduces the capacity and reliability of the battery. On the other hand, studies show that charging at low temperatures is possible if a very low charge current is used. For example at -30º C a Li-ion battery can be charged at 0.02C, i.e. 0.02 times the capacity in ampere-hours. For a 1000 mAh battery this would mean with a maximum charge current of 20 mA, which would charge the battery in 50 hours. Luckily energy harvesters often do charge batteries at such low currents since they are capable of supplying so little power. All things considered lithium-ion polymer is the most suitable chemistry for this project. (Buchmann 2014b.)

The chosen battery was manufactured by Unionfortune Electronic Co, Ltd, has the type number 063450 and capacity 1000 mAh and was bought from SparkFun Electronics. It

features a small protection circuit that according to Great Power Battery Co., Ltd (2012) protects it from over-charging above 4.28 V, over-discharging below 2.9 V and over-current above 4.5 A. It was confirmed by draining the battery that it locks out and allows no current to flow once it drops below 2.9 V. This protection circuit consumes some power, but it is very useful at least for initial trials where the battery can easily be damaged by unforeseen effects. The size of the battery is 50.8 x 33.5 x 5.9 mm and it weighs only 22 g. Similar models are available in different capacities and they can be connected in parallel (after balancing), but have to be charged individually.

Figure 29, reproduced from Sony Corporation (2013), shows how the discharge characteristics of a Li-ion battery are influenced by temperature when a battery is discharged at a constant current of 360 mA. A battery discharged at -20º C is able to output about half the energy it would output at room temperature. To test the battery described above in cold conditions, one such battery was placed charged to 3.86 V without a load in a freezer at a temperature of approximately -20º C. Another battery, charged to 3.84 V was kept at room temperature for reference. These unloaded batteries held their voltages equally well, with very little quiescent current, as shown in Figure 30. The voltage of both batteries dropped only 40 mV, which corresponds to 33 mAh, during 540 hours, or approx. 7 months. The quiescent current and current consumed by the protection circuit was thus approx. 6.55 µA in total. The multimeter with which the voltages were measured showed only two decimal digits. The measurements and MATLAB script used to produce Figure 30 can be found in appendix 11.

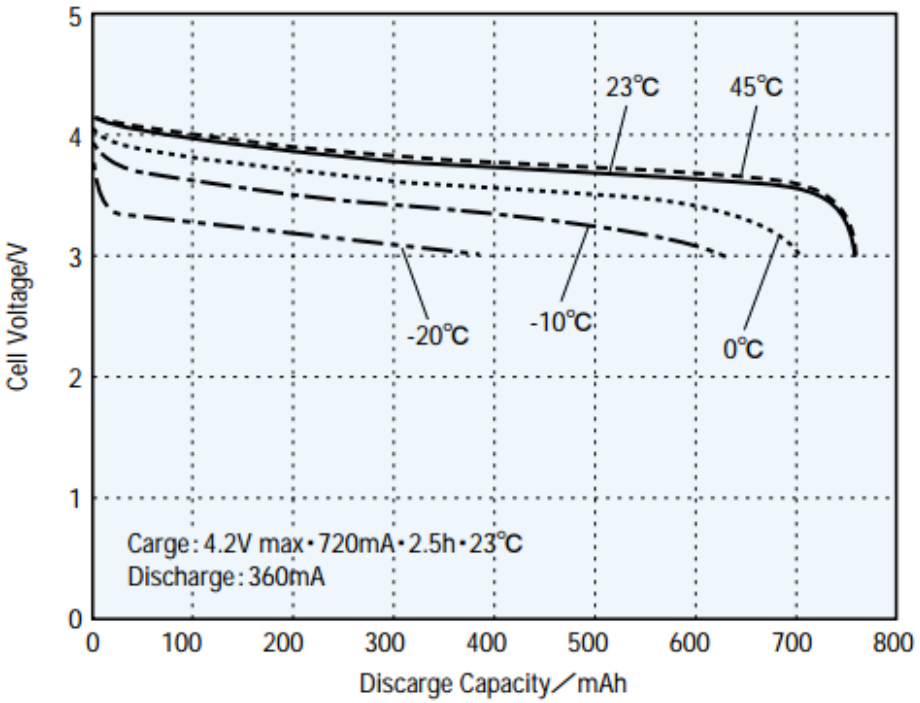

Figure 29. Battery voltage vs. discharged energy

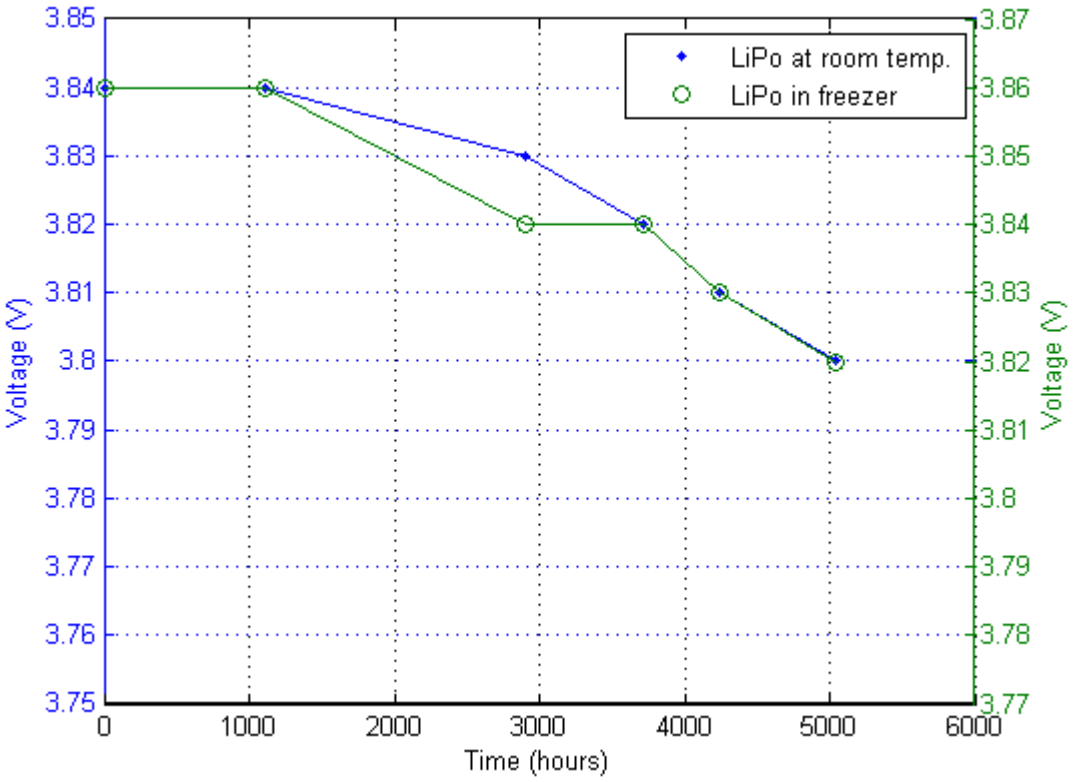

Figure 30. Long term voltage loss of batteries without a load at two different temperatures

Another battery was placed fully charged to 4.2 V in the freezer with a 30.3 Ω resistor as a load and an equal setup was placed in room temperature. The loaded battery at room temperature was discharged down to 2.9 V after approx. 8 hours and the loaded battery in the freezer was discharged down to 2.9 V in approx. the same time, as can be seen in Figure 31. The loaded battery at room temperature was able to keep its voltage higher during the discharge, but it was emptied in approx. the same time as the one in the freezer. This is due to the fact that battery in the freezer output a smaller power since its voltage was lower and its load resistance was constant. The oscillation of the voltage of the battery in the freezer was due to the varying temperature in the freezer. It can be seen that the temperature has a large effect on the voltage of a Li-ion battery. The initial voltage of the battery would have been lower, had it been cooled before the load was applied.

When the loaded battery that had been in the freezer was recharged at 1 A of initial current (the current drops after the constant current phase see chapter 6.6.2), it was charged with 937 mAh of energy over 104 minutes. The loaded battery that had been in room temperature was charged in the same way with 947 mAh over 106 minutes. Based on these values obtained by the charger, the difference in capacity is only about 1 %, but the voltage was probably not taken correctly into account. Calculating the energy based on the measurements plotted in Figure 31, gives a more exact value for the difference of 13 %. Equation 6.3 was used for calculating the energies in the MATLAB script in appendix 10 that also was used to plot Figure 31. The energy provided by each battery in joules is also shown in Figure 31. From this it can be concluded that the capacity decreases with temperature as Figure 29 indicates. The capacity increases when a cooled battery is returned to room temperature.

$$E = Pt = UIt = \frac{U^2 t}{R} \tag{6.3}$$

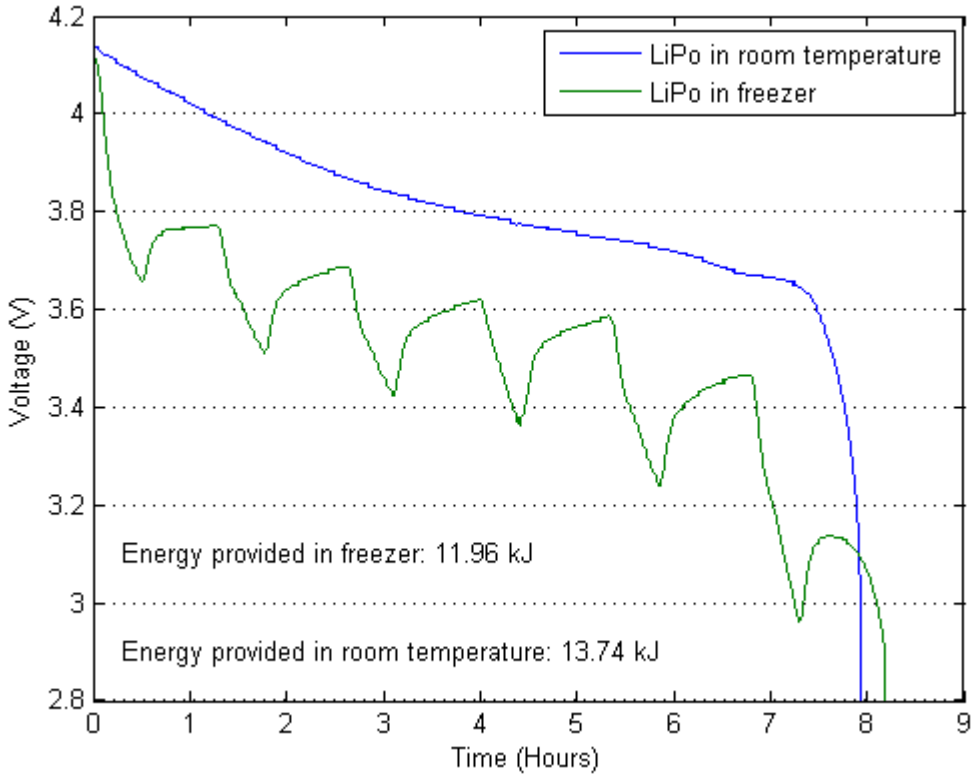

Figure 31. Voltage over time for two batteries discharged at different temperatures.

According to these measurements the battery can supply about 13 kJ, which could power the UWASA Node for approx. 4.5 h, assuming that 800 mW is consumed continuously. This should be more than enough considering that the UWASA Node will be active and consuming energy only intermittently and the energy harvester would take days to charge the battery with this amount of energy, as will be shown in the measurement results in chapter 7. For example the UWASA Node could be allowed to consume 5 kJ during 15 hours of low light conditions per day when no energy is harvested. If the power consumption would be 800 mW, there would be enough energy for the node to wake up and be active for 30 seconds 14 times per hour, as shown in equation 6.4. For many purposes a smaller battery would suffice.

$$\text{Energy consumed: } 0.8\ \text{W} * 30\ \text{s} * 14 * 15 = 5.04\ \text{kJ} \qquad (6.4)$$

6.6.2. Battery Chargers

Usually a Li-ion battery is charged in a special way in order to maximize its lifetime. If charged with too high a current or to too high a voltage, the battery will permanently lose some capacity or be damaged. Therefore Li-ion polymer batteries often come with a protection circuit such as the one found on the battery used in these tests, i.e. the 1000 mAh LiPo battery from SparkFun Electronics. A typical charging scheme can be seen in Figure 32 which is a plot of current and voltage over time, reproduced from Sony Corporation (2013). First the battery is charged with a constant current until the target voltage is almost reached. Then there is a constant voltage phase under which the battery is kept at a constant voltage until the current drops below a certain threshold, after which the battery is considered fully charged. After an hour or so the battery voltage drops a little due to high quiescent current close to the maximum voltage. Some chargers then apply a topping charge, but Li-ion batteries should not constantly be trickle charged as other chemistries can be. (Sony Corporation 2013.)

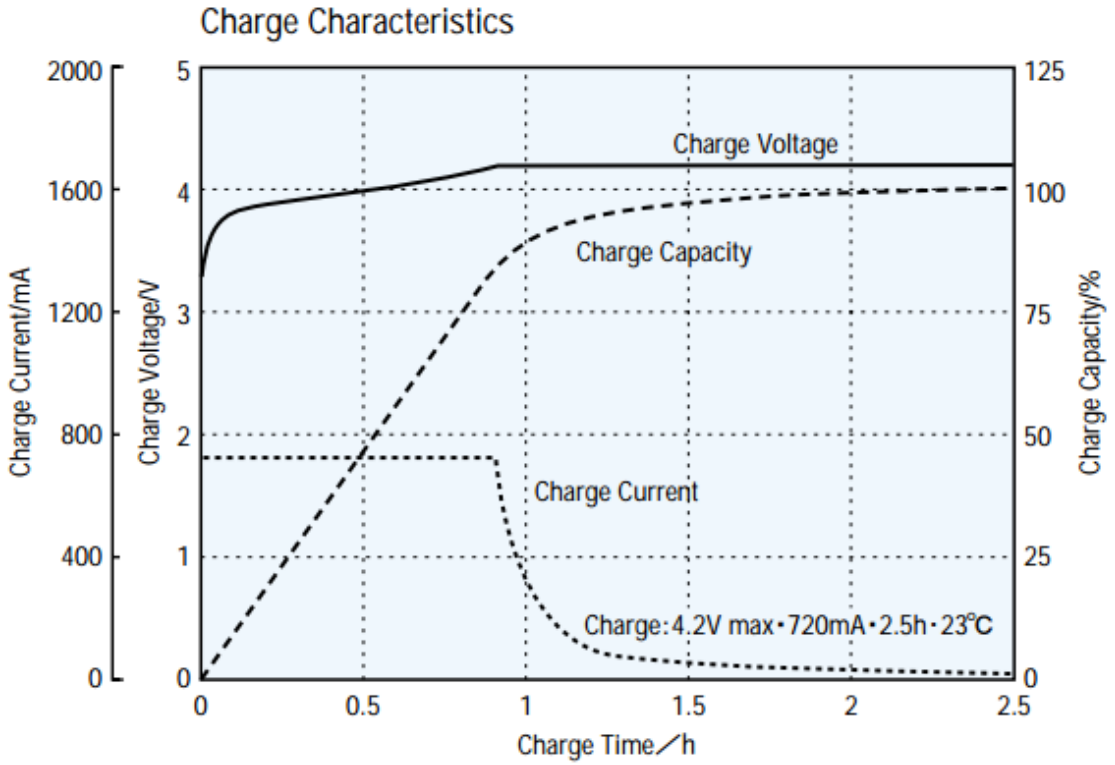

Figure 32. A typical Li-ion 1 cell battery charging curve

To mimic this charger behavior, the battery can simply be supplied with power via a current limiter. The current flowing from the supercapacitors to the battery will thus be constant and limited, and the current will drop when the battery reaches the maximum output voltage of the harvester which is the 4.2 V that the battery accepts maximally, thereby entering the constant voltage phase. The supercapacitor does not store enough energy to charge the battery completely, so it will charge the battery intermittently at the current set by the current limiter as the harvester charges the capacitor back to above the charging threshold.

The voltage thresholds at which power is transferred in the prototype between the supercapacitors, the battery and the WSN are governed by LTC1540 nanopower voltage comparators by Linear Technology. These comparators feature an ultralow quiescent current of 0.3 µA nominally and a voltage reference and a hysteresis, both adjustable by resistor voltage dividers. An example use of the LTC1540 as a low-battery detector can be seen in Figure 33.

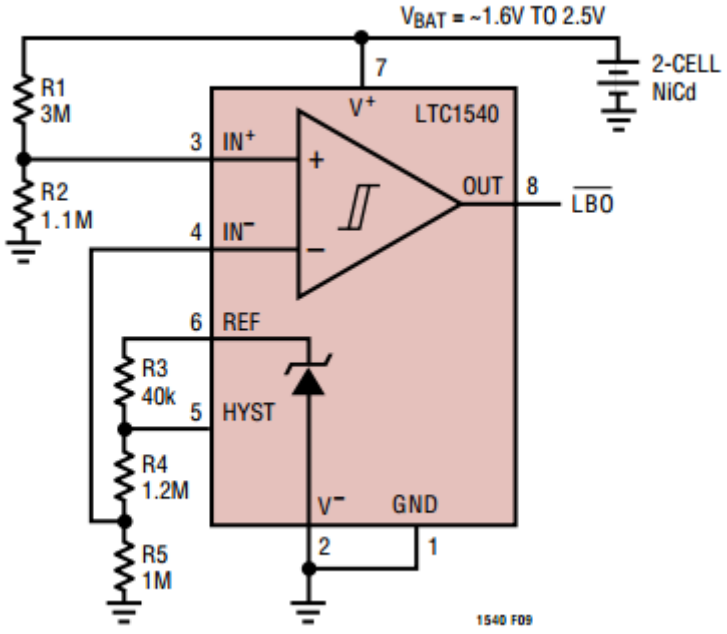

Figure 33. The LTC1540 configured for low-battery detection

In the prototype, one comparator is used for activating the current flow from the voltage rail (supercapacitor) to the battery when the rail voltage is more than 3.7 V. Another comparator is used in the UVLO described later and a pair of comparators is used for activating the current flow from the battery to the voltage rail. The pair checks that the voltage rail is below 3.4 V and that the battery voltage is above 3.4 V. The outputs of these are connected to a small AND gate IC that combines these signals. All comparators were configured for a hysteresis of approx. 100 mV. The operations of all comparators were simulated using LTspice models provided by the manufacturer to confirm the resistor sizing calculations. The AND gate was modeled as a diode-resistor AND gate because the NC7S08M5 IC was not included in LTspice IV. The pair of comparators and the AND gate were first tested on the small PCB shown in Figure 34.

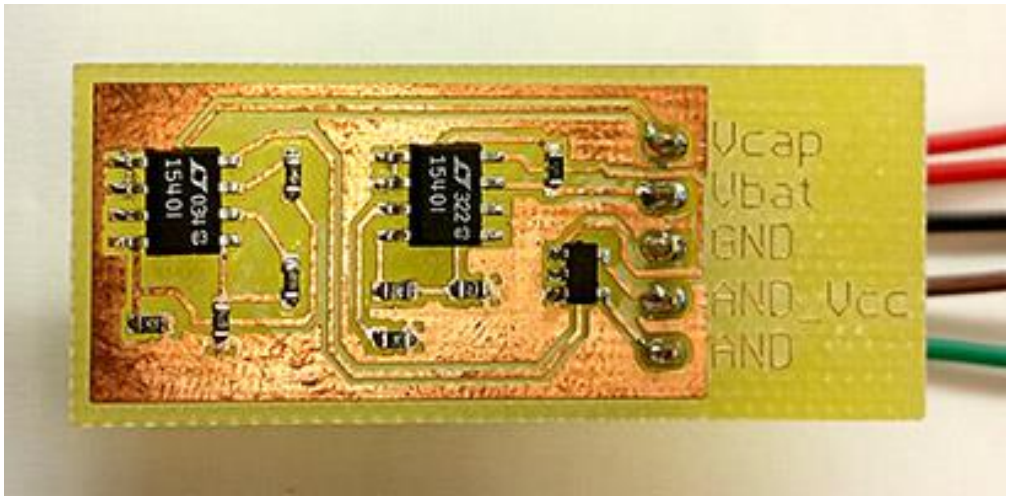

Figure 34. PCB for testing the pair of comparators with AND gate

The single comparator and the AND gate are connected to the enable pins of two separate current limiters that when enabled let current flow through them at a maximum current in one direction. If the enable pin is low, current cannot flow in either direction and if it is high current is limited in one direction and unlimited in the other direction. These current limiters were implemented using TPS2030D power distribution switches by Texas Instruments. They feature a maximum standby supply current of 10 µA and short-circuit and thermal protection. They allow 300 mA to pass through them when activated. When tested, the TPS2030D did not heat up when shorted from a 4.2 V battery to an

empty pair of 22 F supercapacitors. The supercapacitors were charged in under two minutes at 285 mA. In case the voltage of the battery is more than 3.7 V and the voltage of the capacitor is also more than 3.7 V, but less than that of the battery, which can happen only once when the system is installed, there will be backflow through the TPS2030D that is supposed to charge the battery. This is not a problem since it happens only for a few seconds, but can be avoided by charging both the battery and capacitor to 4.2 V initially.

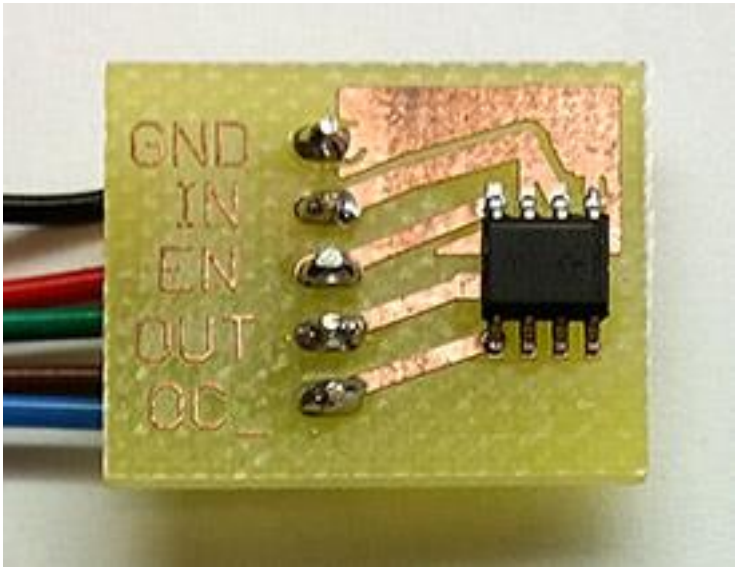

Figure 35. PCB for testing current limiting switch

See appendix 7 for a table of all possible states of the energy management system. The states are described by the voltage of the battery and supercapacitors, and by the paths of current flow (charging the battery, emptying the battery and supplying the node). Appendix 7 also contains example transition paths between the states.

6.6.3. Supercapacitors

Supercapacitors can act as a buffer and be used to store the first energy delivered by the energy harvester until there is enough to charge the battery or supply the WSN. The voltage of the supercapacitor can rise quickly to a voltage where the step-up (or step-down) converter operates the most efficiently because of its much lower capacity compared to a battery. Connecting the harvester directly to the battery would cause its volt-

age to rise very slowly and then energy would be harvested less efficiently because of the step-up inefficiency at lower voltages. Supercapacitors can also smooth out the wide dynamic range of energy harvesters and the WSN load, especially if more than one harvester subsystem is connected in parallel. Another advantage of using supercapacitors is that they can be used to preferentially supply the WSN before the battery is needed. This keeps the battery voltage more even and thus slows down battery aging. If more than one subsystem is used, their individual capacitors should be connected via diodes to the voltage rail. The single supercapacitor (a unit of two in series) of the prototype needs no diode and therefore saves energy that would be lost in the diode. Each subsystems' supercapacitor should be sized to suit the particular harvester so that it reaches a useful voltage. If the power output of a subsystem is low compared to the other subsystems, it should have a smaller supercapacitor. Otherwise this capacitor can never deliver any current because its voltage is always lower than that of the other capacitors. (Park & Chou 2006.)

Supercapacitors can be placed in parallel to increase the capacitance, or in series to increase the allowable voltage. For version 8 of the prototype presented in chapter 6.2 two 22 F, 2.3 V supercapacitors by Philips were used in series to allow them to hold a voltage of 4.2 V (4.6 V maximum). These are only 35 mm in length and 18 mm in diameter. Even so, their size might be a limiting factor in certain applications. When current is drawn from a supercapacitor, there is an instantaneous voltage drop U_{ESR} due to the equivalent series resistance (ESR of the supercapacitor). This voltage drop for a given load current I_{L} is calculated for the previously mentioned Philips supercapacitors in equation 6.5. The resistance R_{ESR} in equation 6.4 is double that of a single supercapacitor since two were used in series. When a battery is supplying the load in parallel with the supercapacitor the ESR and thus also the voltage drop is reduced. The result of equation 6.4 is theoretical but is useful to know because the voltage hystereses in energy management comparators should be larger than U_{ESR} in order to avoid that the load affects the operation of the power routing too much. This voltage drop is more critical in case the supercapacitor is used without a battery because a high load current can cause a high voltage drop. The ESR of the supercapacitor and the internal resistance of the battery could be taken into account for impedance matching with the load, but that was not

done in this project. The internal resistance of the battery causes a voltage drop similar to U_{ESR} when it supplies the load. (Mars 2009.)

$$U_{\mathrm{ESR}} = I_{\mathrm{L}} R_{\mathrm{ESR}} = 200\ \mathrm{mA} * 200\ \mathrm{m\Omega} = 40\ \mathrm{mV} \tag{6.4}$$

It is difficult to specify how large the leakage current of a supercapacitor is. It depends on the capacitance of the supercapacitor, on the voltage and temperature of the supercapacitor and on how long the supercapacitor has been kept at a constant voltage. The leakage current is lower the lower the voltage is. Because of this it is preferable to have a supercapacitor that is rated for a little higher a voltage than the maximum voltage that will be applied to it. According to W. Wang, N. Wang, Vinco, Siddique, Hayes, O'Flynn & O'Mathuna (2013) the leakage current can be reduced by as much as 50 % by keeping the supercapacitor at 85 % of its maximum voltage rating instead of at 100 %. The previously mentioned 22F Philips supercapacitors have a maximum voltage of 2.3 V. With two such in series the maximum voltage becomes 4.6 V, which is 0.4 V higher than what they will be subjected to. The 4.2 V maximum voltage equals about 91 % of the maximum supercapacitor current rating. In version 9.1 of the prototype described in chapter 6.2 the supercapacitors were exchanged for ones with a maximum voltage rating of 2.5 V each, making the corresponding maximum operating voltage percentage 84 %. (Mars 2009.)

As supercapacitors age over time their capacitance is reduced and ESR increased. The rate of ageing approximately doubles for every 10° C increase in temperature. This effect should be taken into account when designing an energy harvester that needs to have a long lifetime so that the capacitance is still sufficiently high and ESR sufficiently low at the end of the expected lifetime. (Mars 2009.)

If two or more supercapacitors are connected in series and their summed voltage is close to the summed maximum voltage, there is the risk of overvoltage on one of the supercapacitors if they become unbalanced due to slightly differing characteristics. Active capacitor balancing can be applied using an ultra-low current rail-rail operational amplifier to avoid overvoltage. This was not deemed necessary for the prototype devised in this

project, as there is room for error, since the maximum voltage of the supercapacitor is much larger than what the circuit will experience. (Mars 2009.)

According to Mars (2009) equation 6.5 gives an approximation for the necessary capacitance C of the supercapacitor assuming there is a constant load current I_L and that the supercapacitor needs to be able to supply I_L for time t. The load voltage is allowed to decrease from U_{max} to U_{min}. Equation 6.5 shows that an approx. 12 F supercapacitor is necessary to supply 250 mA for 60 seconds with the voltage limits of the developed prototype presented in chapter 6.2. In the actual case the current would vary much over time, but this equation gives a good indication how large a capacitor is needed.

$$C = \frac{I_L t}{U_{max} - U_{min} - I_L R_{ESR}} = \frac{250 * 10^{-3}\ \text{A} * 60\ \text{s}}{4.2\ \text{V} - 2.9\ \text{V} - 250 * 10^{-3}\ \text{A} * 200^{-3}\ \Omega} = 12\ \text{F} \qquad (6.5)$$

6.6.4. Undervoltage Lock-Out Circuit

The undervoltage lock-out circuit depicted in Figure 36 was designed to cut off the power from the WSN when the voltage rail is below 2.9 V. There is a 20 MΩ feedback resistor (2x10 MΩ) that creates an extra high hysteresis of 350 mV to allow the WSN enough energy to wake up and measure the voltage without letting the turn-on current surge and any startup tasks drain the voltage rail to below the UVLO threshold again. The switching is done using a 2N7002 small signal N-channel MOSFET and an IRLML6401 (or IRFD9024 in older versions) P-channel power MOSFET.

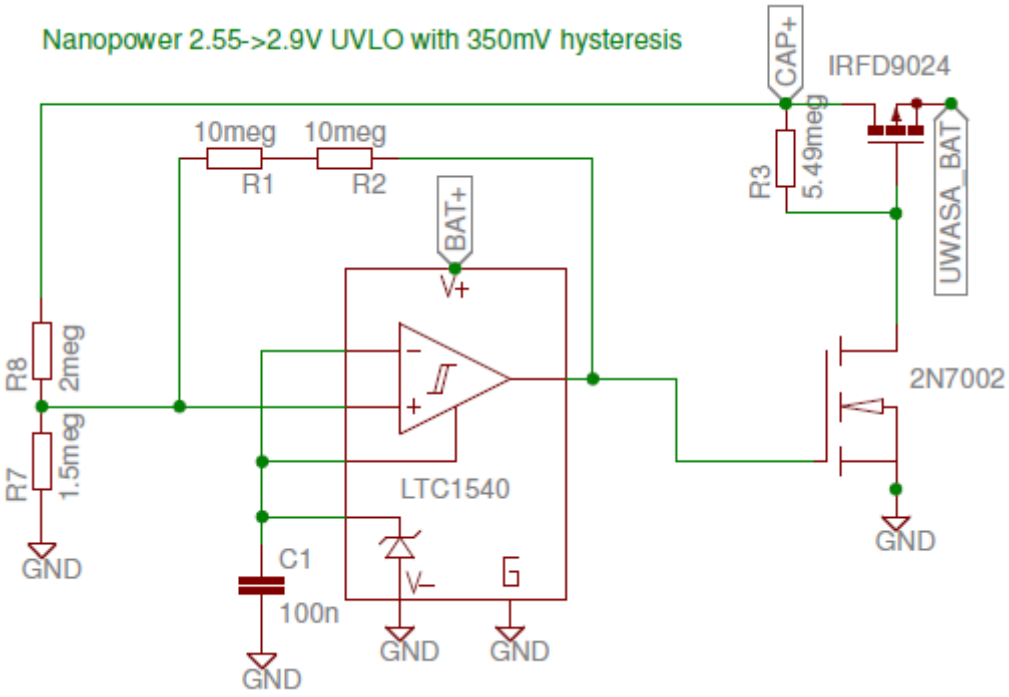

Figure 36. The UVLO circuit schematic

The UVLO circuit was first tested as a separate PCB shown in Figure 37. It was simulated using LTspice IV before manufacturing to ensure the resistors were correctly chosen. There was a complete simulation block for the LTC1540 included with the software. The measured hysteresis was close to the nominal one of 350 mV. The resistors have extra high resistance in order to minimize the power they waste. The voltage limits worked well and the quiescent current was just a few microamperes. The comparator triggered when rising above 2.87 V and falling below 2.53 V, which corresponds to a hysteresis of 340 mV.

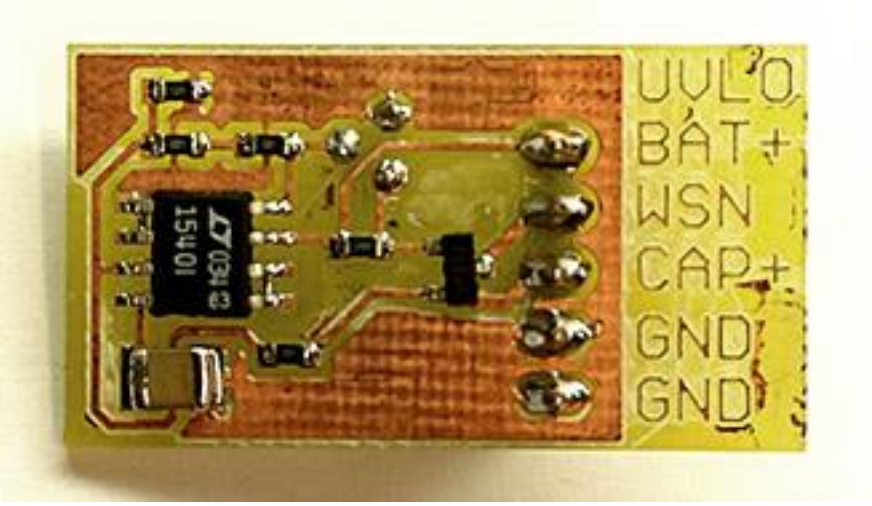

Figure 37. PCB for testing the UVLO circuit

6.6.5. Real-Time Clock Switch

On the UWASA Node there is a real-time clock (RTC) integrated into the main controller and it can be used to set the main controller to sleep mode. This would save much energy, but there are many parts on the power module that would still consume power. The alarm pin of the main controller RTC could be connected to an external switch for switching off the power to everything except the RTC itself, but the alarm pin is not broken out on any PCB designed for the UWASA Node. The alarm pin can be found on one of the stackable headers. Instead of using this RTC, a separate RTC was placed on the energy harvester and power management PCB prototype developed in this project (versions 9.0 and 9.1). Having the RTC on the energy harvester PCB has the added benefit of allowing the board to be used not only by the UWASA Node, but by any WSN.

The RTC has an alarm output that can be set to trigger at the point in time when the WSN should be powered on. The RTC consumes only a few microamperes of current. The alarm output is connected to a latch IC that turns on or off the current flow through two MOSFETs that supply the WSN with power. The WSN can request the RTC to activate the latch at a specific time in the future, turning the power supply on at that time, and then use the reset line of the latch to shut itself down. The RTC switch circuit can be found in appendix 1.8.

7. PERFORMANCE OF THE PROTOTYPE

All working versions of the energy harvester prototype were tested and measured under laboratory conditions. The voltages at which the energy management circuit switches the current flows were measured by connecting supercapacitors to both the supercapacitor net and the battery net of the PCB. The supercapacitor should begin charging the battery when the supercapacitor exceeds 3.7 V nominally, with a small hysteresis. The measured voltage at which this happened was 3.65 V with a hysteresis of 80 mV. The battery should charge the supercapacitor when the battery voltage is larger than 3.4 V and the supercapacitor voltage is smaller than 3.4 V. Measurements showed that the battery began charging the supercapacitor already when the battery reached 3.3 V (normally the supercapacitor is charged before the battery). When the supercapacitor voltage reached 3.39 V the charging stopped (when the battery voltage was higher than that). The UVLO should cut off the power to the sensor node when the voltage rail falls below 2.9 V nominally. Without a load the UVLO cut off the supply when the voltage rail fell below 2.63 V and turned it back on when it rose above 2.87 V, exhibiting a 240 mV hysteresis.

When testing the performance of the energy harvester measurements were conducted indoors using a 20 W adjustable halogen light bulb as the light source with paper for dispersing the light more evenly across the solar cell. The illuminance was measured using a handheld lux meter. The lowest level of illuminance at which the LTC3105 was able to harvest was a few hundred lux, depending on the voltage of the supercapacitor. Once the illuminance dropped so much that the LTC3105 stopped harvesting, the illuminance had to increase to much higher than it had previously been when harvesting, before the step-up converter of the LTC3105 turned back on. This large hysteresis should not be a problem, unless the illuminance is very low and varies much.

Version 8 of the energy harvester prototype was tested in a long term test that lasted six days in March 2014 on a roof where the solar cell was not shadowed by anything at any time of the day. There was no load connected to the prototype. The Arduino data logger described in chapter 5 was connected to the prototype and used for measuring time, il-

luminance and the voltages of the supercapacitor, battery, solar cell and MPPC pin of the LTC3105. During the test the temperature was a few degrees below freezing and there was occasionally light snowfall, but the snow was manually removed from the solar cell every morning if the wind had not blown it away. Power for the Arduino data logger was supplied by an external AC adapter. All electronics except the solar panel were kept in a plastic bag to protect against moisture.

Figure 38 shows how the prototype performed over six days. A larger print of this plot can be found in appendix 12.3. The energy harvester was active for 9.0 hours per day on average (the sunny hours) and harvested at 35.6 mW on average from the 92 x 61 mm solar cell. On average 1.16 kJ was harvested per day, or 2.14 J per minute active. In 6 days 6.9 kJ, or 51% of the 1000 mAh, 3.7 V LiPo battery capacity was harvested. Once the battery was fully charged the voltage rail reached the set point of the energy harvesting circuit and the solar cell was automatically disconnected, causing a voltage of more than 5 V over the solar cell. There is clipping at the end of the solar cell voltage data because it was higher than the reference voltage.

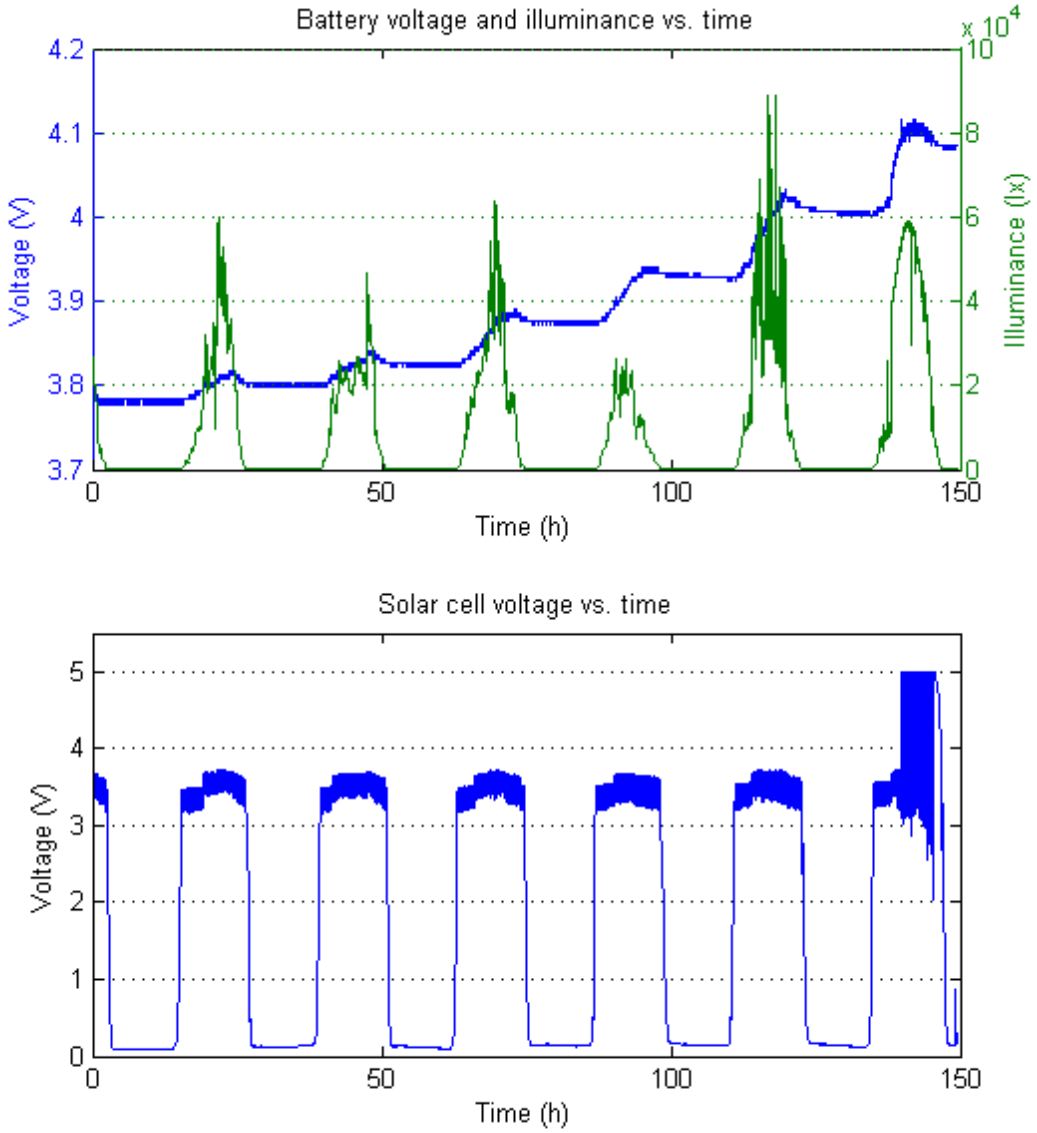

Figure 38. Performance of the prototype over six days in March 2014

Since the current was not measured in this experiment, the energy had to be estimated instead. All the previously mentioned values for power and energy were calculated assuming that the total capacity of the battery was 13.74 kJ as described in chapter 6.6.1 and shown in Figure 31 where the battery was discharged at room temperature. The analyzeLog1.m MATLAB script that was used to plot Figure 38 can be found in appendix 12.1. This script uses the energyBetweenVoltages.m MATLAB function found in appendix 12.2 for calculating the harvested energy. The battery draining data from the ex-

periment at room temperature was used for estimating the energy required to charge the battery from one voltage to another. The voltages at the beginning and end of each day in the data are input into the MATLAB function. The function calculates the approximate energy harvested between two voltages by utilizing one regression for converting voltage into seconds and another regression for converting seconds into power. The regressions were calculated using the MATLAB curve fitting tool box. The function then integrates this power over the corresponding time interval and the integral is the energy that it returns. The returned value is the energy that the battery needs to be charged with to reach the higher voltage from the lower voltage, or vice versa (discharged).

The energy harvester prototype was also tested with two solar cells in parallel and the power output doubled as can be seen in Figure 39. For a larger cell area it might be more efficient to use a cell rated at a higher voltage and a step-down converter. Figure 39 was made using a script very similar to the one in appendix 12.1. The fact that the energy harvester was activated at 80 hours, but not much the day before, was probably caused by the supercapacitor draining over time due to leakage current.

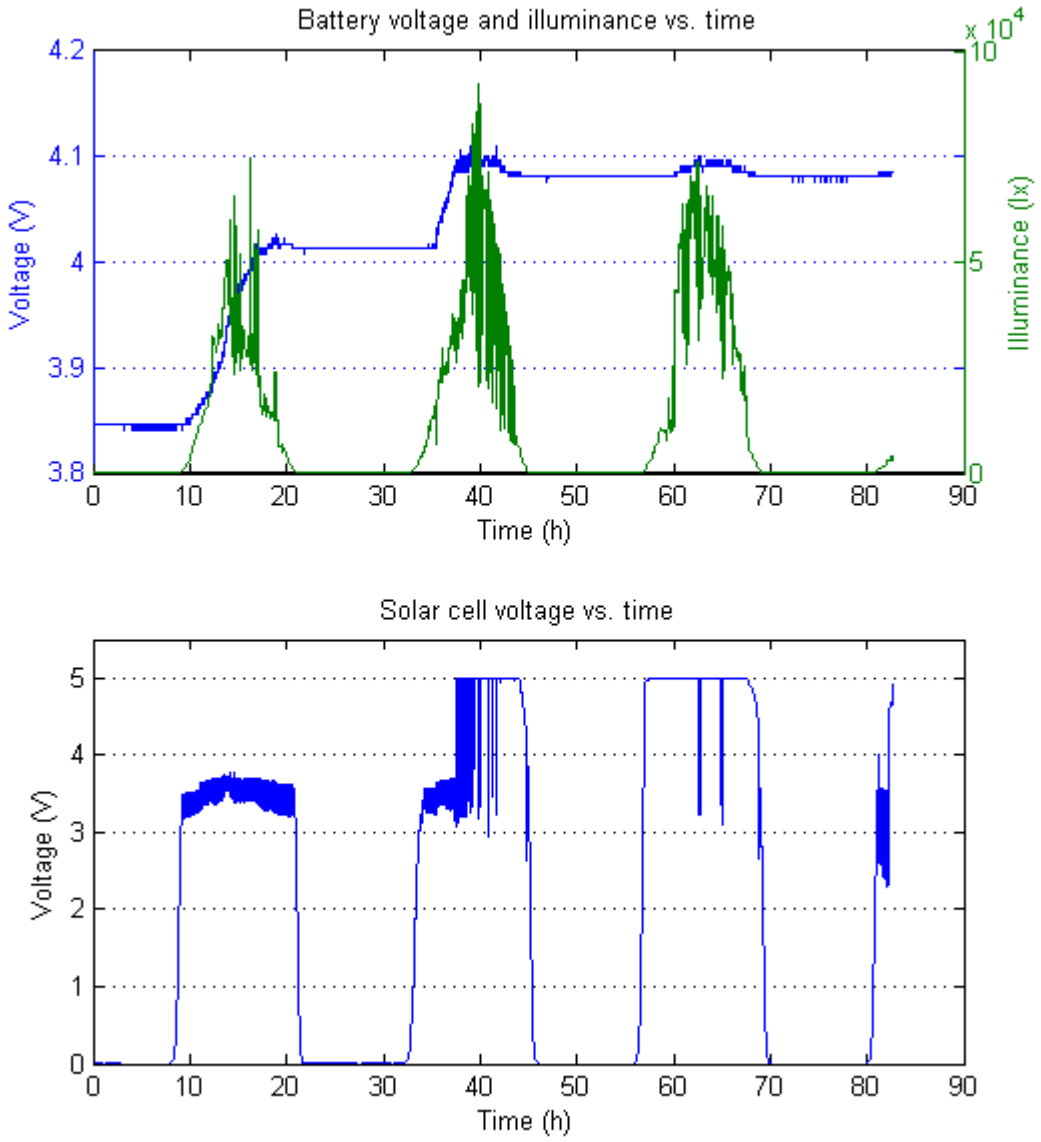

Figure 39. Performance of the prototype over three days with two solar cells

For most applications one solar cell of the type tested should be enough and the 1000 mAh battery capacity is good to have to ensure the WSN can operate during days of low illuminance. Overall the solar cell, battery and energy harvester of the prototype were well dimensioned, but for very specific installations and uses the sizes of these parts could be further optimized.

8. WIND POWER STATION APPLICATIONS

A goal of the project that this thesis was written for was to prove the wireless measurement and monitoring capabilities of the UWASA Node. The node could conceivably be attached to a wind turbine blade and be used there for measuring primarily vibration. The vibration data could be used to analyze the efficiency of the blade under different circumstances and to monitor the forces on and the structural health of the blade. The effect of the pitch of the blade and how the blade behaves when passing the tower could be measured.

The UWASA Node could also be attached to other parts of a wind turbine, such as the stays of the tower if it has such. The vibrations and elongations of the stays could be monitored using an accelerometer and a strain gauge to make sure the stays are suitably tautened and working as they should.

The environmental conditions a wireless sensor node would be subjected to on a wind turbine are harsh. The node has to operate in rain and in freezing temperatures. Therefore also all parts of the energy harvester need to be specified to work down to at least -20°C and be sealed and protected from humidity. The WSN and harvester would also be subjected to large accelerations and vibrations and should therefore be mechanically durable.

Changing or servicing a WSN on a wind turbine is expensive, since a lift is required and the turbine has to be stopped. Therefore the lifetime of the WSN application needs to be as long as possible and the WSN and energy harvester need to be tested to make sure they are robust before they are installed.

Unfortunately there was not enough time to install the UWASA Node with an energy harvester on a wind turbine before the RIWA project ended. Some preparations were made and software was written for the UWASA Node, but there was only time to finish and test the hardware, not the software. The software and field test may be completed in the future.

The UWASA Node is unnecessarily large for installation on a wind turbine blade, where weight and size are of importance. Because the UWASA Node needs its power module and the generic slave module for most tasks, it has to be stacked to a height of three modules, which is about 3 cm high. This is more than the height of the energy harvester with supercapacitors and battery. The supercapacitors can also be replaced with flat types if height needs to be minimized. Also using several capacitors in parallel the overall dimensions of the energy harvester could be reduced.

9. CONCLUSIONS AND FUTURE WORK

The goal of this project was to build and test an energy harvester and power management prototype for the UWASA Node, primarily for wind turbine monitoring applications. The prototype was developed in several iterations and each of its functions was tested and reported in detail. The prototype works as expected and is able to harvest at a high power output compared to what the energy harvesting industry is focusing on.

Energy harvesting was only tested using a common solar cell, but the prototype was designed with modularity in mind so that more energy harvesting sources could easily be added. Every part of the energy harvester and power management were optimized to operate at voltages optimal for the UWASA Node with power module. In the future a new power module could be designed to include the energy harvesting and power management components and leave out components that are superfluous when using an energy harvester.

Illuminance conditions in an installation are difficult to predict and should be measured to evaluate the amount of energy that can be harvested. Based on that information the WSN can be programmed to consume energy at an optimal schedule in a laboratory environment before being deployed.

The implementation of piezoelectric energy harvesting and microscale wind energy harvesting were left for future research. In order to get any useful energy out of a vibration energy harvester (in terms of what the UWASA Node consumes), the available vibrations first need to be measured so that the harvester can be tuned to work at the resonant frequencies of the vibrating element that it is to be installed onto.

Microscale wind energy harvesting would be feasible in fixed installations where a large amount of energy is necessary. This could be used in parallel with the solar energy harvester to even out the fluctuations in the available sunlight and wind. It would be difficult to design a microscale wind turbine that does not jam when subjected to snow and icing.

The UWASA Node consumes more power than usual WSN designed specifically for energy harvesting do. It could still easily be powered by a slightly larger energy harvester such as the 2.5 W solar cell discussed in this report, or a miniature wind turbine. These would be easy to use in stationary installations. The requirement for small size has to be weighed against the duty cycle of the operation of the WSN. Overall, it is confirmed that the UWASA Node can be powered by energy harvesting, and the prototype can now be used for further trials and research.

Energy harvesting continues to receive a lot of attention and there were many research results published in 2013 and 2014. Some methods such as photovoltaic energy harvesting are already widely deployed in custom wireless sensor networks and other electronics. The newest microcontrollers made for being powered by energy harvesting require much less energy than their predecessors. These can be used with much smaller energy harvesting devices, or with less common methods that output less energy but have other benefits.

Powering the UWASA Node by energy harvesting is a good idea, as it makes the node self-sufficient and allows it to operate in places where servicing would be prohibitively expensive or impossible. Using energy harvesters, WSNs can potentially operate independently for several years, provided that the rest of the platform is robust enough. An example wind power station application is monitoring vibrations on the turbine blades intermittently to see how they vary with varying weather conditions and mechanical wear.

An energy harvester similar to the AmbiMax of Park & Chou (2006) was constructed. The prototype has been tested in laboratory conditions and outdoors and its performance has been proven. The next step would be to do field tests and optimize the software running on the UWASA Node. The developed prototype could also be used with other WSNs, but many things need to be optimized for a specific solution as described in Chapter 4.

REFERENCES

Azevedo, J.A.R. & F.E.S Santos (2012). *Energy harvesting from wind and water for autonomous wireless sensor nodes* [online]. University of Madeira [cited 25.2.2013]. Available from the World Wide Web: <URL: http://ccm.uma.pt/publications/2012/Azevedo2012a.pdf>.

Buchmann, Isidor (2014a). *Comparison Table of Secondary Batteries* [online]. Battery University [cited 24.8.2014]. Available from the World Wide Web: <URL: http://batteryuniversity.com/learn/article/secondary_batteries>.

Buchmann, Isidor (2014b). *Charging at High and Low Temperatures* [online]. Battery University [cited 24.8.2014]. Available from the World Wide Web: <URL: http://batteryuniversity.com/learn/article/charging_at_high_and_low_temperatures>.

Çuhac, Caner (2012). UWASA Node Reference Manual 3.0.0. Aalto University & University of Vaasa, ComSys group [cited 1.10.2013]. Unpublished, internal document.

Gilbert, James M. & Farooq Balouchi (2008). Comparison of Energy Harvesting Systems for Wireless Sensor Networks. *International Journal of Automation and Computing* [online]. University of Hull [cited 5.2.2013]. Available from the World Wide Web: <URL: http://web.eecs.umich.edu/~prabal/teaching/eecs598-w10/readings/GB08.pdf>.

Great Power Battery Co., Ltd (2012). *Battery Protection* [online]. Great Power Battery Co., Ltd, [cited 24.8.2014]. Available from the World Wide Web: <URL: http://dlnmh9ip6v2uc.cloudfront.net/datasheets/Prototyping/BatteryProtection.pdf>.

Harrop, Peter (2009). *An Introduction to Energy Harvesting* [online]. IDTechEx Ltd, [cited 28.1.2013]. Available from the World Wide Web: <URL: http://www.energyharvestingjournal.com/new-to-energy-harvesting.asp>.

Höglund, Thomas (2014). Energy Harvesting for the UWASA Wireless Sensor Node: Applications for Wind Turbine Monitoring. University of Vaasa.

Jones, David L. (2010). *The µCurrent: A professional precision current adapter for Multimeters* [online]. EEVBlog [cited 19.8.2014]. Available from the World Wide Web: <URL: http://www.eevblog.com/files/uCurrentArticle.pdf>.

Mars, Pierre (2009). *Using a supercapacitor to manage your power* [online]. IDTechEx Ltd, [cited 24.8.2014]. Available from the World Wide Web: <URL: http://www.energyharvestingjournal.com/articles/using-a-supercapacitor-to-manage-your-power-00001921.asp>.

Park, Chulsung & Pai H. Chou (2006). *AmbiMax: Autonomous Energy Harvesting Platform for Multi-Supply Wireless Sensor Nodes* [online]. IEEE [cited 18.3.2013].

Pololu Robotics & Electronics (2014). *Pololu Adjustable Step-Up/Step-Down Voltage Regulator S7V8A* [online]. Pololu Robotics & Electronics, [cited 5.3.2014]. Available from the World Wide Web: <URL: http://www.pololu.com/product/2118>.

Sony Corporation (2013). *Lithium Ion Rechargeable Batteries Technical Handbook* [online]. [cited 28.1.2014]. Available from the World Wide Web: <URL: http://www.sony.com.cn/products/ed/battery/download.pdf>

Tan, Yen Kheng, Sanjib Kumar Panda (2011). *Self-Autonomous Wireless Sensor Nodes With Wind Energy Harvesting for Remote Sensing of Wind-Driven Wildfire Spread* [online]. IEEE, [cited 27.2.2013].

Toh, Tzern Tzuin (2011). *A Gravitational Torque Energy Harvesting System for Rotational Motion* [online]. Imperial College London [cited 5.3.2013]. Available from the World Wide Web: <URL: https://workspace.imperial.ac.uk/opticalandsemidev/Public/Publications/2011_Toh_PhDThesis_GravitationalTorqueEnergyHarvester.pdf>.

Wang, Wensi, Ningning Wang, Alessandro Vinco, Rashid Siddique, Mike Hayes, Brendan O'Flynn, Cian O'Mathuna (2013). *Super-capacitor and Thin Film Battery Hybrid Energy Storage for Energy Harvesting Applications* [online]. IOP Publishing, Journal of Physics: Conference Series 476 (2013) 012105, [cited 24.8.2014]. Available from the World Wide Web: <URL: http://iopscience.iop.org/1742-6596/476/1/012105/pdf/1742-6596_476_1_012105.pdf/>.

APPENDICES

Appendices 1.1-1.8 show the electrical schematic of the energy harvester and power management PCB prototype version 9.1.

Appendix 1.1: The parent sheet with terminals, supercapacitors, I^2C pull-up resistors and all other sheets

Appendix 1.2: The UVLO sheet with comparator and MOSFETs

Appendix 1.3: The DoubleComparator sheet with comparator pair, AND gate and current limiter for supplying the voltage rail from the battery

Appendix 1.4: The SolarHarvester sheet with the LTC3105

Appendix 1.5: The ChargerCAP_BAT sheet with comparator and current limiter for charging the battery from the voltage rail

Appendix 1.6: The SHT11 sheet with the temperature and humidity sensor and zero-ohm links for disconnecting the sensor to save power

Appendix 1.7: The V_SENS sheet with voltage dividers for measuring the battery and capacitor voltages with a reference voltage of 3.3 V

Appendix 1.8: The RTC_Switch sheet with RTC, latch and MOSFETs

Appendix 2: PCB layout of the energy harvester and power management prototype version 9.1

Appendix 3: Photographs of the top and bottom sides of the energy harvester prototype version 9.1

Appendix 4: Electrical schematic of the energy harvester and power management PCB prototype version 8

Appendix 5: PCB layout of the energy harvester and power management prototype version 8

Appendix 6: Photographs of the top and bottom sides of the energy harvester prototype version 8

Appendix 7: The states and operating modes of the power management system

Appendix 8: Arduino program for data logging

Appendix 9: MATLAB script for the resistance vs. illuminance regression plot

Appendix 10: MATLAB script for battery discharge plot (Figure 29) and energy calculation

Appendix 11: MATLAB script for 7 month LiPo voltage plot

Appendix 12.1: MATLAB script for the 6-day prototype test

Appendix 12.2: MATLAB function for calculating energy between two voltages of the battery

Appendix 12.3: Plots of the 6-day prototype test

Appendix 1.1.

Version 9.1
4.8.2014

To-do:

- The v9.0 can probably not be used with the latch because of latch power supply.
- The R34 1M pulldown on LATCH may not be necessary.
  R34 can be turned and connected to BAT+ instead if necessary.

Notes

- I2C can be pulled up externally if 3.3V is left disconnected

I2C pullup

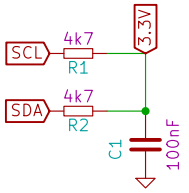

Super capacitors

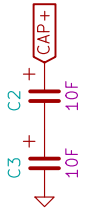

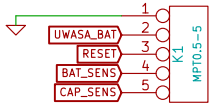

5-pole terminal:
GND (UWASA Node)
UWASA_BAT
RESET
BAT_SENS
CAP_SENS

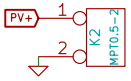

2-pole terminal:
PV+
GND (PV)

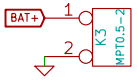

2-pole terminal:
BAT+
GND (battery)

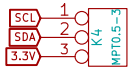

3-pole terminal:
SCL
SDA
3.3V (for I2C pullups)

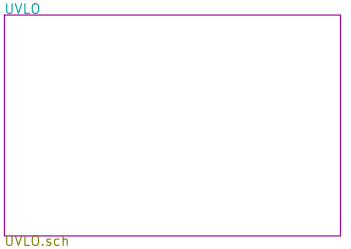

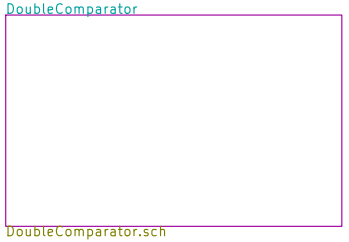

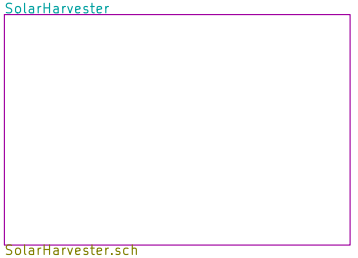

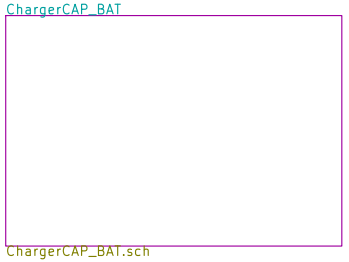

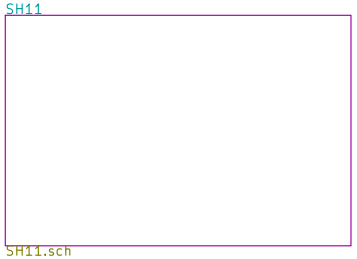

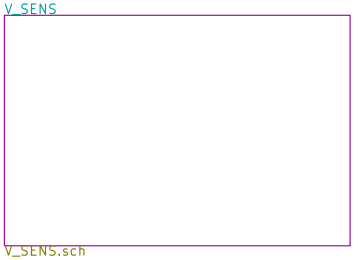

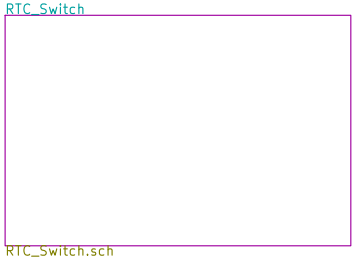

File: EHv9.sch		
Sheet: /		
Title:		
Size: A4	Date: 5 sep 2014	Rev:
KiCad E.D.A.		Id: 1/8

Appendix 1.2.

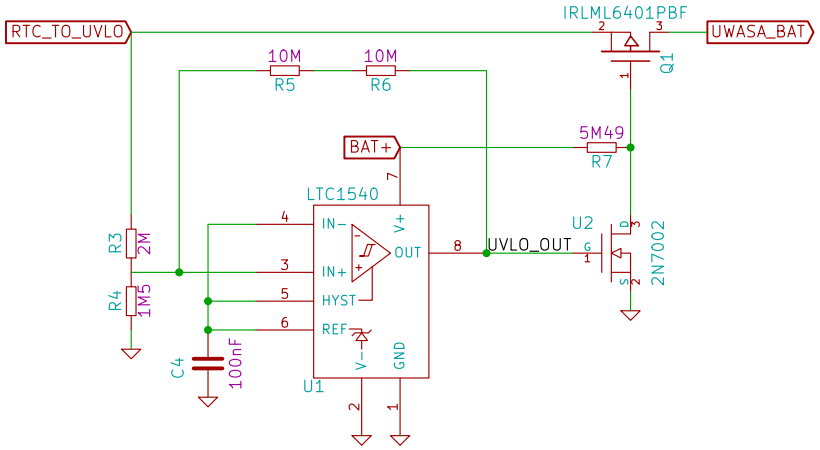

File: UVLO.sch		
Sheet: /UVLO/		
Title:		
Size: A4	*Date: 5 sep 2014*	*Rev:*
KiCad E.D.A.		Id: 2/8

Appendix 1.3.

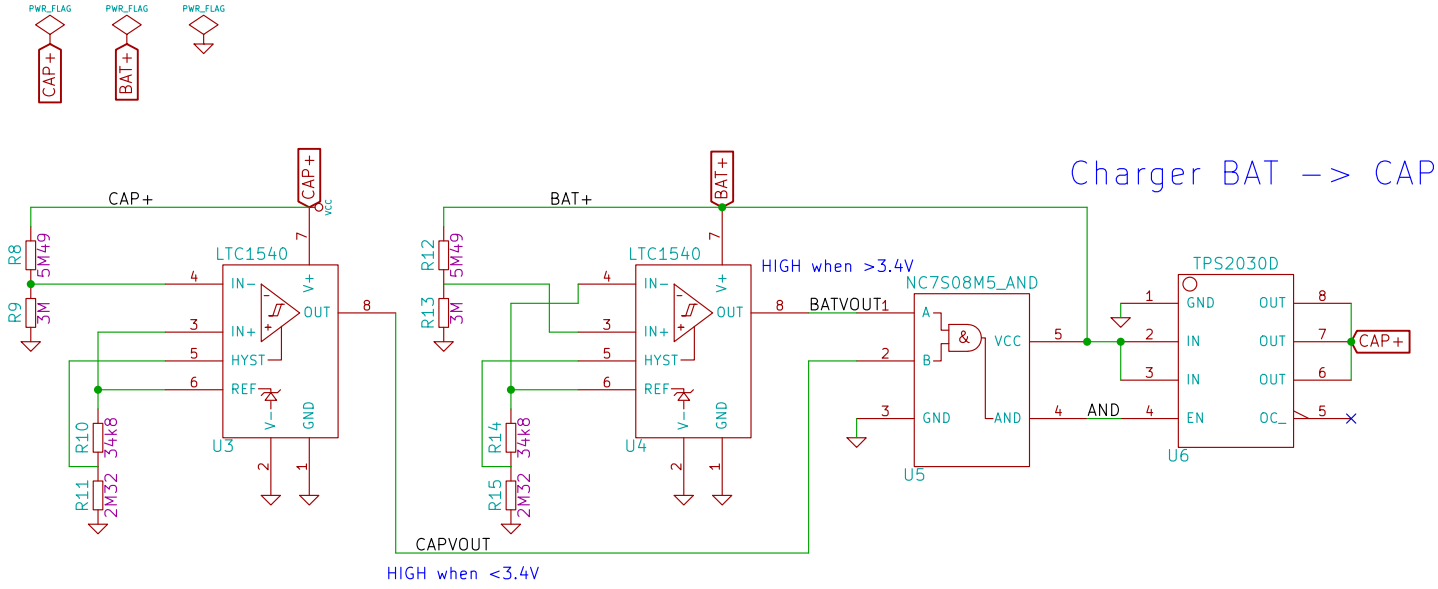

File: DoubleComparator.sch		
Sheet: /DoubleComparator/		
Title: Double comparator switch		
Size: A4	*Date: 5 sep 2014*	*Rev:*
KiCad E.D.A.		Id: 3/8

Appendix 1.4.

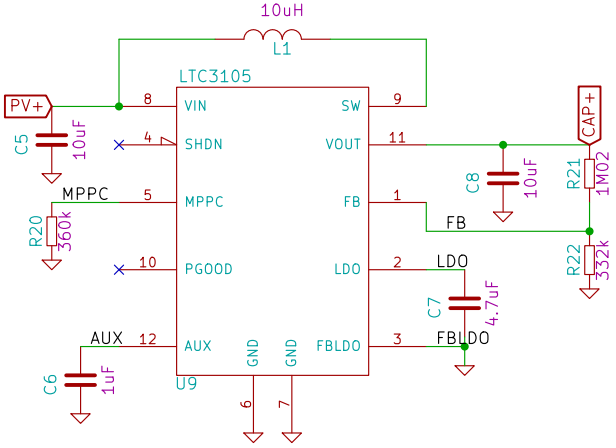

File: SolarHarvester.sch		
Sheet: /SolarHarvester/		
Title: noname.sch		
Size: A4	Date: 5 sep 2014	Rev:
KiCad E.D.A.		Id: 5/8

Appendix 1.5.

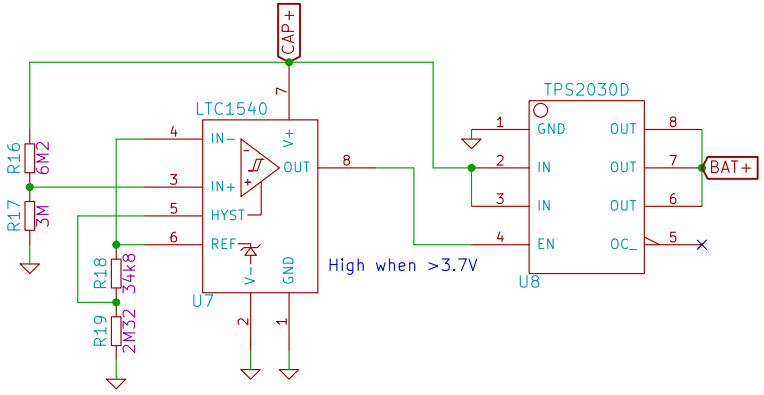

File: ChargerCAP_BAT.sch		
Sheet: /ChargerCAP_BAT/		
Title: noname.sch		
Size: A4	*Date: 5 sep 2014*	*Rev:*
KiCad E.D.A.		Id: 4/8

Appendix 1.6.

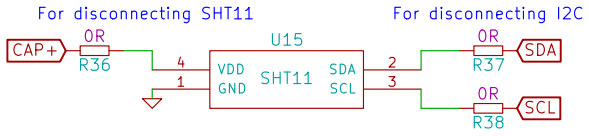

File: SH11.sch		
Sheet: /SH11/		
Title:		
Size: A4	*Date: 5 sep 2014*	*Rev:*
KiCad E.D.A.		Id: 8/8

Appendix 1.7.

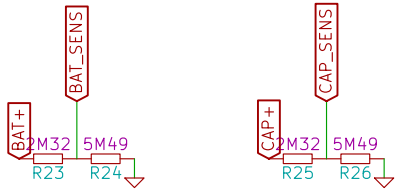

File: V_SENS.sch		
Sheet: /V_SENS/		
Title:		
Size: A4	Date: 5 sep 2014	Rev:
KiCad E.D.A.		Id: 6/8

Appendix 1.8.

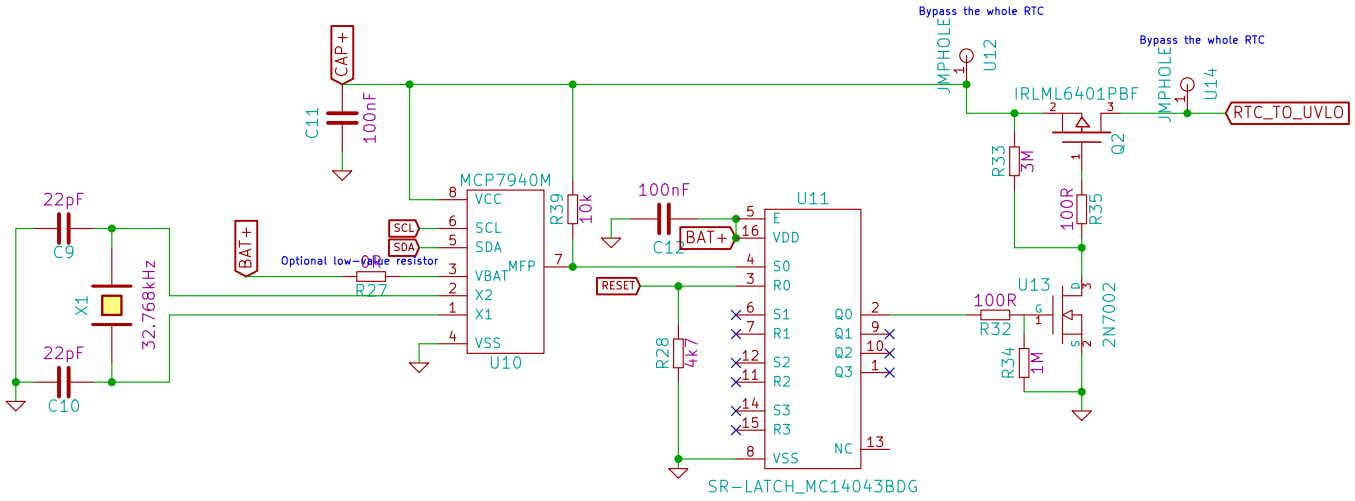

File: RTC_Switch.sch		
Sheet: /RTC_Switch/		
Title:		
Size: A4	Date: 5 sep 2014	Rev:
KiCad E.D.A.		Id: 7/8

Appendix 2.

Top

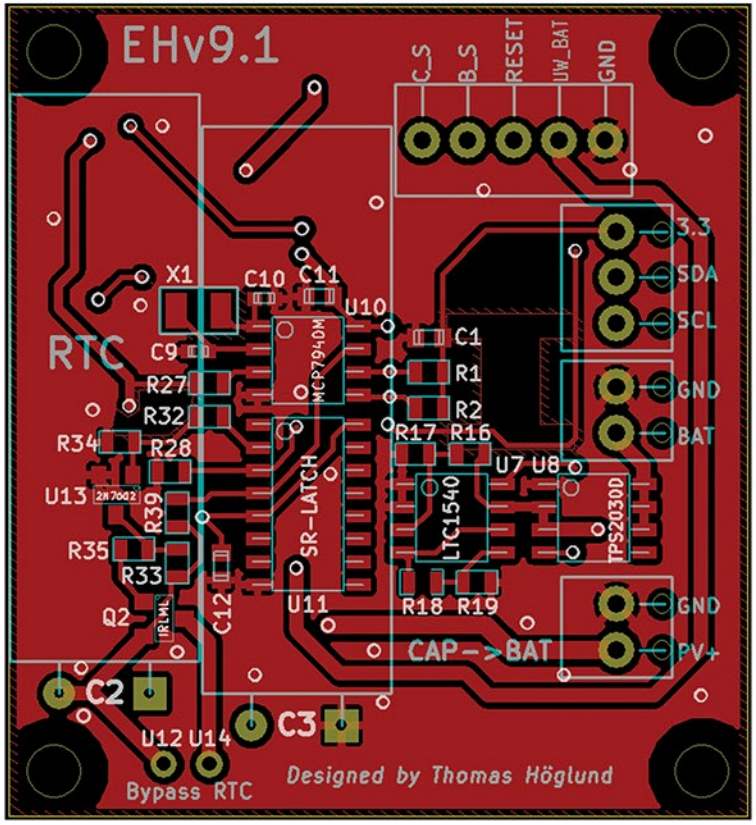

Bottom

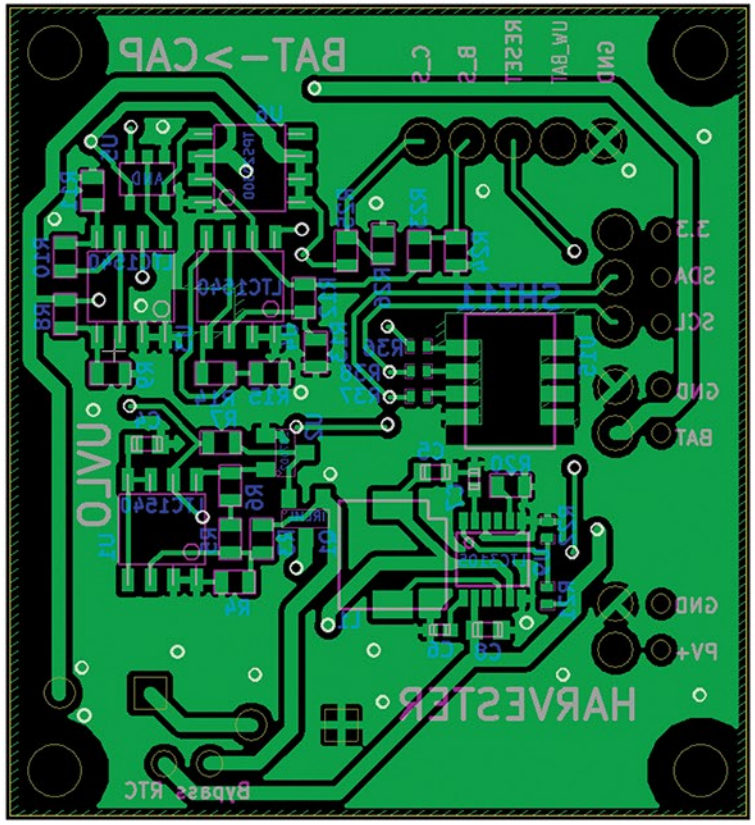

Not to scale, actual size 41 x 45 mm

Appendix 3.

Top

Bottom

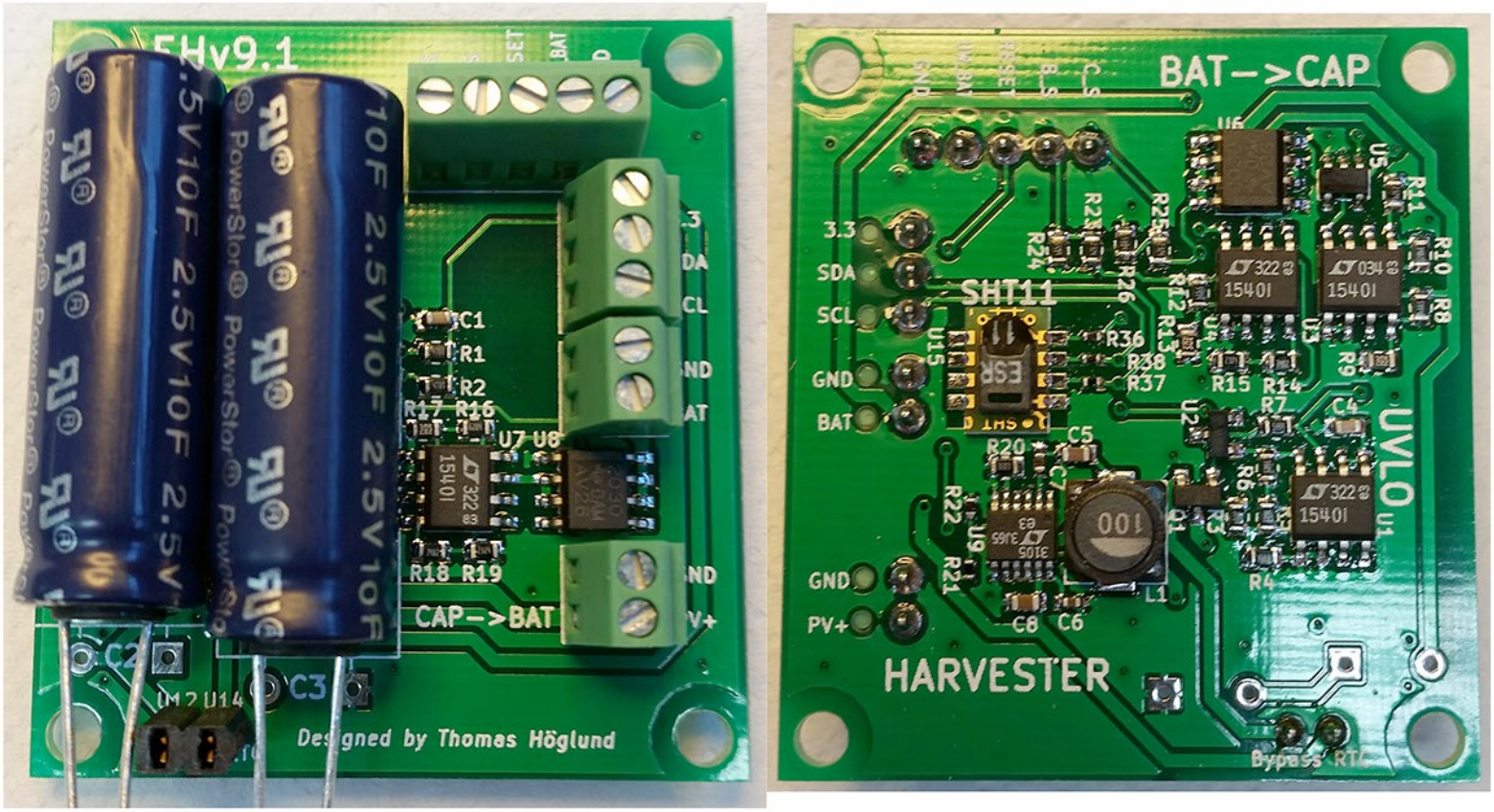

Not to scale, actual size 41 x 45 mm

Appendix 4.

Energy Harvester for the UWASA Node

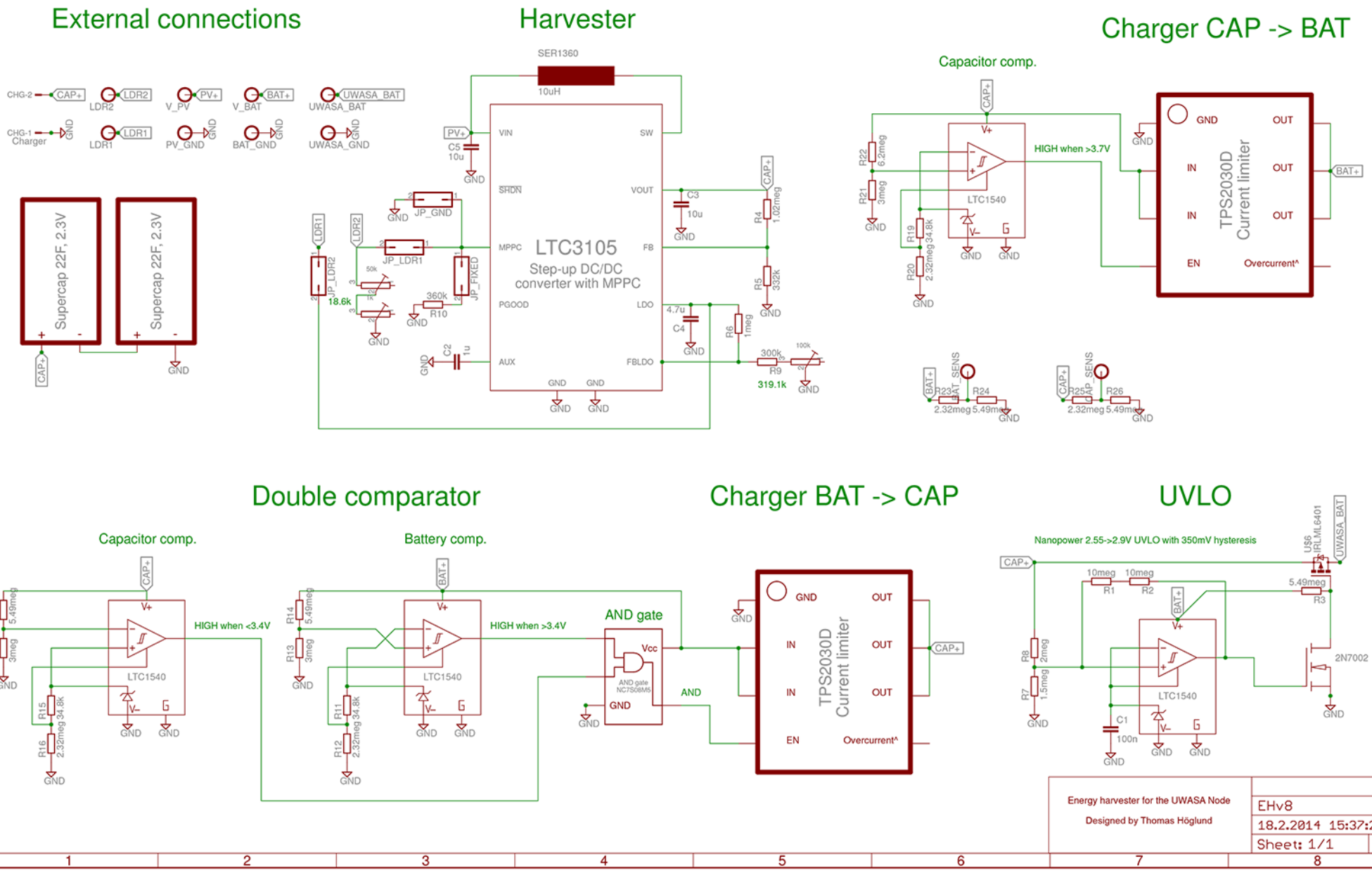

Appendix 5.

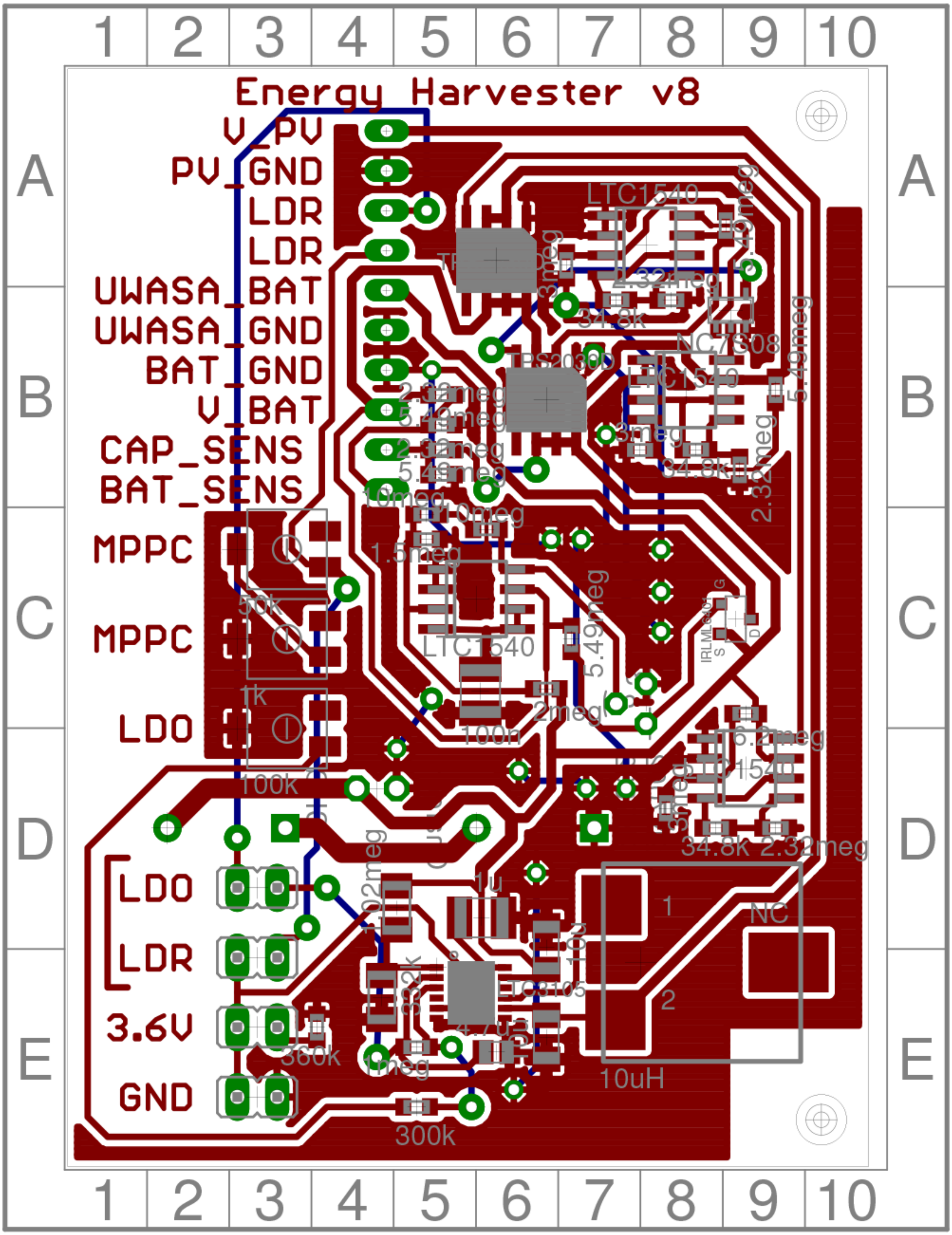
Energy Harvester v8
V_PV
PV_GND
LDR
LDR
UWASA_BAT
UWASA_GND
BAT_GND
V_BAT
CAP_SENS
BAT_SENS
MPPC
MPPC
LDO
LDO
LDR
3.6V
GND
LTC1540
LTC1540
LTC3105
10uH
300k
360k
100k
1k
50k

Appendix 6.

Top

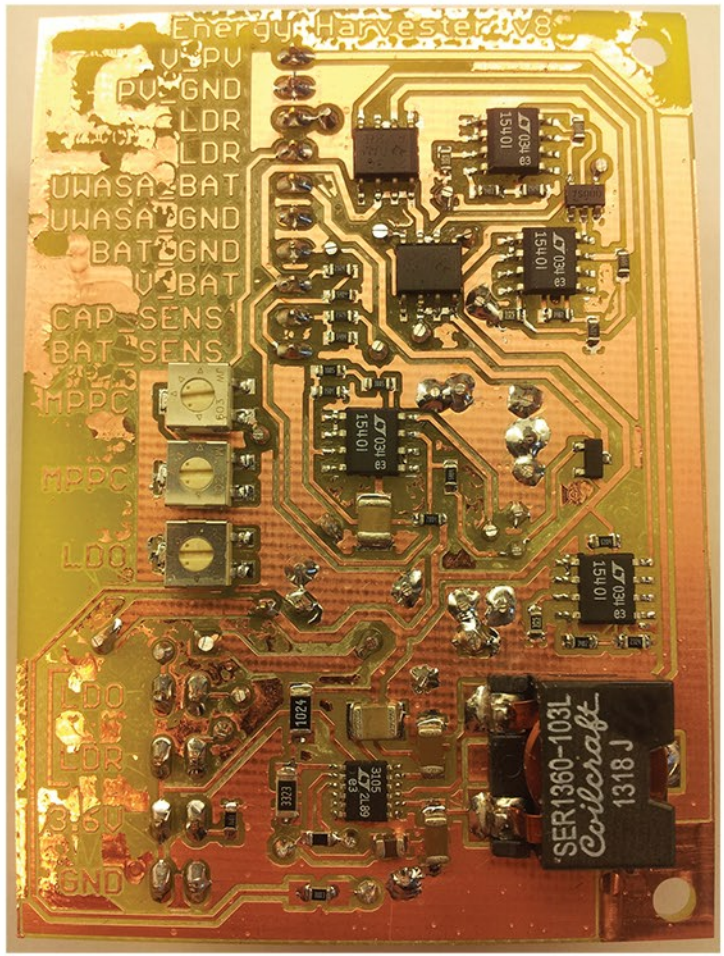

Bottom

Not to scale, actual size 51 x 70 mm

Appendix 7. All possible states of the power management system

State #	<2.9V	2.9-3.4V	3.4-3.7V	3.7-4.1V	Vcap>3.7V **Charging battery**	Vcap<3.4V & Vbat>3.4V **Emptying battery**	Vcap>2.9V **Supplying node**
1	Supercap.	Battery			0	0	0
2	Supercap.		Battery		0	1	0
3	Supercap.			Battery	0	1	0
4		Battery, Supercap.			0	0	1
5		Battery	Supercap.		0	0	1
6		Battery		Supercap.	1	0	1
7		Supercap.	Battery		0	1	1
8			Battery, Supercap.		0	0	1
9			Battery	Supercap.	1	0	1
10		Supercap.		Battery	0	1	1
11			Supercap.	Battery	0	0	1
12				Battery, Supercap.	1	0	1

Cases:

Initially bat 4.1V, cap 0V, low harvesting, high load, states:	3,10,11,12,11,10,11,…,10,8,7,8,…,7,4,1,4,1,…
Initially bat 4.1V, cap 3.5V, low harvesting, high load, states:	11,10,11,…,8,7,8,…,7,4,1,4,1,…
Initially bat 3.0V, cap 4.1V, high harvesting, high load, states:	6,5,4,3,1,4,1,4,1,…
Initially bat 3.0V, cap 4.1V, high harvesting, no load, states:	6,5,6,5,…,6,8,9,8,9,8,…,9,12

```
/*
 Logs EH over several days

 Logs:
 milliseconds, capacitor voltage, battery voltage, solar cell voltage,
 LDR (voltage), MPPC pin voltage (from 3.6V jumper)

 Connect the LDR9060 in a voltage divider with a 4.5 kOhm resistor,
 LDR on GND side

 SD card attached to SPI bus as follows:
 MOSI - pin 11
 MISO - pin 12
 CLK - pin 13
 CS - pin 8

 created 6.3.2014 by Thomas Höglund
 */

#include <SD.h>

#define CHIP_SELECT  8 // Chip Select pin is tied to pin 8 on the
SparkFun SD Card Shield
#define LED_PIN 1
#define CAP_PIN A0
#define BAT_PIN A1
#define PV_PIN A2
#define LDR_PIN A3
#define MPPC_PIN A4
#define MEAS_INTERVAL 10 // seconds

File dataFile;
unsigned long time=0;

void setup(){
  pinMode(CHIP_SELECT, OUTPUT);
  pinMode(LED_PIN, OUTPUT);
  SD.begin(CHIP_SELECT);
  delay(5000);
  dataFile = SD.open("vlog.txt", FILE_WRITE);
  if (dataFile){//if the file is available
    dataFile.println("millis,Vcap,Vbat,Vpv,LDR,MPPC");
    dataFile.close();
  }
}

void loop(){
  // This opens the file and appends to the end of file
  // If the file does not exist, this will create a new file.
  dataFile = SD.open("vlog.txt", FILE_WRITE);
  if (dataFile){//if the file is available
    while(millis()-time<MEAS_INTERVAL*1000);//wait
    time=millis();
```

```
52        dataFile.print(time);
53        dataFile.print(",");
54        dataFile.print(analogRead(CAP_PIN));
55        dataFile.print(",");
56        dataFile.print(analogRead(BAT_PIN));
57        dataFile.print(",");
58        dataFile.print(analogRead(PV_PIN));
59        dataFile.print(",");
60        dataFile.print(analogRead(LDR_PIN));
61        dataFile.print(",");
62        dataFile.print(analogRead(MPPC_PIN));
63        dataFile.println();
64        dataFile.close();
65      }
66    }
```

```
% Resistance of LDR vs. illuminance and regression
% Data in LDR9060.mat

clc;clf
clear all
load 'LDR9060.mat'
res=res/1000; % change to kOhm
L=length(lux);

figure(1)
plot(lux,res)
hold on
plot(lux,res,'.')
set(gca,'ygrid','on','xgrid','on','xscale','log')
xlabel('Illuminance (lx)')
ylabel('Resistance (k\Omega)')

% Power fit:
% General model Power2:
%      f(x) = a*x^b+c
% Coefficients (with 95% confidence bounds):
%        a =       495.8  (449, 542.5)
%        b =     -0.5812  (-0.5959, -0.5665)
%        c =      0.4339  (0.3451, 0.5228)
% Goodness of fit:
%   SSE: 0.2243
%   R-square: 0.9991
%   Adjusted R-square: 0.999
%   RMSE: 0.08794

resFit=495.8*lux.^-0.5812+0.4339;
plot(lux,resFit,'r')
```

```
% LiPo discharge plot and energy calculation
% 30.3 Ohm load, logging with Arduino

clc;clf;clear all

load 'vlogR.mat'% R = room pemperature
% plot(millisR,adcR,'.-')
% Remove zeros
zs=find(~adcR);
zs(1)=[];% keep the first zero
adcR(zs)=[];
millisR(zs)=[];
hoursR=millisR/1000/60/60;
voltsR=5/1023*adcR;
% Calculate total energy:
powerR=voltsR.*voltsR/30.3;% P=U^2/R
energyR=sum(powerR*10);% E=P*t, 10s/sample
sR=['Energy provided in room temperature: ',num2str(energyR/1000,4),'
kJ'];

load 'vlogF.mat'% F = freezer
% plot(millisF,adcF,'.-')
% Remove zeros
zs=find(~adcF);
zs(1)=[];% keep the first zero
adcF(zs)=[];
millisF(zs)=[];
hoursF=millisF/1000/60/60;
voltsF=5/1023*adcF;
% Calculate total energy:
powerF=voltsF.*voltsF/30.3;% P=U^2/R
energyF=sum(powerF*10);% E=P*t, 10s/sample
sF=['Energy provided in freezer: ',num2str(energyF/1000,4),' kJ'];

figure(1)
plot(hoursR,voltsR,hoursF,voltsF)
xlabel('Time (Hours)');ylabel('Voltage (V)')
legend('LiPo in room temperature','LiPo in freezer')
ylim([2.8 4.2])
set(gca,'ygrid','on')
text(0.3,2.9,sR)
text(0.3,3.1,sF)

% For comparison:
% Room temp.: charged at 1C with 947mA for 106min
% Freezer: charged at 1C with 937mA for 104min
% E=P*t=U*I*t:
% 3.7*.947*3600% 3.7*947mA*3600s=12.61 kJ
% 4.2*.947*3600% 4.2*947mA*3600s=14.32 kJ
```

```
% Plot the voltage over time with 1000mAh LiPo in freezer and room
% temperature without load

% Room temperature:
% 27.1.2014 3.84V
% 14.3. 3.84
% 28.5. 3.83
% 1.7. 3.82
% 23.7. 3.81
% 25.8. 3.80
%
% Freezer:
% 27.1.2014 3.86V
% 14.3. 3.86
% 28.5. 3.84
% 1.7. 3.84
% 23.7. 3.83
% 25.8. 3.82

clf;clc;clear all
Vr=[3.84 3.84 3.83 3.82 3.81 3.80];%voltage at room temperature
Vf=[3.86 3.86 3.84 3.84 3.83 3.82];%voltage in freezer
clocks={    2014 1 27 0 0 0;...
            2014 3 14 0 0 0;...
            2014 5 28 0 0 0;...
            2014 7 1 0 0 0;...
            2014 7 23 0 0 0;...
            2014 8 25 0 0 0;...
       };
seconds=zeros(1,size(clocks,1));
for i=1:size(clocks,1)-1
    seconds(i+1)=seconds(i)+etime(cell2mat(clocks(i+1,:)),cell2mat(
    clocks(i,:)));
end
hours=seconds/60/60;
disp(hours')

figure(1)
[AX1,H1,H2]=plotyy(hours,Vr,hours,Vf)
legend('LiPo at room temp.','LiPo in freezer','location','northeast')
ylabel(AX1(1),'Voltage (V)')
ylabel(AX1(2),'Voltage (V)')
hold on
[AX2,H3,H4]=plotyy(hours,Vr,hours,Vf);
set(H1,'LineStyle','.')
set(H2,'LineStyle','o')
set(AX1(2),'ylim',[3.77 3.87])
set(AX2(2),'ylim',[3.77 3.87])
set(AX1(1),'ylim',[3.75 3.85])
set(AX2(1),'ylim',[3.75 3.85])
set(AX1(1),'ygrid','on','xgrid','on','YTick',[3.75:0.01:3.85])
set(AX1(2),'YTick',[3.77:0.01:3.87])
xlabel('Time (hours)')
```

```
% log1 contains voltages from the first EHv8 test outside with Arduino
% SD logger. The LDR9060 is connected in a voltage divider with a
% 4.5 kOhm resistor, LDR on GND side

% Results: In 6 days 6.9kJ, or 51% of the battery capacity was charged
% Average harvesting hours/day = 9.017 h
% Average energy harvested/hour = 128.3 J
% Average energy harvested/day = 1.157 kJ
% Average energy harvested/minute = 2.138 J
% Average power = 35.63 mW (about 9.4 mA)

clc;clear all;clf
load('log1')% load the dataset for 8-14.3.2014
log1.Properties.VarNames'
l=1:length(log1);

% % Plot all
% figure(1)
% plot(l,log1.(2),l,log1.(3),l,log1.(4),l,log1.(5),l,log1.(6))
% legend(log1.Properties.VarNames(2:end-1))

% % Find the restart and create hours
% ind=find(log1.millis==10000);
% hours=log1.millis(ind(2):end)+log1.millis(ind(2)-1);% find last part
% hours=[log1.millis(1:ind(2)-1);hours];% add first part
% hours=hours/1000/60/60;
% log1.hours=hours;
% plot(log1.hours)
% ylabel('hours')
% save('log1.mat','log1')

% % Convert ADC values to voltages
% log1.Vcap=log1.ADCcap*5/1023;
% log1.Vbat=log1.ADCbat*5/1023;
% log1.V_PV=log1.ADC_PV*5/1023;
% log1.V_LDR=log1.ADC_LDR*5/1023;
% log1.V_MPPC=log1.ADC_MPPC*5/1023;
% figure(1);plot(log1.V_LDR),ylabel('V LDR')
% save('log1.mat','log1')

% % Calculate LDR resistance
% % log1.R_LDR=4.5e3*log1.V_LDR/5./(1-log1.V_LDR/5);
% V_LDR_corrected=log1.V_LDR;% correct values rounded to 5V to 4.9V
(220.5kOhm)
% V_LDR_corrected(find(log1.V_LDR>4.9))=4.9;
% log1.R_LDR=4.5e3*V_LDR_corrected/5./(1-V_LDR_corrected/5);
% figure(1);plot(l,log1.R_LDR,l,log1.V_PV)
% save('log1.mat','log1')

% % Calculate illuminance (lx)
% % The following formula was found using LDR9060notkOhm.m and the
% % Curve fitting tool box:
% % calculatedLx=nthroot((measuredResistance-433.9)/4.958e+05,-0.5812)
```

```
53  % log1.lx=nthroot((log1.R_LDR-433.9)/4.958e+05,-0.5812);
54  % figure(1);plot(l,log1.lx/1000);ylabel('Illumination (kLx)')
55  % save('log1.mat','log1')
56
57  % % Plot illuminance vs time (hours)
58  % figure(1)
59  % plotyy(log1.hours,log1.lx/1000,log1.hours,log1.Vbat)
60  % legend('Illuminance','Vbat','location','northwest')
61  % % hold on;plotyy(log1.hours,log1.lx/1000,log1.hours,log1.Vbat)
62  %
63  % %
    [AX1,H1,H2]=plotyy(Loadresistance,Loadpower,Loadresistance,Efficiency);
64  % % % title('hmm')
65  % % legend('Power','Efficiency')
66  % % xlabel('Resistance (\Omega)')
67  % % ylabel(AX1(1),'Power (mW)')
68  % % ylabel(AX1(2),'Efficiency (%)')
69  % % hold on
70  % %
    [AX2,H3,H4]=plotyy(Loadresistance,Loadpower,Loadresistance,Efficiency);
71  % % set(H1,'LineStyle','.')
72  % % set(H2,'LineStyle','o')
73  % % ylim([0 300])
74  % % set(AX1(1),'ygrid','on','YTick',[0:50:300],'xgrid','on')
75  % % % set(AX1(1),'ygrid','on','YTick',[0:50:300])
76  % % % % set(AX2(1),'ygrid','on','YTick',[0:1:5])
77  % % % set(AX1(2),'ylim',[80 86],'ytick',[80:2:86])
78  % % % set(AX2(2),'ylim',[80 86],'ytick',[80:2:86])
79
80  % Calculate energy harvested per day, hour and minute
81  fig1h=figure(1);subplot(211)
82  [AX1,H1,H2]=plotyy(log1.hours,log1.Vbat,log1.hours,log1.lx);
83  title('Battery voltage and illuminance vs. time');xlabel(AX1(1),'Time
    (h)');
84  set(AX1,'YGrid','on')
85  ylabel(AX1(1),'Voltage (V)');ylabel(AX1(2),'Illuminance (lx)')
86  subplot(212)
87  plot(log1.hours,log1.V_PV);title('Solar cell voltage vs. time')
88  xlabel('Time (h)');ylabel('Voltage (V)')
89  set(gca,'YGrid','on','ylim',[0 5.5],'YTick',[0:1:5])
90  text(0.5,14,'Appendix 12.3.','FontSize',14)
91  %# centimeters units
92  X = 29.7;                   % A4 paper size
93  Y = 21.0;                   % A4 paper size
94  xMargin = 1;                % left/right margins from page borders
95  yMargin = 1.5;                % bottom/top margins from page borders
96  xSize = X - 2*xMargin;      % figure size on paper (widht & hieght)
97  ySize = Y - 2*yMargin;      % figure size on paper (widht & hieght)
98  % figure size printed on paper
99  set(fig1h, 'PaperUnits','centimeters')
100 set(fig1h, 'PaperSize',[X Y])
101 set(fig1h, 'PaperPosition',[xMargin yMargin xSize ySize])
102 set(fig1h, 'PaperOrientation','portrait')
```

```
103  % export to PDF and open file
104  print -dpdf -r0 out.pdf
105  winopen out.pdf
106
107  % Voltages: Day1: 3.783->3.803, day2: 3.803->3.827, day3: 3.827->3.876,
108  % day4: 3.876->3.93, day5: 3.93->4.008, day6: 4.008->4.086
109  Vlow=[3.783 3.803 3.827 3.876 3.93 4.008];
110  Vhigh=[3.803 3.827 3.876 3.93 4.008 4.086];
111  for d=1:length(Vlow)
112      energyOnDay(d)=energyBetweenVoltages(Vlow(d),Vhigh(d));
113  end
114  energyOnDay
115  disp('Sum of energy harvested (J): ');disp(sum(energyOnDay))
116  % % Illustrate that the energy difference is not linearly proportional
     to the
117  % % voltage difference:
118  % energyOnDay/max(energyOnDay)% normalized
119  % Vdiff=Vhigh-Vlow
120  % Vdiff/max(Vdiff)% normalized
121  harvestingHours=[8.3 8.8 9.9 9.7 8.2 9.2];% how many hours
     harvested/day, manually calculated
122  disp('Average harvesting hours per day:')
123  disp(mean(harvestingHours))
124  disp('Average energy harvested per hour (J): ')
125  energyPerHour=mean(energyOnDay./harvestingHours);
126  disp(energyPerHour)
127  disp('Average energy harvested per minute (J): ')
128  energyPerMin=energyPerHour/60;
129  disp(energyPerMin)
130  clear Vlow Vhigh Vdiff d
131  % Calculate average power harvested at daytime
132  % E=P*t, P=E/t
133  format short eng
134  averagePower=energyPerHour/3600
```

```
function [ energy ] = energyBetweenVoltages( v1,v2 )
%ENERGYBETWEENVOLTAGES Calculates the energy the LiPo can provide being
%discharged between two voltages, or conversely, how much it can
accept when charged.

    load('fitFunctions');
    evalPoints=1e6;
    s1=secondsFromVoltage(v1);
    s2=secondsFromVoltage(v2);
    s=linspace(s1,s2,evalPoints);
    energy=sum(powerFromSeconds(s)*abs(s2-s1)/evalPoints);
end
```

Appendix 12.3.